

AMERICAN UNIVERSITY OF BEIRUT

CURCUMIN BASED HYBRID NANOCAPSULES: SELF-
ASSEMBLY, CHARACTERIZATION AND BIOMEDICAL
APPLICATION

by
LAYAL MAJID SLIKA

A thesis
submitted in partial fulfillment of the requirements
for the degree of Master of Science
to the Department of Chemistry
of the Faculty of Arts and Sciences
at the American University of Beirut

Beirut, Lebanon
February 2019


AMERICAN UNIVERSITY OF BEIRUT

CURCUMIN BASED HYBRID NANOCAPSULES: SELF-
ASSEMBLY, CHARACTERIZATION AND BIOMEDICAL
APPLICATION


by
LAYAL MAJID SLIKA

Approved by:

Dr. Digambara Patra, Associate Professor
Chemistry


Advisor

Dr. Rabih Sultan, Professor
Chemistry


Member of Committee

Dr. Elias Baydoun, Professor
Biology


Member of Committee

Date of thesis/dissertation defense: February 1, 2019

AMERICAN UNIVERSITY OF BEIRUT

THESIS, DISSERTATION, PROJECT RELEASE FORM

Student Name: Slika Layal Majid
Last First Middle

Master's Thesis Master's Project Doctoral Dissertation

I authorize the American University of Beirut to: (a) reproduce hard or electronic copies of my thesis, dissertation, or project; (b) include such copies in the archives and digital repositories of the University; and (c) make freely available such copies to third parties for research or educational purposes.

I authorize the American University of Beirut, to: (a) reproduce hard or electronic copies of it; (b) include such copies in the archives and digital repositories of the University; and (c) make freely available such copies to third parties for research or educational purposes after : **One --- year from the date of submission of my thesis, dissertation, or project.**
Two --- years from the date of submission of my thesis, dissertation, or project.
Three ~~1~~ years from the date of submission of my thesis, dissertation, or project.

Layal Slika

Signature

Feb. 8/2019

Date

ACKNOWLEDGMENTS

First of all, I would like to express my sincere appreciation and thanks to my advisor Dr. Patra and thesis committee members Dr. Sultan and Dr. Baydoun for their valuable time, suggestions and comments.

I also want to specially thank Dr. Patra for being the amazing person you are, thanks for your patience, guidance and distinguished kindness. I always think that if it weren't for your understanding and support I wouldn't have gone this far. Now, I knew I've made the best choice by working with you.

I want to especially thank Dr. Baydoun for the offered lab facilities in order to conduct the biological part of the study. Thanks for his kind help that I really appreciate. I would like also to thank my professors throughout my past years of masters who enriched my learning experience each in his own way.

I'm always grateful for the ones who were there to assist and support me throughout my past 3 years especially the Central Research Science Laboratory Mr. Joan, Ms. Rania and Mr. Shady.

Special thanks also for Mahmoud, Nisreen and Ghiwa for the emotional and technical support every time I needed it. And I needed it a lot!

Wissam Al Moubarak, my husband, thanks for being there for me every single moment ever since I started my Masters, thanks for all the emotional, motivational and technical support you provided me. Thanks for always proving you are my better half.

Finally, I want to thank my close family, my mom, dad, Rayan and Raghied, my lovely husband's family and my close friends Bushra, Zeina and Manal for all the love, care and support.

I am very blessed to have you all around believing in me and helping me to achieve my dreams and goals. I promise to always be there for all of you <3

AN ABSTRACT OF THE THESIS OF

Layal Slika for

Master of Science

Major: Chemistry

Title: Curcumin Based Hybrid Nano Capsules: Self-Assembly, Characterization and Biomedical Application

Chapter I provides an introduction into the thesis topic and enlists the major aims, and Chapter II provides a literature review. Curcumin (CUR) is a natural polyphenol present in the rhizomes of *Curcuma longa* and possesses diverse pharmacological effects especially anti-carcinogenic effects against several types of cancers. Unfortunately, this novel compound has been clinically proven to have poor aqueous solubility and bioavailability that limit its pharmaceutical effects. Several nanotechnological approaches such as liposomes, adjuvants, and polymeric nanocapsules have been applied in order to overcome such problems. Thus, our present study aimed at developing two novel polymeric nanoparticle systems that encapsulate either curcumin alone (CUR-PAH NP) or with piperine (CUR-PIP-PAH NP). Piperine (PIP) was chosen based on its role as a glucuronidation inhibitor that has been shown to increase the bioavailability of curcumin.

Chapter III describes the materials and methods used to achieve our aims. The NPs were successfully designed by self-assembled nanoprecipitation method and their characteristics were identified by FTIR, XRD, SEM, DLS, and Zeta potential. The drug release profiles were monitored under different pH, and their effects against colon cancer were investigated both in *vitro* and *in vivo*.

Chapter IV discusses our findings. The FTIR analysis showed that both CUR and PAH are present inside the CUR-PAH NP confirming a strong involvement of NH₂ of PAH and enol form of CUR inside the NPs. Similarly, this analysis of CUR-PIP-PAH NP showed that CUR and piperine are present inside the NPs. The SEM images showed that CUR-PAH NP and CUR-PIP-PAH NP are spherical and their sizes are in the range of 80-100 nm depending on ratio of CUR:PAH and PIP:CUR. The XRD analysis proved the amorphous structure of the produced NPs. Results also showed that adding piperine to the prepared NP while fixing the concentration of PAH and CUR facilitates the encapsulation and drug loading of CUR within PAH. *In Vitro* drug release study showed that pH triggers the maximum release of curcumin from the capsule in basic medium compared to acidic and neutral media. The drug release profile of curcumin follows Higuchi model. Apart from drug delivery, the cytotoxic effects of curcumin

within the two different types of nanocapsules were high. They were confirmed by % viability and fluorescent images that showed the cellular localization of NPs inside the Caco-2 (human epithelial colorectal adenocarcinoma) cells and a distorted morphology of cancer cells indicating apoptosis. The *in vivo* application of CUR-PAH NP in mouse model of colorectal carcinogenesis that is discussed in chapter V showed that CUR-PAH NP downregulates the Wnt signaling pathway that is known to drive colorectal cancer. It also acts as an anti-inflammatory agent inhibiting cyclooxygenase (COX-2) and inducible nitric oxide synthase (iNOS).

Our findings indicated that curcumin nanoencapsulation enhances the physiochemical properties of curcumin whereby it reduced particle size, formed an amorphous state, and enhanced the drug loading and release. The addition of piperine enhanced the observed results. Furthermore, *in vitro* and *in vivo* studies showed that curcumin NPs exerted selective and potential cytotoxic effects against colon cancer cells. Accordingly, we suggest that curcumin nanoencapsulation enhanced the solubility and bioavailability of curcumin rendering it more effective against colorectal cancer.

CONTENTS

ACKNOWLEDGEMENTS.....	v
ABSTRACT.....	vi
LIST OF ILLUSTRATIONS.....	xii
LIST OF TABLES.....	xiv
LIST OF ABBREVIATIONS.....	xv
I. INTRODUCTION.....	1
II. LITERATURE REVIEW.....	3
A. Curcumin.....	3
1. Traditional uses.....	3
2. Pharmacological properties.....	5
a. Anti-diabetic and hypolipidemic effects.....	6
b. Anti-inflammatory and antioxidant activities	6
c. Antitumor and chemoprotective effects.....	8
d. Curcumin against colorectal cancer.....	10
i. <i>In vitro</i>	10
ii. <i>In vivo</i>	11
iii. Main activities and targets of curcumin.....	12
iv. Clinical trials.....	13
3. Structural and chemical properties.....	14
4. Photophysical properties of curcumin.....	16
5. Stability of curcumin.....	17
a. Aqueous stability.....	17
b. Spectral and photophysical stability.....	18
c. Photochemical stability.....	20
d. Thermal stability.....	21
6. Bioavailability problems.....	22
7. Recent advances.....	22
a. Adjuvants.....	22

b. Nanoparticles.....	23
c. Liposomes, micelles and phospholipid complexes.....	23
d. Metal complexes.....	24
e. Derivatives and analogues.....	25
B. Nanotechnology.....	25
1. Nature & uses.....	25
2. Different types of nanoparticles.....	26
a. Inorganic nanoparticles.....	26
b. Solid lipid nanoparticles.....	27
c. Liposomes.....	27
d. Nanocrystals.....	27
e. Quantum dots.....	28
f. Carbon nanotubes and fullerenes.....	28
g. Dendrimers.....	29
h. Polymeric nanoparticles and nanocapsules.....	29
3. Different types of curcumin nanoparticles.....	31
C. Polymeric nanocapsules	32
1. Properties.....	33
a. Particle size.....	33
b. Surface properties.....	34
c. Drug loading and drug release.....	34
i. Drug release systems.....	35
ii. Methods of assessing drug release profiles.....	36
iii. Drug release kinetic models.....	38
2. Applications.....	40
3. Preparation of different nanocapsules for drug delivery.....	40
a. Layer by layer.....	41
b. Emulsifications/solvent diffusion.....	43
c. Solvent displacement and interfacial deposition.....	44
d. Self-assembly.....	45
4. Curcumin-based polymeric nanocapsules.....	48
D. PAH.....	50
1. Applications of PAHs.....	51
2. PAH driving forces.....	52
3. Curcumin and PAH.....	53

III. MATERIALS AND METHODS.....	56
A. Chemicals and reagents.....	56
B. Methods.....	56
1. Preparation of curcumin-PAH nanoparticles.....	56
2. Preparation of curcumin-piperine-PAH nanoparticles.....	57
3. Preparation of calibration curves.....	58
4. Drug loading of curcumin nanocapsules.....	59
5. Encapsulation efficiency of curcumin nanoparticles.....	59
6. Characterization.....	60
a. Fourier Transform Infrared Spectroscopy (FTIR) Analysis.....	60
b. Scanning Electron Microscopy (SEM) Analysis.....	60
c. X-Ray Diffraction Studies (XRD) Analysis.....	61
d. Dynamic Light Scattering (DLS) and Zeta Potential Analysis...	61
7. <i>In vitro</i> Analysis.....	61
8. Culture of Caco2 cells	62
9. Drug preparation for cell culture treatment	63
10. Cytotoxicity and cell viability studies.....	63
IV. RESULTS AND DISCUSSION.....	64
A. FTIR analysis.....	64
B. SEM analysis.....	68
1. Formation and morphology.....	68
2. Size.....	68
C. XRD analysis.....	71
D. DLS and Zeta Potential analysis.....	75
E. <i>In Vitro</i> drug release analysis.....	79
F. Cytotoxic effect of CUR-PAH NP and CUR-PIP-PAH NP.....	86
V. IN VIVO STUDY.....	92

VI. CONCLUSION.....	95
---------------------	----

REFERENCES.....	96
-----------------	----

ILLUSTRATIONS

Figure		Page
1	Curcuma longa, turmeric and curcumin.....	3
2	Stages in tumor progression inhibited by curcumin.....	8
3	Chemical structures of the three major natural curcuminoids.....	14
4	Tautomerism of curcumin under different physiological states. In acidic and neutral media, the bis-keto form (top) dominates, while the enol-form exists at pH > 8.....	15
5	Curcumin's degradation products. (A) vanillin, (B) ferulic acid, (C) feruloylmethane, (D) vanillic acid, and (E) ferulic aldehyde.....	18
6	(A) Ground-state absorption spectra and (B) Normalized fluorescence spectra of curcumin in cyclohexane (•••••), benzene (---), acetonitrile (—), methanol (•-•-) and TX-100 (.....) due to excitation at 355 nm...	20
7	Structural formula of piperine.....	23
8	Basic methods of in vitro drug release assessments. A sample and separate method, B continuous flow method and C dialysis method.....	38
9	Process of LbL assembly (a) on a solid substrate; (b) on a colloidal core.....	42
10	Schematic illustration of the ESD technique.....	43
11	Schematic representation of the solvent displacement technique. **Surfactant is optional. ***In interfacial deposition method, a fifth compound was introduced only on preparation of nanocapsules.....	44
12	Molecular level of directed self-assembly.....	47
13	Chemical structure of poly (allylamine hydrochloride) (PAH).....	50
14	Conversion of curcumin powder into stable nanocolloids.....	54
15	FT-IR spectra of CUR (A), CUR-PAH NP (B), CUR-PIP-PAH NP (C), PAH (D) and PIP (E).....	67
16	SEM images of 1:4 CUR:PAH (A), 1:2 CUR:PAH (B) and 1:1 CUR:PAH NPs (C).....	69
17	SEM images of 1:4 PIP:CUR (A), 1:2 PIP:CUR (B) and 1:1 PIP:CUR NPs (C).....	71
18	XRD images of curcumin (A), PAH (B), and 1:2 CUR:PAH (C).....	73

19	XRD images of PIP (A) and 1:2 PIP:CUR (B)	75
20	% Cumulative release of 1:2 CUR-PAH NP (A) and CUR-PIP-PAH NP (B)	80
21	Plots showing the drug release of CUR:PAH NPs plotted using three different mathematical models: (a) zero order kinetic model, (b) first order kinetic model, and (c) Higuchi kinetic model.....	83
22	% Viability of Caco-2 cells treated with different concentrations of 1:2 CUR:PAH NPs.....	86
23	Fluorescence inverted microscope images of Caco-2 cell uptake of different concentrations of CUR-PAH NP at 24 and 48 hours.....	88
24	% Viability of Caco-2 cells treated with CUR, 1:2 CUR:PAH, and different ratios of PIP:CUR NPs	89
25	Fluorescence inverted microscope images of untreated Caco-2 cells (control), CUR and 1:2 PIP:CUR NPs treated cells at 24 and 48 hours.....	91
26	Effect of CUR-PAH NP on the expression of Wnt (A), b-Catenin (B), APC (C), and Cyclin D1 (D) genes. Expression levels of control and treated samples were normalized to their respective GAPDH, and the fold change was determined relative to the control. All bars represent mean of three determinations \pm SEM. (*), (**), (***), and (****) on bars correspond to p-value < 0.05, < 0.01, < 0.001, and <0.0001 respectively.....	93
27	Effect of CUR-PAH NP on the COX-2 level and iNOS activity. Data are represented as mean \pm SD. (****) corresponds to p-value < 0.0001.....	94

TABLES

Table		Page
1	Summary of main activities of curcumin.....	12
2	% EE and % DL of different ratios of CUR-PAH NP and CUR-PIP-PAH NP.....	78
3	R ² values of zero-order, first-order and Higuchi kinetic models for 1:2 CUR:PAH NPs release at different pH.....	84
4	R ² values of zero-order, first-order and Higuchi kinetic models for 1:2 PIP:CUR NPs release at different pH.....	84
5	R ² values of zero-order, first-order and Higuchi kinetic models for CUR-PAH NP and CUR-PIP-PAH NP release at 2 phases of pH=10.	85
6	Experimental protocol.....	92

LIST OF ABBREVIATIONS

ACF	Induced aberrant crypt foci
AOM	Azoxymethane
APC	Adenomatous polyposis coli
BSA	Bovine serum albumin
Caco-2	Human epithelial colorectal adenocarcinoma cells
COX	Cyclo-oxygenase
CRC	Colorectal cancer
CS	Chitosan
CUR	Curcumin
CUR-PAH	Curcumin-PolyallylAmine Hydrochloride
CUR-PIP-PAH	Curcumin-Piperine-PolyallylAmine Hydrochloride
DL	Drug loading
DLS	Dynamic light scattering
DM	Dialysis membrane
DCM	Diabetic Cardiomyopathy
DDW	Double Distilled Water
DMEM	Dulbecco's Modified Eagle's medium
DMH	Dimethylhydrazine
DSA	Directed self-assembly
EE	Encapsulation efficiency

ESD	Emulsifications/solvent diffusion
ESIHT	Excited state intramolecular hydrogen transfer
FA	Ferulic acid
FBS	Fetal bovine serum
FDA	US Food and Drug Administration
FTIR	Fourier transform infrared spectroscopy
GAPDH	Glyceraldehyde-3-phosphate dehydrogenase
IL-1 β	Interleukin-1 β
iNOS	Inducible nitric oxide synthase
LbL	Layer by Layer
LDL	Low-density lipoprotein
LOX	Lipo-oxygenase
LPS	Lipopolysaccharide
MIP-1	Monocyte inflammatory protein-1
MP2	Møller-Plesset perturbation
MS	Mass spectrometry
MWNTs	Multiple-walled nanotubes
NaHCO ₃	Sodium bicarbonate
NF-kB	Nuclear factor kappa B
NMR	Nuclear magnetic resonance
NP	Nanoparticle
P/S	Penicillin/Streptomycin

PAH	Polyallylamine hydrochloride
PBCA	Poly(butylcyanoacrylate)
PCA	Poly-cyanoacrylate
PEG	Polyethylene glycol
PEO	Polyethylene oxide
PIP	Piperine
PLA	Poly (lactic acid)
PLG	Poly (L-glycolide)
PLGA	Poly(lactide-co-glycolide)
qRT-PCR	Real time polymerase chain reaction
ROS	Reactive oxygen species
SEM	Scanning electron microscopy
SLN	Solid lipid nanoparticles
SWNTs	Single-walled nanotubes
TD-DFT	Time-dependent density functional theory
TEM	Transmission electron microscopy
TNF- α	Tumor necrosis factor- α
VA	Vanillic acid
XRD	X-ray diffraction

CHAPTER I

INTRODUCTION

Curcumin (CUR) is a well-documented natural polyphenol which possesses anti-inflammatory, antioxidant, and anti-carcinogenic properties. This agent holds great promise in the field of cancer chemoprevention and suppression of different types of cancers. However, it has poor aqueous solubility and bioavailability that reduce its pharmaceutical effectiveness. To enhance its solubility and subsequent bioavailability, applying nanotechnological approaches in order to develop curcumin nanocapsules can be performed. Recently, the use of nanocapsules on the basis of well-documented biocompatible polymers, such as polyallylamine hydrochloride (PAH), for targeted drug delivery is being applied in the treatment of many diseases.

Hence, we aimed in this study to:

- develop polymeric nanoparticle systems that encapsulate curcumin into PAH assembled nanocapsules by simple nanoprecipitation method
- incorporate piperine into the curcumin-PAH nanocapsules
- characterize the physicochemical properties of the two types of the designed nanocapsules using FTIR, SEM, XRD, DLS, and zeta potential
- monitor the drug delivery of both NPs at different pHs (4, 6, 7, 8, and 10)
- investigate the *in vitro* cytotoxic effects of curcumin nanocapsules against Caco-2 (human epithelial colon cancer cells) cell line

- examine the *in vivo* antiproliferative effects of curcumin nanocapsules against DMH-induced colorectal cancer in mice

CHAPTER II

LITERATURE REVIEW

A. Curcumin

Curcumin (diferuloylmethane) is the major polyphenol found in the Indian spice turmeric¹. Turmeric is derived from the rhizomes of *Curcuma longa* Linn – a perennial plant native to Southeast Asia that belongs to the family of ginger “Zingiberaceae” (see **Figure 1**). Curcumin is the chief constituent of turmeric; it comprises ~ 2-5% of the spice. Turmeric is mainly made up of a class of curcuminoids, including curcumin, that are responsible for its bright yellow color. Other members of the curcuminoid family found in turmeric include: desmethoxycurcumin and bisdemethoxycurcumin².

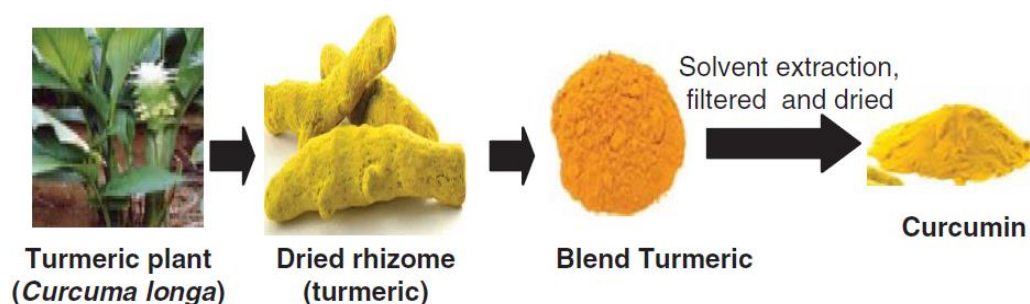


Figure 1. *Curcuma longa*, turmeric and curcumin.

1. *Traditional uses*

Due to its vibrant yellow color, curcumin has been widely applied as a food color as well as a food additive referred to as E100. In cooking, curcumin is used as a

spice to add a flavor commonly to curry and mustard. As a food color, it is used to color many foods including cheese and butter. In addition, curcumin has been recently marketed in many countries worldwide as tablets, capsules, energy drinks, ointments, cosmetics, and soaps³.

Curcumin is well-recognized for its worldwide use in various forms and each country uses it in a different form; for example, it is commonly used in India in curries. In Japan, it is used in the form of a tea while in Thailand it is more involved in cosmetics. Curcumin is also used as a colorant in China, an antiseptic in Malaysia and anti-inflammatory agent in Pakistan, a preservative coloring agent in the United States in mustard sauce, cheese, butter, and chips, and served as a drink in Korea. The US Food and Drug Administration (FDA) have approved the use of curcumin as a safe tolerable agent at doses of 4000-8000 mg/day⁴.

Curcumin has not been only used in food flavoring, dyeing and cosmetics, but also in the traditional medicine of many Asian countries, mainly India and China, over centuries⁵. As a major constituent of the traditional Indian holistic system, Ayurveda, turmeric poultices have been used in treating eye infections and diverse dermatological conditions including skin rashes, infections, bites, burns and acne. In Ayurvedic medicine, curcumin is well-known in treating diverse respiratory ailments including asthma, cough, sinusitis, and allergy. It is also used to treat various liver disorders, rheumatoid arthritis, anorexia, dental diseases, as well as digestive disorders like acid reflux, indigestion and flatulence^{6,7}.

In Chinese herbal medicine, it is used in relieving abdominal pain, while in Hindu traditional medicine; it is used in augmenting sprains, pain and swelling. Throughout East Asia, it is used to alleviate a wide array of inflammatory conditions⁸.

The most powerful and key reason for the continuous usage of curcumin in traditional folk remedies is its highly desirable safety profile. To date, no studies either in vivo or in vitro have revealed any curcumin-associated toxicity even at high doses³.

2. Pharmacological properties

Globally, the scientific community is showing great emphasis on the use of natural traditional medicines, which possess tested pharmacological properties, in Western medicine. Surprisingly, extensive research has showed that curcumin possesses a wide array of pharmacological benefits such as being an anti-inflammatory, antioxidant, antitumor and chemopreventive agent. Such findings have been revealed in both in vitro and in vivo models, and have created an explosive growth of interest in curcumin that paved the way for progressing toward human clinical trials⁶.

Currently, curcumin is being a well-known plant-based drug in treating many chronic diseases including cardiovascular, pulmonary, hepatic, kidney, and skin diseases, as well as gut inflammation, rheumatoid arthritis, premenstrual syndrome, and depression⁹. Such abilities are due to the well-recognized biological activities which involve anti-inflammatory, antioxidant, anti-proliferative, anti-angiogenic, pro-apoptotic, anti-tumor, anti-thrombotic, anti-viral, and anti-bacterial effects¹⁰. In addition, curcumin has showed beneficial effects in ocular diseases such as corneal disorders, eye dryness, conjunctivitis, uveitis, pterygium, cataracts, and glaucoma¹¹.

a. Anti-diabetic and hypolipidemic effects

Many clinical trials have examined curcumin's beneficial effects against various chronic human diseases such as obesity, metabolic syndromes and diabetes. The anti-diabetic and hypolipidemic activities of curcumin were widely investigated in the literature¹². For example, clinical trials that studied the effect of curcumin supplementation on diabetes and diabetic cardiomyopathy (DCM) presented that curcumin acts on specific mechanisms that mitigate diabetes and DCM¹³.

Regarding its hypolipidemic effects, curcumin was shown to result in reducing the total cholesterol and low-density lipoprotein (LDL) levels in patients with acute coronary syndrome. It also effectively caused significant reductions in platelet aggregation and hyperlipidemia and promoted cardiac repair¹⁴. A meta-analysis of randomized controlled trials reported that turmeric and curcumin supplementation protected patients who are at risk of cardiovascular diseases through enhancing their serum lipid profiles¹⁵.

b. Anti-inflammatory and antioxidant activities

Curcumin has been well-documented for its potential activities in suppressing acute and chronic inflammation. Several in vitro studies have reported that curcumin inhibits the activities of major pro-inflammatory enzymes: lipooxygenase (LOX) and cyclooxygenase (COX) in phorbolmyristate acetate (PMA)-induced inflammation in mouse fibroblast cells, and the production of nitricoxide in RAW264.7 macrophages¹⁶⁻¹⁸.

Similarly, in vivo studies have illustrated the inhibitory bioactivities of curcumin against inflammation. For instance, it inhibited carrageenan-induced

inflammation¹⁹ and cyclophosphamide-induced acute lung injury in rats²⁰. In addition, curcumin has been shown to exhibit anti-inflammatory responses that are as effective as cortisone or phenylbutazone. Moreover, curcumin administration to rats with Freund's adjuvant-induced arthritis, showed significant reduction in the inflammatory swelling^{21,22}. The evaluation of turmeric extracts and curcumin in the treatment of arthritis symptoms provided scientific evidence that highlights their efficacy in alleviating the symptoms associated with arthritis²³. Curcumin has been shown to possess anti-inflammatory properties through its ability to regulate NF-kB pathway that plays a significant role in various diseases such as multiple sclerosis, rheumatoid arthritis, ulcerative colitis, Crohn's disease, autoimmune and auto-inflammatory diseases, and cancer. Curcumin has been greatly reported to downregulate the transcription factor NF-kB and thus prevents many diseases pathology²⁴.

Regarding its antioxidant activity, curcumin exhibits potent antioxidant properties when compared to vitamins C and E²⁵. Physiologically, oxidative stress caused by reactive oxygen species (ROS), plays a key role in the pathogenesis of many ailments such as myocardial/cerebral ischemia, neurodegenerative diseases, aging, and cancer. On the other hand, antioxidants act as a defense mechanism against oxidative stress and thus provide protection against many diseases. Among these antioxidants, curcumin has been well-valued for its scavenging activities of many ROS such as superoxide anion radicals, hydroxyl radicals and nitrogen dioxide radicals^{17, 19}.

Due to its neuroprotective activities, evidence suggests that the dietary supplementation of curcumin can be beneficial in Alzheimer's disease²⁵⁻²⁸. In a rat model of cerebral ischemia, curcumin showed high level of neuroprotection as it inhibited lipid peroxidation and ROS generation, and enhanced the body's antioxidant

defense mechanisms^{5,30}. Furthermore, Curcumin is endowed by numerous protective functionalities against oxidative associated liver diseases. It exerts notable protective and therapeutic activities that ameliorate cellular responses to oxidative stress, scavenge free radicals via its phenol, β -diketone and methoxy groups³¹.

c. Antitumor and chemoprotective effects

A vast array of animal and cell culture studies have revealed the potency of curcumin in preventing carcinogenesis at different stages: promotion, growth, angiogenesis, and metastasis (see **Figure 2**). Curcumin has been widely valued for its ability to suppress the tumorigenesis of many carcinogens in the colon, duodenum, esophagus, head and neck, stomach, liver, breast, prostate, and leukemia³².

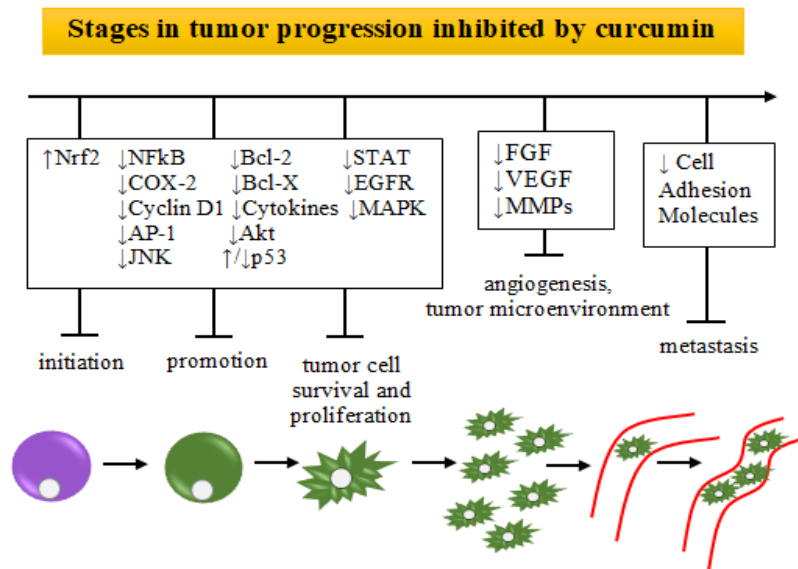


Figure 2. Stages in tumor progression inhibited by curcumin.

Curcumin has been shown to possess anti-tumor activities through affecting several biological pathways that play roles in mutagenesis, cell proliferation, tumor

progression, angiogenesis and metastasis³³. It inhibits the expression of a variety of growth factors and oncogenes while it activates many tumor suppressor genes.

Curcumin has been found to be a potential candidate that exerts selective toxicity and therapeutic activities against head and neck cancer – the sixth most common cancer worldwide³⁴.

In animal models, numerous studies have evaluated curcumin's efficacy against various cancers. In mice, curcumin inhibited 7,12-dimethylbenz[a]anthracene and 12-O-tetradecanoylphorbol-13-acetate-induced skin cancer³⁵. Besides, it has shown potent suppressive activities against mammary tumors³⁶. Other studies have shown the antitumor effects of curcumin in Wistar rats with hepatic cancer mainly through preventing the decrease of hepatic antioxidant defense mechanisms and suppressing lipid peroxidation^{37,38}. Moreover, curcumin has been reported to exert chemopreventive effects against the N-methyl-N-nitro-N-nitrosoguanidine-induced stomach carcinogenesis; this effect was mediated through the suppression of *Helicobacter pylori* which is implicated in stomach cancers³⁹. Furthermore, other studies have shown that curcumin can induce apoptosis and suppress angiogenesis in head and neck cancer, prostate cancer, and pancreatic cancer in rodent models of carcinogenesis³⁴.

In vitro studies have shown that curcumin inhibits the proliferation of an extremely wide set of cancer cell types. This set includes cell lines from bladder, breast, lung, pancreatic, prostate, ovarian, cervical, head and neck, brain, and kidney cancers⁴⁰. Besides, in androgen-dependent and independent prostate cancer cell lines, curcumin has been shown to suppress tumor proliferation, and to induce apoptosis and cell cycle arrest at G2/M phase. In addition, the application of curcumin to human gastric cancer MGC-803 cell line resulted in significant suppression of cell proliferation accompanied

by cell cycle arrest and apoptosis. Mechanistically, such potent antitumor activities of curcumin are achieved through its blockage of ROS production and oncogenic pathways, and activation of apoptotic and tumor suppressor pathways^{41,42}.

d. Curcumin against colorectal cancer

Globally, colorectal cancer (CRC) is the third common cancer⁴³. Since several epidemiological studies attributed the low incidence rates of CRC in India to the antitumor and antioxidant properties of curcumin-enriched diets, curcumin received a great attention from researchers all over the world. Due to being more bioavailable in the gastrointestinal tract than other organs, curcumin became a well-documented molecule that potentially treats many functional and organic gastrointestinal diseases including inflammatory bowel diseases, colorectal cancer and hepatic fibrosis⁴⁴.

i. *In vitro*

Curcumin has been widely proven as a potent therapeutic agent against various colorectal cancer cell lines. Such antitumor activities are mechanistically due to the ability of curcumin to interact with various target molecules that play key roles in colorectal carcinogenesis. For instance, curcumin has been reported to induce cell cycle arrest at the S and G2/M phases in LoVo cells (colon adenocarcinoma cell line). Also, curcumin has been shown to downregulate the driver pathway of colorectal carcinogenesis – the Wnt signaling, leading to reduced cell proliferation in HCT-116 cells. Besides suppressing the Wnt signaling pathway, curcumin induces apoptosis through activating the Fas signaling and reducing the formation of DNA adducts in different human colorectal cell lines. During the apoptotic process that is induced by

curcumin, cell shrinkage, chromatin condensation and DNA fragmentation in colorectal cancer cells such as HT-29 and HCT-116 cells, occur⁴⁵.

Moreover, several studies have shown that curcumin, alone or combined to chemotherapeutic drugs such as 5-Fluorouracil or celecoxib, downmodulates COX-2 expression and thus inhibit prostaglandin synthesis in colorectal cancer cell lines. In cancer cells, COX-2 promotes tumor development, inhibits apoptosis and facilitates metastasis; therefore, it has emerged as a novel target for studying the chemopreventive efficacy of many agents⁴⁶.

ii. *In vivo*

Several in vivo studies have proven the chemopreventive and antitumor efficacy of curcumin against colorectal cancer. Wargovich *et al.* showed that curcumin is a powerful chemopreventive agent against azoxymethane (AOM) induced aberrant crypt foci (ACF) in the colon of F344 rat model⁴⁸. Similarly, curcumin showed antitumor activities during promotion and progression stages of CRC in different carcinogen-induced colonic tumors in rats^{49,50}. Away from chemically induced CRC models, other studies investigated the chemopreventive ability of curcumin in C57BL/6J-Min/+ (Min/+) mice that possess a germline mutation in the Apc tumor suppressor gene and spontaneously develop many colorectal adenomas. The results obtained in these studies showed that curcumin induces apoptosis, inhibits COX-2 expression and reduces cell proliferation^{51,52}.

iii. Main activities and targets of curcumin

The molecular basis of the above-mentioned anti-tumor and chemopreventive bioactivities of curcumin are imputed to its activities on various target molecules and regulators that play roles in transcription, growth and angiogenesis, adhesion, apoptosis, and cellular signaling⁴⁵. **Table 1** summarizes the general activity and mechanisms involved in the tumor preventive activity of curcumin.

Table 1. Summary of main activities of curcumin.

General Activity
*Chemosensitizing activity of curcumin *Radiosensitization and radioprotection *Chemopreventive, chemotherapeutic *Inhibition of angiogenesis and metastasis *Immunologic modulation
Mechanism
*Inhibition of NF- κ B *Downstream of NF-KB: Inhibition of cyclin D1 *Downstream of NF-KB: Inhibition of COX-2 *Downstream of NF-KB: Inhibition of Bcl-2 and Bcl-XL *Inhibition of cytokines inhibits the pro-survival kinase Akt *Effects of curcumin on tumor suppressor p53 *Induction of Phase II enzymes *Modulation of growth factors and their signaling pathways *Inhibition of STAT3 activation by curcumin *Effect of curcumin on mitogen-activated protein kinases

iv. Clinical trials

Research has gone further where the pharmacodynamic and pharmacokinetic effects of oral curcumin uptake in patients with CRC were assessed. In a study involving fifteen patients with advanced CRC refractory to conventional chemotherapy, their uptake of curcumin on daily basis over 4 months revealed no toxicity accompanied with dose dependent inhibition of COX-2 activity. Accordingly, these findings implicated the efficacy of curcumin in the management of advanced colorectal cancer⁵³. Another study, in patients with advanced CRC, reported that a daily consumption of 3 g curcumin causes around 55 to 60 % reductions in inducible prostaglandin production in different blood samples taken on the first and 29th day, respectively⁴⁷.

Moreover, a pilot trial, including twelve patients with hepatic metastases from CRC who received 450–3600 mg of curcumin daily over 1 week before undergoing surgery, showed that curcumin was found to be sufficiently concentrated in the hepatic tissue to trigger a pharmacological activity. Also, it is deduced that a daily dose of 3.6 grams of curcumin is safe and pharmacologically efficient to reach the colorectal tissues and exert antioxidative changes commensurate with long-term chemopreventive benefits⁵⁴. Furthermore, a case report by Braumann *et al.* showed that combining oxaliplatin, 5-Fluorouracil and leucovorin, to a 5 g daily dose of curcumin, administered to an old woman (age: 75 years) with advanced CRC metastasized to the liver over 5 months, led to partial remission with no side effects⁵⁵. Another recent study showed that capsulated curcumin administration (360 mg/3 days per week; over 1 month) to CRC patients after their diagnosis and prior to surgery, decreased serum tumor necrosis factor alpha (TNF- α) levels, increased apoptotic cells, and enhanced p53 expression in tumor tissue⁵⁶.

3. Structural and chemical properties

Curcumin is a diaryl heptanoid composed of two aromatic rings linked by a chain of seven carbons. Curcumin's chemical name is 1,7-bis(4-hydroxy-3-methoxyphenyl)-1,6-heptadiene-3,5-dione⁵⁷. It has several functionally active groups: two o-methoxy phenolic groups, two enone moieties and a keto-enol moiety (see **Figure 3**). Its molecular formula is C₂₁H₂₀O₆, and it has a molecular weight of 368.38 Daltons. It is a lipophilic polyphenol that is insoluble in water but soluble in organic solvents such as ethanol and acetone. It is also insoluble at acidic and neutral pH but highly soluble at alkali or extremely acidic medium^{58,59}.

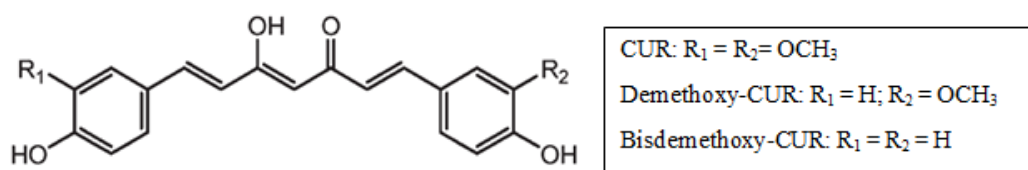


Figure 3. Chemical structures of the three major natural curcuminoids.

Curcumin is a bis- α,β -unsaturated β -diketone where its structure shows a ketoenol tautomerism and a cis-trans isomerism that depend on the solution's acidic state⁶⁰. At acidic and neutral pH as well as in the cells, the dominant form is the keto-form. At such pHs, curcumin potentially donates H-atom because its keto-form contains a highly active Carbon atom in its heptadienone linkage between the two methoxyphenol rings. This carbon has very weak C–H bonds since the unpaired electrons on the adjacent oxygens are delocalized as shown in **Figure 4**. On the other hand, at alkali pH the enol-form predominates where curcumin donates electrons in a

mechanism that reflects its antioxidant scavenging activities. The resonance-assisted hydrogen bonding in the enol-form of curcumin stabilizes its structure^{61,62}.

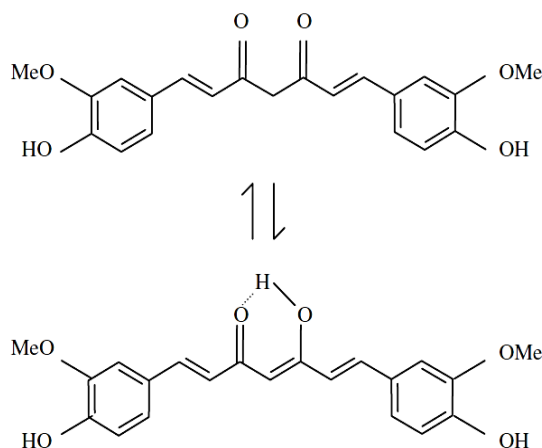


Figure 4. Tautomerism of curcumin under different physiological states. In acidic and neutral media, the bis-keto form (top) dominates, while the enol-form exists at pH > 8.

The anti-inflammatory and antioxidant properties of curcumin are attributed to the presence of enolic center and two phenolic groups separated by a hydrophobic bridge. These hydrophobic and hydrophilic features facilitate the penetration of curcumin into the blood-brain barrier which have been proven by density functional and Møller-Plesset perturbation (MP2) computations. More importantly, the enolic form was shown to be the most favored form with the ideal antioxidant properties including its binding ability to human proteins such as amyloid β that is involved in Alzheimer's disease⁶³.

4. Photophysical properties of curcumin

Curcumin has been shown to possess anti-oxidant properties that are contributed to its potent H-atom donating ability. Several studies have revealed that curcumin, in its enolic form, undergoes Excited State Intramolecular Hydrogen Transfer (ESIHT) that in turn plays crucial roles in the antioxidant bioactivities of curcumin. ESIHT is a state occurring in molecules with a hydrogen donor group such as: OH and NH₂ as well as a hydrogen acceptor group such as: N and carbonyl. Besides, the ground state of these groups is connected through an intramolecular hydrogen bonding, and their exposure to light induces ESIHT. In this case, the hydrogen atom that is covalently linked to hydroxyl oxygen (in the ground state) undergoes migration to the carbonyl oxygen in the (excited state)^{64,65}.

ESIHT has aroused remarkable interests in the in-depth understanding of several biochemical intrinsic mechanisms. The unimolecular basis of ESIHT allows for its use as a model that represents catalytic reactivity and explains medicinal bioactivities⁶⁶. Several computational studies explained the ESIHT of conjugated curcumin and showed that in the large conjugated systems, low reaction barrier in the ground state but high barrier in the excited state are exhibited⁶⁷.

ESIHT is one of the kinetic processes that affect the molecular environment of a fluorophore. Time resolved fluorescence measurements such as fluorescence spectroscopy has been widely used in studying of the structure and dynamics of many fluorophores including curcumin⁶⁸. Several Synchronous fluorescence spectroscopic studies by Patra *et al.* assessed the absorption and fluorescence spectra of curcumin using in thirteen different solvents^{68,69}. These methods were shown to be sensitive, simple, easy and fast in investigating solvent/solute interactions as well as

general/specific solvent effects⁶⁹. Moreover, fluorescence temperature sensing has been used to assess the impact of pH on curcumin where results showed that in acidic, neutral and slightly alkaline media curcumin underwent ESHT emitted from enol form⁷⁰. Material research is focusing on the photoluminescence and fluorescence spectroscopic methods to achieve favorable physicochemical behaviors that can be applied for imaging and sensing purposes⁷¹.

5. *Stability of curcumin*

a. Aqueous stability

In aqueous media, curcumin's stability is pH-dependent, and this stability is commonly proven by the color change of curcumin at different pH values. For example, at very low pH (<1), the color of curcumin in solution is red due to the predomination of its protonated form. At a pH range from 1 to 7, curcumin exhibits a yellow color where its molecules being in their neutral form. At pH values > 7.5, curcumin becomes orange in color. Moreover, according to the used buffer system, curcumin tends to do complexes with borate, citrate, and phthalate; however, it is inert with potassium chloride (KCl), potassium dihydrogen phosphate (KH₂PO₄), and sodium bicarbonate (NaHCO₃)^{58, 72}.

Kinetic degradation of curcumin was studied under different buffer systems at different pH values. Results showed that at neutral pH, curcumin appears to be unstable where it hydrolyzes into smaller products. In phosphate buffer of pH 7.4, it has been proposed that curcumin undergoes degradation within 30 minutes. As pH increases, the rate of curcumin's degradation increases as well. The three most important degradation products of curcumin are: vanillin, ferulic acid (FA) and ferulic aldehyde (see **Figure**

5). Of these, vanillin was the major product. In other biological buffers such as 0.1 M phosphate buffer or serum-free medium of neutral pH, curcumin undergoes rapid degradation over a period of 3 hours. Similarly, the degradation products were vanillin, FA, and feruloylmethane (see **Figure 5**)⁷³.

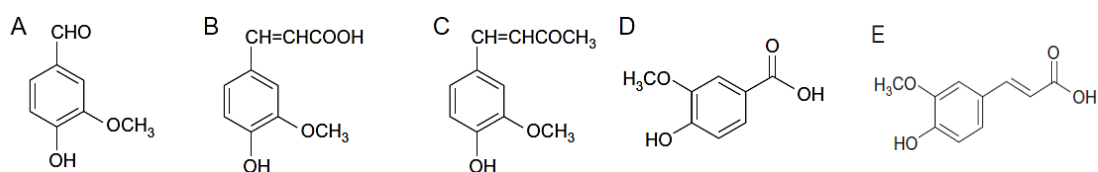


Figure 5. Curcumin's degradation products. (A) vanillin, (B) ferulic acid, (C) feruloylmethane, (D) vanillic acid, and (E) ferulic aldehyde.

In addition, in phosphate buffered saline of neutral pH, upon adding human serum albumin, the rate of curcumin's degradation was significantly slowed down. Similar to albumin, in the presence of surfactants, cell culture media and biological fluids, curcumin's degradation is inhibited. For example, in human blood, the rate of curcumin's degradation is relatively very slow; only 20% of curcumin is degraded within 1 hour^{57,58}.

b. Spectral and photophysical stability

Due to its relatively low solubility in aqueous media, several studies have focused on curcumin's stability in other organic solvents. Curcumin possesses optical absorption at 408-430 nm, in different solvent; while at its excited state, the emission

maximum ranges from 460 to 560 nm. Many studies revealed that as the pH of the solution becomes more acidic, the rate of curcumin's fluorescence-decay increases. Similarly, this rate increases in more polar solvents. For example, the fluorescence-decay spectra of curcumin and its products was found to be much higher in methanol than that in hexane⁷⁴. Time-dependent density functional theory (TD-DFT) is one of the major methods used to provide reliable absorption spectra of curcumin^{75,76}.

Moreover, a study by Chignell *et al.* showed that curcumin strongly fluoresces in toluene⁷⁷. Curcumin's absorption spectra, that has been drawn-out in various solvents, is presented in **Figure 6**. In each solvent, a strong intense absorption band is observed between wavelengths of 300 and 500 nm. A large shift of the absorption maxima is clear in solvents of high polarity. It was also shown that the intensity of curcumin's fluorescence was highly sensitive to the solvent's nature. As shown in **Figure 6B**, the fluorescence spectra of curcumin in different solvents. The maximum of the fluorescence spectra (at 560 nm) was observed in methanol, which acts as hydrogen bond-donating and accepting solvent. The fluorescence spectral width of curcumin increases with high polarity as well as hydrogen bond-donating or accepting potential of the solvent^{64, 77}.

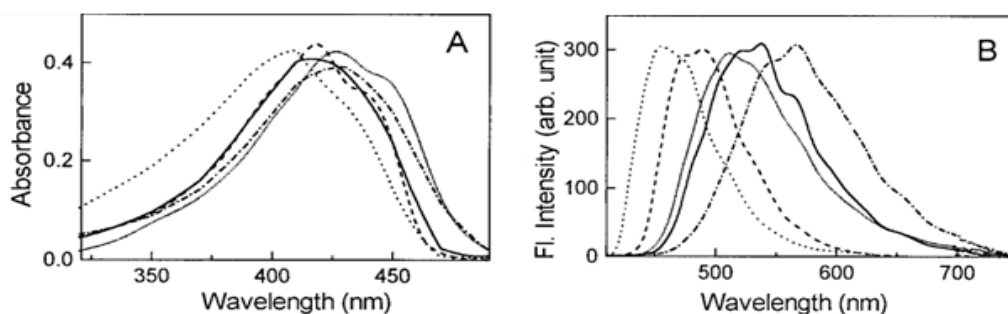


Figure 6. (A) Ground-state absorption spectra and (B) Normalized fluorescence spectra of curcumin in cyclohexane (· · · · ·), benzene (---), acetonitrile (—), methanol (· - · -) and TX-100 (·····) due to excitation at 355 nm.

c. Photochemical stability

An in-depth study has reported the photodegradation products of curcumin in isopropanol medium. Upon dissolving curcumin in isopropanol and exposing it to light (λ 400–510 nm) over four hours, the degradation products were determined through TLC, mass spectrometry (MS) and nuclear magnetic resonance (NMR). The main degradation product of curcumin was identified as: $C_{12}H_{18}O_6$. This product was also characterized by a mass spectrum exhibiting a molecular ion at m/e 4366, which indicates the removal of two hydrogen atoms from the structure. Moreover, this product was suggested to be resulted from a cyclization process induced by light irradiation and detected within 15 minutes of irradiation. Furthermore, other minor degradation products of curcumin were identified as vanillin, vanillic acid (VA), FA, and vinylguaiacol⁷⁸.

Another study showed that curcumin's exposure to methanolic or ethanolic solutions, over a long period of 5 days in the presence of sunlight, caused its degradation. Such degradation resulted in many products including vanillin, hydroxybenzaldehyde, ferulic aldehyde, hydroxybenzoic acid, VA, and FA. Also, it has

been revealed that the dried form of curcumin was relatively more stable against the exposure of sunlight exposure, than in suspended form ⁷⁹.

Several studies tackled examining the stability of curcumin against light of different wavelengths in various solvents: methanol, chloroform, ethyl acetate, and acetonitrile. The light wavelengths ranged from 400 to 750 nm and from 240 to 600 nm. In these media, the photodegradation of curcumin followed the first-order kinetics. Curcumin's half-life in these solutions followed this series of stability: "methanol>ethyl acetate>chloroform>acetonitrile". On the other hand, upon drying curcumin's solution in each tested solvent, curcumin's half-life apparently followed the second-order kinetics. the stability series being with this order: "acetonitrile>chloroform>ethyl acetate>methanol". Additionally, it was highly recommended to use brown glass for storing curcumin as it transmits light of wavelengths only above 500 nm. At such wavelengths, curcumin has no absorption ^{57, 73}.

d. Thermal stability

Regarding its thermal stability, curcumin has been shown to be stable up to 70°C for 10 minutes. Above 70°C, curcumin begins degrading, and at 100°C, its rate of decomposition increases as its absorbance decreases. Besides, curcumin's boiling for 15-20 min led to the partial loss of curcumin by 27% and 32%, respectively. It has been also shown that turmeric processing in a pressure cooker for 10 min at 15 psi, caused the loss of 53% of curcumin ⁵⁷.

6. *Bioavailability problems*

Several clinical studies reported the safety of curcumin consumption, but unfortunately it has low bioavailability that limits its therapeutic efficacy. During its rapid metabolism, curcumin is highly conjugated through glucuronidation and sulfation which make it poorly absorbed, and thus its free levels in plasma and tissues become very low⁷⁹. Many studies, in animals and humans, have shown that curcumin possesses several bioavailability problems such as: low levels in serum, limited distribution to tissues, excessive metabolism in the liver and intestine as well as short half-life. A dose of 3.6g of curcumin per day showed to release only 11.1 ng/mL into the blood⁸⁰. Such bioavailability problems limit both the concentrations of curcumin in the gastrointestinal tract and the bioactivities including its antitumor potential⁸¹.

7. *Recent advances*

Various strategies have been devised to overcome the low bioavailability of curcumin. These promising strategies include the following curcumin formulations: adjuvants, nanoparticles, liposome, micelle and phospholipid complexes, metal complexes, and derivatives and analogues⁸².

a. Adjuvants

Curcumin's complexation with piperine (see **Figure 7**), an inhibitor of glucuronidation, was administered to rats and humans aiming to increase the bioavailability of curcumin. Unfortunately, piperine was found to be toxic in animals and the levels of curcumin in plasma increased for a short time. However, studies in humans showed that piperine combination to curcumin increases curcumin's

bioavailability. The presence of piperine doubled curcumin's absorption and elevated its tissue-uptake². Similarly, combining well-documented antitumor bioactive compounds such as: quercetin, EGCG (epigallocatechin-3-gallate), and genistein to curcumin enhanced curcumin's bioavailability and uptake in tissues⁸³.

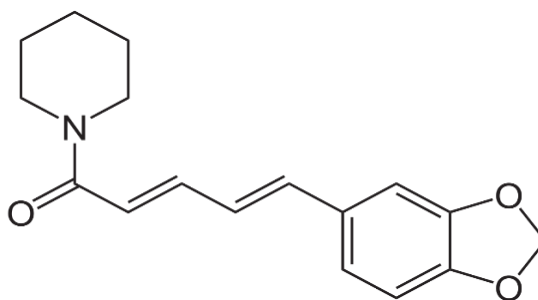


Figure 7. Structural formula of piperine.

b. Nanoparticles

Lately, the application of nanotechnology to targeted systems of drug delivery became one of the notable solutions to many bioavailability problems of therapeutics. It is especially appropriate for hydrophobic agents with poor aqueous solubility such as curcumin. Over the recent years, many forms of curcumin nanoparticles have been studied. Some examples include poly(butylcyanoacrylate) (PBCA) nanoparticles, poly(lactide-co-glycolide) (PLGA) nanoparticles, chitosan (CS) nanoparticles, albumin nanoparticles, and solid lipid nanoparticles (SLN)^{2,84}. Advances in nanotechnology-based delivery systems for curcumin are more discussed in **part B.5**.

c. Liposomes, micelles and phospholipid complexes

Liposomes are outstanding drug delivery systems. They deliver hydrophilic and hydrophobic agents. Liposomal curcumin has been shown to exert antitumor

activities against human pancreatic carcinoma cells and colorectal cancer (Colo205) cells. Its antitumor activities included growth-inhibitory, apoptotic and antiangiogenic effects⁸⁵. Other *in vivo* studies have reported a higher bioavailability of liposomal curcumin over free curcumin. Moreover, micelles and phospholipid complexes enhance the absorption of many drugs by the gastrointestinal tract as well as their plasma levels. In rats, the intestinal absorption of micellar curcumin formulation with phospholipid increased, and thus enhanced the bioavailability of curcumin. The half-life of curcumin increased upon its formulation with polymeric micelles⁸⁶. Another study revealed a 3-fold increase in the aqueous solubility of curcumin when complexed with phospholipid; it exerted greater hepatoprotective effects compared to free curcumin⁸⁷.

d. Metal complexes

Zinc (II) curcumin complexes were shown to have higher stability and antitumor activity against in prostate cancer and neuroblastoma cell lines. Similar observations were reported for the use of (arene)ruthenium (II) curcumin complexes against several cell lines. Other studies showed that cobalt (III) and copper complexes of curcumin enhanced its cellular delivery to tumor cells and showed better antitumor effects than the parent compound. Moreover, curcumin manganese complexes exerted more potent neuroprotective activities than curcumin *in vitro* and *in vivo*⁸⁸.

e. Derivatives and analogues

The chemical structure of curcumin and its isomerization have greatly influenced its antioxidant and antitumor activities. Thus, researchers focused on dealing with structural modifications such as using derivatives and analogues, to enhance

curcumin's bioavailability and biological effects. A curcumin analogue nominated EF-24 was shown to display higher antitumor activities than curcumin. Besides, different curcumin formulations from curcumin derivatives (bisdemethoxycurcumin, demethoxycurcumin and tetrahydrocurcumin) showed increased oral absorption and enhanced solubility^{80, 89}.

B. Nanotechnology

1. Nature & uses

Nanotechnology is commonly defined as a technology that involves structures in the nanometer scale, referred to as “nanoparticles”⁹⁰. Nanoparticles are promising drug carriers due to their small size (between 10 and 1000 nm diameter), custom-made surface, enhanced solubility, and multi-functional characteristics⁹¹. In addition, nanoparticles allow the transportation, protection, at the site localization, and targeted-tissue distribution of many drugs. Indeed, these modern characteristics of nanoparticles provide insights into enhanced drug loading and delivery, and thus treat various devastating diseases including cancer, as well as neurovascular and neurodegenerative diseases^{92,93}.

According to the US National Institute of Health, applying nanotechnology in treating, diagnosing, monitoring, and controlling diseases has lately been known as “nanomedicine”⁹⁴. Nanosystems of variable compositions have novel physical and biological characteristics that allow their use in ways that overcome the previous limitations of conventional drug delivery ways^{90,95}.

Cancer is a major “killer” in modern societies, and its conventional treatment methods, including surgery, radiotherapy, and chemotherapy, have many serious side

effects on healthy tissues, low cure and high recurrence rates. In this context, nanomedicine aims to design therapeutic modalities with higher safety, effectiveness and lower side effects⁹⁶. A major advantage of nanosystems is their ability to improve the preferential accumulation of antitumor therapeutics in cancer cells. In the field of cancer therapy, nanobiotechnology progressed rapidly with promising achievements⁹⁶⁻⁹⁸.

2. Different types of nanoparticles

a. Inorganic nanoparticles

Inorganic nanoparticles are commonly made up of silica and alumina. The nanoparticle core may also involve metals, metal oxides and sulfides. In general, inorganic nanoparticles may be designed with variable sizes, pores and surface compositions that allow them to escape the immune system attacks⁹³. Examples of silica nanoparticles involve calcium phosphate-based nanoshells that have a porous surface leading to the entrapped molecular payload. Other types include mesoporous silica-based nanoparticles which have been proven to potentially deliver different drugs such as ibuprofen and some neurotransmitters⁹⁹. Overall, inorganic nanoparticles are characterized by their easily modifiable surfaces that can undergo various chemical transformations leading to unique activities. Moreover, they have stability over a broad range of temperatures and pHs; however, their long-term administration lacks safety as they evade biodegradable processes and have slow dissolution¹⁰⁰.

b. Solid lipid nanoparticles

Solid lipid nanoparticles have a solid lipid matrix that solubilizes lipophilic molecules and have been designed as more stable alternatives than liposomes. Their stability in the biological system is attributed to the rigid core made up of solid lipids – at body and room temperature – encapsulated with a phospholipid monolayer. These lipid core constituents are also stabilized by a high level of surfactants/emulsifiers¹⁰¹. Due to their easy biodegradation, solid lipid nanoparticles are considered as the safest nanoparticles compared to the polymer and ceramic-based ones. They have been widely used in delivering oral, topical and inhaled drugs⁹³.

c. Liposomes

Liposomes are spherical bilayered vesicles with a phospholipid membrane that provides them with amphiphilic characteristics¹⁰². They are also characterized by an easily modifiable surface and high biocompatibility which in turn increase the circulatory half-life of many biomolecules. They may also encapsulate a hydrophilic compound in an aqueous core, as well as a hydrophobic compound, associated with the phospholipid membrane⁸⁷. Liposomes are formulated to either adhere to cell membranes and deliver drugs payload or deliver their load after being endocytosed. Although liposomes received a substantial amount of investigations, they have not shown a significant therapeutic impact due to their limited stability^{87,93}.

d. Nanocrystals

Nanocrystals are molecules aggregated into a single or poly-crystalline drug form. They are surrounded by a layer of surfactant for solubilization. These

nanosystems have been extensively applied in chemical and biological research as quantum dots⁹⁰. Nanocrystals are mainly formulated from lipophilic compounds while their coating is of hydrophilic nature. This hydrophilic coating enhances the bioavailability of drugs and avoids the formation of aggregated nanocrystals which in turn boosts the delivery of the drug material¹⁰¹. An advantage of these nanocrystals is their ability to deliver high doses of drugs especially those of low solubility where the coating layer can improve their distribution. On the other hand, the formulation methods of nanocrystals involve only therapeutic agents that can be crystallized¹⁰³.

e. Quantum dots

Quantum Dots are semiconductor nanocrystals. They mainly consist of a semiconducting inorganic core and an outer aqueous organic-coated shell ready for conjugation. The core can be also made to fluoresce in the presence of light, and the conjugation of quantum dots can be customized based on the targeted biomolecules. They also consist of a cap that provides them with a high solubility in aqueous media⁹⁰. These systems have been widely applied as sensitive probes to track and monitor various intracellular processes, which help in the diagnosis and treatment of many diseases. Their therapeutic applications include gene therapy, cancer treatments through targeted delivery of drugs, DNA hybridization, and cell labeling¹⁰⁴.

f. Carbon nanotubes and fullerenes

A nanotube is a tubular structure made up of hexagonal carbon-based networks (1-100 nm length). These networks have the arrangement of graphite sheets that are rolled up into a cylindrical configuration^{90,93}. Common configurations of carbon

nanotubes are the single-walled nanotubes (SWNTs), multiple-walled nanotubes (MWNTs) and C60 fullerenes. Due to their attractive size, geometrical and surface properties, carbon nanotubes are remarkable drug carriers. SWNT and C60 fullerenes are of 1 to 2 nm diameter while MWNT have up to ten nm diameter. Carbon nanotubes and fullerenes have shown a great potential in tissue-specific deliver of drugs either through endocytosis or direct membrane insertion. Several experiments showed that fullerenes exert antioxidant and antitumor activities¹⁰⁵.

g. Dendrimers

Dendrimers are highly branched tree-like nanoparticles. They are designed from monomers, and their branching size depends on a controlled number of branchings. Through polymerization, many branches extend from the core resulting in a sphere with many cavities to entrap the therapeutic molecules. The free ends of the branches may conjugate or attach to other molecules depending on their way of customization¹⁰⁶. Dendrimers are promising drug carriers as they are characterized by easily functionalized surface, stability, biocompatibility, and easy incorporation methods of drugs of interest. These nanosystems have been applied in chemotherapy, gene therapy and transfer and as contrast agents for imaging. Disadvantages include toxicity profile where some cationic dendrimers were shown to cause cell lysis and membrane instability¹⁰⁷.

h. Polymeric nanoparticles and nanocapsules

The degradable and biologically compatible characteristics of polymeric nanoparticles make them the most preferred method for drug delivery. These colloidal

carrier systems have a modifiable surface that can undergo many biochemical transformations. Hence, they are excellent regarding their controllable pharmacokinetics and their ability to entrap and deliver a vast array of therapeutic drugs^{108,109}. Commonly used polymeric nanoparticles involve those created from gelatin, chitosan, poly (L-glycolide) [PLG], poly(D,L lactide), poly (lactic acid) [PLA], poly(lactide-co-glycolide) [PLGA], and poly-cyanoacrylate [PCA]¹¹⁰. In addition, the distribution of nanoparticles can be enhanced through functionalizing different polymer coatings. For instance, the covalent linkage of the polymer polyethylene glycol (PEG) onto the surface of nanoparticles has been found to decrease immune responses especially phagocytosis of nanoparticles thus increasing the availability of drugs in tissues¹⁰¹.

The US Food and Drug Administration (FDA) has recently approved the usage of polymer-based nanoparticles in humans. They have been designed to encapsulate different therapeutic drugs, and it has been proven that their application in gene therapy against breast cancer cells resulted in antiproliferative effects. Indeed, the biocompatibility and biodegradation properties of polymer-based nanoparticles are interesting especially with formulations that necessitate appropriate dosing, in contrast to inorganic nanoparticles¹¹¹.

Nanocapsules are polymeric nanoparticles comprising a thin polymeric outer protective wall of a surfactant or a phospholipid, and an inner oily core. They are hollow structures and their size ranges from 10 to 1000 nm. Their well-defined shell and core distinguish them from other nanosystems. Polymeric nanocapsules are colloidal drug delivery systems that have acquired great attention within the past three decades since they enhance the potency of therapeutic drugs and decrease the risk of side effects¹¹². Such systems have proven an increased efficiency of their loaded bioactive

substances compared to their free form. The basis of using colloidal nanocapsules involve: efficient drug encapsulation, targeted drug delivery to specific body organ or tissue and controlled drug release at these sites¹¹³.

Moreover, polymer-based drug delivery systems display the following benefits¹¹⁴:

- ability to incorporate poorly-water soluble molecules
- control of drug accumulation in different organs and tissues depending on particle size
- substantial decrease in the amount of drug needed to trigger treatment

3. Different types of curcumin nanoparticles

Over the past decade, a great progress has been shown in the use of curcumin drug delivery nanosystems especially in the form of curcumin liposomes, nanocapsules, microemulsions, cyclodextrin inclusions, solid dispersions, and nanotubes^{82,115,116}.

Curcumin polymeric nanoparticles that are made up of butylcyanoacrylate, a common medical cyanoacrylate glue used clinically, showed a great potential in treating b-amyloid-induced cytotoxicity in Alzheimer's disease⁸⁴. Another study by Mars *et al.* showed that curcumin-graphene quantum dots were promising effects against Apolipoprotein E (ApoE) that plays major roles in Alzheimer's disease¹¹⁷. Other curcumin-loaded biodegradable polymers include curcumin-chitosan-PNVCL nanoformulations which showed anticancer effects against MCF 7 (human breast cancer cell line), KB (oral cancer cell line), and L929 (mouse fibroblast cell line) cells¹¹⁸.

Moreover, the use of curcumin loaded dextran sulphate–chitosan nanoparticles showed

preferential apoptotic effects of curcumin against cancer cells without targeting normal cells¹¹⁹.

A study by Gangwar *et al.* showed that curcumin conjugation with silica nanoparticles improved the bioavailability and anticancer properties of curcumin against HeLa and fibroblast cell lines¹²⁰. Curcumin gold nanoparticles showed enhanced targeted drug delivery onto cancer cells resulting in significant cellular uptake, internalization of curcumin and cytotoxic effects compared to free curcumin¹²¹. Solid lipid nanoparticles incorporating curcuminoids were applied in *in vivo* studies for treating inflammatory reactions, especially for radiodermatitis¹²². The application of curcumin nanotechnology-based formulations in cancer prevention and therapy showed promising results against brain, prostate, pancreatic, breast and colorectal cancers^{123,124}. Curcumin nanoparticles led to improved physicochemical properties of curcumin. They effectively enhanced curcumin's antioxidant and antihepatoma activities¹²⁵. Formulations involving the complex conjugation of curcumin with bovine casein micelles (CMs) showed significant cytotoxicity against HeLa cells *in vitro*¹²⁶.

C. Polymeric nanocapsules

Polymeric nanocapsules have been widely used in the medical and pharmaceutical domains where such application requires the used polymers to have some characteristics such as^{127,128}:

- being biocompatible and biodegradable
- being of high molecular weight in order to circulate in blood over a period of time

- containing functional groups (-OH, -NH₂, -CHO, -COOH) that are required for polymer-drug conjugations and surface alterations
- being commercially available, easily designed and cheap
- being easily administered

To formulate a polymeric nanocapsule with the above-mentioned requirements, several properties must be taken into consideration.

1. Properties

The size, surface and drug loading into polymeric nanocapsules are easily customized properties of these systems. Such customizations provide exact defined physical, optical, magnetic and biochemical properties that in turn easily serve specified functions.

a. Particle size

It is a major property of nanocapsules as it reflects how the drug will be distributed *in vivo* as well as its capacity to target the biological system. It is also important to determine the nanocapsule size since it influences the desired capacity, releasing dosage, time relapse if action, and stability of the drug payload¹²⁹. When the particle size is small, high surface area is created which also allows the instant release of drugs. However, when the particle size is large, the core of the nanocapsule is large enough to cause a gradual outward diffusion of the drug¹³⁰. Moreover, particle size plays a crucial role in affecting the degradation of the polymer. For instance, as the particle size of PLGA nanocapsules increased, the rate of its degradation was higher *in vivo*. Some techniques that can be used to assess polymeric nanocapsules include

dynamic light scattering (DLS), X-ray diffraction (XRD), transmission electron microscopy (TEM), and scanning electron microscopy (SEM)¹³¹.

b. Surface properties

Creating an optimum nanocapsule requires manipulating specific surface properties that involve the incorporation of targeting ligands, as well as controlling surface curvature and reactivity¹¹¹. Also, it is crucial to customize the surface properties of nanocapsules in a way that limits their opsonization by the immune system, increases their circulatory period, prevents their aggregation, and ensures their stability and receptor binding^{111,132}. To achieve this, the addition of hydrophilic polymeric coatings or surfactants can be applied. Besides, formulating nanocapsules with biodegradable copolymers of polyethylene glycol (PEG), polyethylene oxide (PEO) or polysaccharides such as chitosan and dextran can increase the therapeutic drug's bioavailability¹³². To characterize the surface charge of nanocapsules, zeta potential can be determined¹⁰⁸.

c. Drug loading and drug release

Although the size and surface properties have been shown to ensure bioavailability, diminish clearance, and enhance stability; however, it would not be significant if this practice cannot release its drug content¹³³. Therefore, it is crucial to study factors that regulate the release of drug from the nanocapsule matrix such as pH, temperature, solubility, desorption of the surface-bound or adsorbed drug, diffusion through the matrix, swelling or erosion of the matrix. Based on the type of nanocapsule, the release of drug differs¹³⁴. Nanocapsules are considered heterogeneous systems that encapsulate a drug inside the reservoir that is made up of the polymer¹¹³. In such

systems, the release of the drug is controlled by how the drug diffuses through the polymeric layer. Thus, drug diffusibility through the polymer is the major factor responsible for its targeted delivery. The presence of ionic interactions between the drug and polymer will cause the formation of complexes that may not allow the release of drug from its capsule. To avoid such complexes, supplementary agents such as PEO may be added to allow for better release of drug to target tissues. Similarly, various water-soluble carriers were studied in order to enhance the dissolution of poorly soluble drugs, for example, the release of rofecoxib was enhanced with the use of diverse carriers such as PEG, polyglycolized fatty acid ester, polyvinylpyrrolidone K25 (PVP), mannitol, sorbitol, citric acid, urea, and nicotinamide¹³⁵.

i. Drug release systems

In general, there are several drug release systems from polymeric nanocapsules^{127,136}:

- **Diffusion-controlled systems:** drug release takes place after either desorption of the surface-bound drug or diffusion of the drug from inner part of the particles. In such systems, the release rate of drug is dependent on the wall thickness, porosity, and the drug concentration.

- **Chemically/Erosion controlled systems:** These systems involve a biodegradable capsule. Drug is released after the degradation of the polymer itself or after polymer-drug bond breaking.

- **Responsive drug delivery systems:** also called membrane-controlled reservoir systems. Drug release happens through diffusion of the drug into a responsive shell that has a controlled pH, temperature, ionic strength, magnetic or ultrasonic

properties. In such systems, the drug is released after the application of an external trigger that enhances the diffusion rate of drug through the shell.

- **Solvent-activated systems:** These systems may involve an osmotically-controlled delivery nanocapsule that has a semipermeable shell. This shell allows the movement of water into the capsule and the drug will only be released after the creation of an osmotic pressure.

ii. Methods of assessing drug release profiles

Experimentally, different apparatuses have been developed in order to assess the *in vitro* release profiles of drugs from their nanocapsules. As such, the drug release profile can be assessed using sample and separate, continuous flow or dialysis membrane methods¹³⁷.

- **Sample and Separate:** This widely used method is based on introducing the nanoparticle into a vessel containing a selected release medium/buffer at a specific temperature. The released drug is assessed after physically separating the release medium from the nanocapsules. The most commonly used physical separation method is centrifugation. Once separated, drug release is examined by sampling either the release medium (supernatant) or the nanocapsules at selected intervals of time. Then, another amount of release medium/buffer is added to the nanocapsules, in a step known as buffer replacement, by which the sampling is repeated over the entire duration of the study (see **Figure 8A**). This method is a direct, simple, efficient, and practical approach of monitoring the *in vitro* drug release profiles of nanocapsulated dosage forms^{137,138}.

- **Continuous Flow:** This method relies on the use of USP apparatus (flow-through cell holding the sample, pump and water bath) that ensures the constant circulation of a release medium/buffer through a column that contains immobilized nanocapsules. Drug release profile is assessed by the collection of eluents at specific periods of time. Only few examples of this method have been documented for nanocapsules release profiles in the literature (see **Figure 8B**). This method suffers from low flow rates and thus slow and partial release of drugs, high instrumental costs, complicated set-ups, and clogging of filters that lead to variations in the obtained results^{137,138}.

- **Dialysis Membrane:** This method depends on the physical separation of drugs using a dialysis membrane/bag and over selected periods of time. In this method, nanocapsules are introduced into a dialysis bag, that contains the release medium/buffer. The bag is then sealed and moved into a large container that contains a significantly larger volume of release medium than that inside the bag. Sampling from the outer compartment is subsequently performed (see **Figure 8C**)^{138,139}.

This method is easy and straightforward. It is applied on different nano-sized forms such as nanocapsules, liposomes, emulsions, and suspensions. However, drawbacks of this method include (1) the leakage of media from the two ends of the dialysis bag that occur in cases of improper sealing, (2) slow equilibration with outer media does not allow for precise analysis of initial drug amounts in forms of high burst release, and (2) being incompatible for some drugs that may bind to the dialysis bag¹³⁸.

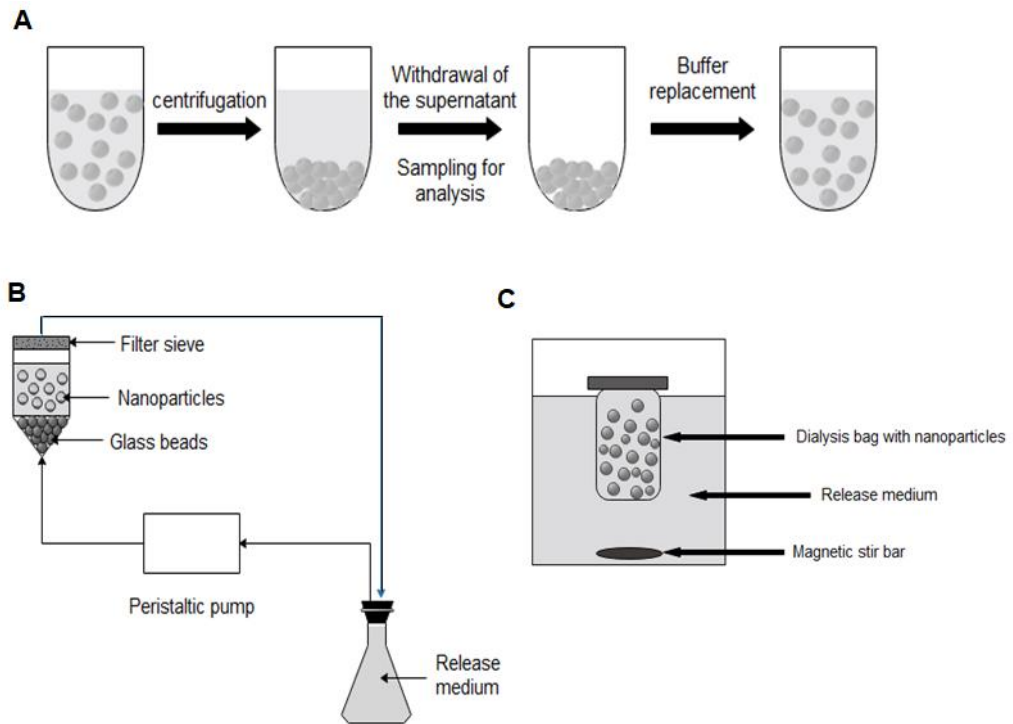


Figure 8. Basic methods of *in vitro* drug release assessments. **A** sample and separate method, **B** continuous flow method and **C** dialysis method.

iii. Drug release kinetic models

There are different kinetic models on drug release from controlled drug delivery systems.

- **Zero order kinetic model:** Based on pharmacokinetic principles, the slow dissolution of drugs from their dosage form can be represented by this equation:

$$Q_t = Q_0 + K_0 t$$

Where: Q_t is the amount of drug released at time t

Q_0 is the initial amount of drug at time $t=0$

K_0 is the zero-order rate constant (concentration/time).

Zero order kinetics explains the profile of constant drug release from its delivery system. It shows that the level of drug remains constant throughout the delivery process¹³⁶.

- **First order kinetic model:** The release of drug that follows first order kinetics is represented by the following equation:

$$\log C = \log C_0 - K_1 t / 2.303$$

Where: C_0 is the initial concentration of the drug,

C is the percent of drug remaining at time t .

K_1 is the first order rate constant, expressed in time^{-1} or per hour

In this model, the rate is directly proportional to the amount of drug that underwent the reaction. It is commonly used to describe the absorption and/or elimination of drugs¹³³.

- **Higuchi model:** This is the first mathematical model that was proposed by Higuchi in 1961, aiming to explain the process of drug release from a matrix system¹⁴⁰. Higuchi equation is a prominent kinetic equation, also known as the most commonly used controlled-release equation¹³³. It can be represented in the following form:

$$Q = K_H \times t^{1/2}$$

Where: K_H is the Higuchi dissolution constant.

It should be noted that a few hypotheses are made in this Higuchi model:

- (i) the initial drug concentration in the matrix is much higher than drug's solubility
- (ii) Perfect sink conditions are attained in the release system
- (iii) The diffusivity of the drug is constant and in one dimension
- (iv) polymer swelling is negligible
- (v) the size of drug particles is smaller than the system thickness

2. Applications

Nanocapsules are smart drugs by which they have a specified binding to selective receptors. This characteristic allows for the use of nanocapsules in targeting cancer cells for instance⁹⁰. Other advantages of nanocapsule pharmaceutical usage include their ability to load high doses and low volumes of drugs, long retention, rapid absorption, high compatibility, safety and bioavailability of drugs. Nanocapsules have been applied in food science and agriculture, genetic and chemical engineering⁹³.

Creating polymeric nanoparticles and nanocapsules is of great importance in treating diseases that involve thorough and long-term therapies with drugs at high doses¹⁴¹. The limitations of chemotherapy in treating cancer and other diseases such as tuberculosis include their unfavorable side effects, low treatment efficacy and high recurrence rates. Nowadays, the use of nanocapsules - on the basis of well-documented biocompatible polymers - for targeted drug delivery is being applied in the treatment of several tumors¹⁴².

3. Preparation of different nanocapsules for drug delivery

Choosing the appropriate method of preparation of nanocapsules depends mainly on the goal, advantage, and properties of both the entrapped drug and the used polymeric material¹¹². Several methods of synthesizing nanocapsules include emulsion polymerization, emulsifications/solvent evaporation, diffusion, interfacial polycondensation, salting out, nanoprecipitation, as well as solvent displacement¹⁴³.

Producing nanoparticles with entrapped drugs imposes a serious challenge that requires harsh synthesis conditions especially when dealing with sensitive drug molecules. Thus, in such cases, encapsulation with a preformed polymer, rather than

from monomer polymerization, can be applied. Recently, various preparation methods including layer-by-layer deposition, emulsifications/solvent diffusion, solvent displacement and interfacial deposition, and direct self-assembly have been used¹¹².

a. Layer by Layer

LbL assembly is a technique adopted by Decher *et al.*, which uses alternating layers of cationic and anionic polyelectrolytes to generate a multilayered film¹⁴⁴. This method can be applied to a vast array of charged substances such as proteins, DNA, carbohydrates, and virus particles. The LbL assembly process results in the formation of films with a nanometer-scale thickness¹⁴⁴. Such films can be conducted in an aqueous media in the presence of mild surrounding conditions. The driving force for the LbL assembly is mainly based on electrostatic interactions as well as other interactions including hydrogen bonding and metal coordination¹⁴⁵.

As shown in **Figure 9**, LbL technique is based on the adsorption of a cationic polyelectrolyte that is immersed in a solution of anionic charged polymer over a period of time, usually 30 min. Then, the solid support is rinsed with water to eliminate excess free polyelectrolyte, followed by immersion in a solution of anionic polyelectrolytes to induce adsorption. This causes a reversal in surface charge. Repeating this process through subsequent adsorption steps and alterations of the surface charge, allows for the continuous formulation of the layered structure^{146,147}.

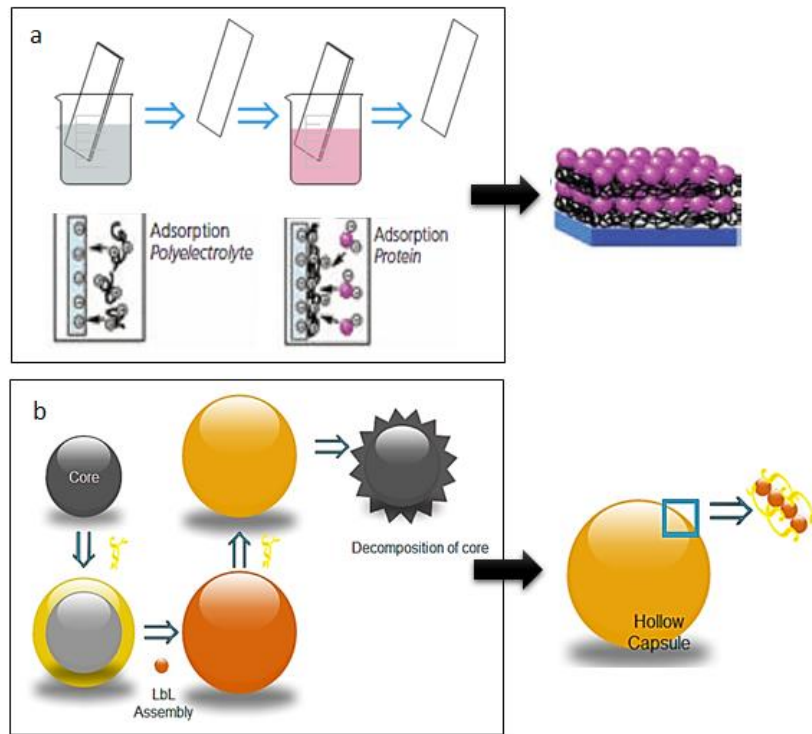


Figure 9. Process of LbL assembly (a) on a solid substrate; (b) on a colloidal core.

Moreover, LbL assembly involved the introduction of template synthesis using colloidal particles where the LbL films are assembled on a colloidal core and later the central particle core is destroyed resulting in the formation of hollow capsules¹⁴⁸. Several biocompatible and biodegradable natural polymers have been used in the formation of LbL assembled nanocapsules for gene and antitumor drug delivery, and they include: chitosan, gelatin, albumin, PLA, PGA, PLGA, PEG, polyanhydrides, polyalkylcyanoacrylates (PACA), poly(N-vinyl pyrrolidone), poly (methacrylic acid), poly(styrene sulfonate), and poly(allylamine) hydrochloride^{148,149}.

b. Emulsifications/solvent diffusion

This method involves the encapsulating polymer to be dissolved in a hydrophilic solvent and then saturated with water¹⁵⁰ (see **Figure 10**). The production of a precipitated polymer and consequent formation of nanocapsules, require the diffusion of the solvent by diluting it with water if the used organic solvent is partially water miscible. Then, the polymer-water saturated solvent phase is exposed to emulsification in an aqueous medium that contains a stabilizer. This causes the diffusion of solvent to the external phase and subsequent formation of nanocapsules based on the oil-to-polymer ratio. At the end, the solvent is either evaporated or filtrated depending on its boiling point¹⁰⁸.

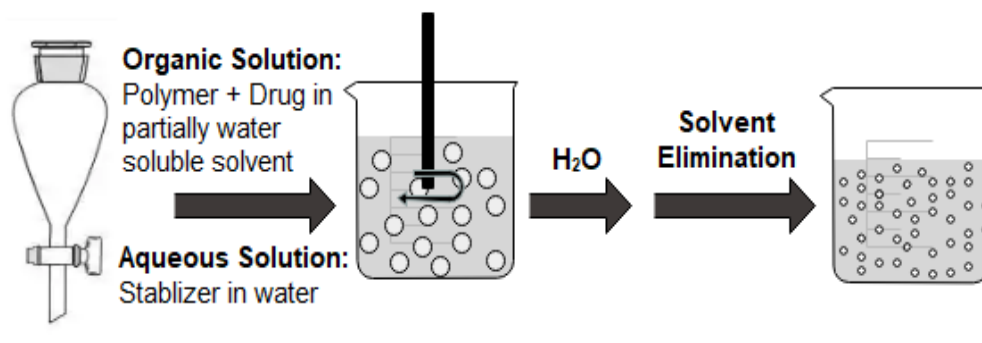


Figure 10. Schematic illustration of the ESD technique.

This method has some advantages that include high encapsulation efficiency, high reproducibility, and being simple and easily scaled-up. However, its disadvantages include the involvement of high-water volumes that should be eliminated from the suspension, and leakage of drug into the external phase that leads to reduced encapsulation efficiency¹⁵¹.

c. Solvent Displacement and Interfacial Deposition

Solvent displacement and interfacial deposition are similar methods where both rely on instantaneous emulsifying the organic internal phase that contains a dissolved polymer, into an aqueous external phase as shown in **Figure 11**. The major difference between these methods is that solvent displacement leads to the formation of nanospheres or nanocapsules, while interfacial deposition formulates nanocapsules only¹⁵².

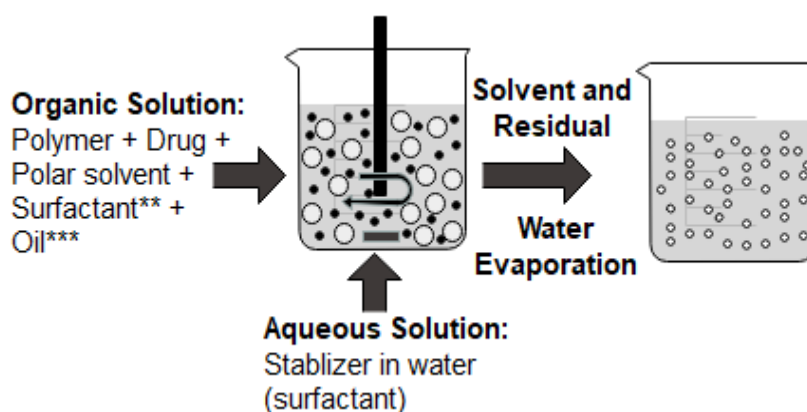


Figure 11. Schematic representation of the solvent displacement technique.
Surfactant is optional. *In interfacial deposition method, a fifth compound was introduced only on preparation of nanocapsules.

Solvent displacement includes precipitating a polymer from an organic solution as well as diffusing the organic solvent into an aqueous medium either in the presence or absence of a surfactant. The polymer is commonly dissolved in a water-miscible solvent which precipitates nanospheres. Then, this phase is subjected into an aqueous solution that contains a stabilizer so that the polymer deposits on the interface between water and the organic solvent. The fast diffusion of the solvent creates a spontaneous colloidal suspension^{153,154}.

This method formulates nanocapsules in cases when a small amount of nontoxic oil is added to the organic phase with high loading efficiency especially for lipophilic drugs. Also, this method is simple but limited to water-miscible solvents that create spontaneous emulsification. Moreover it may involve toxic compounds such as dichloromethane that increase particle size, and it is only applied to lipophilic drugs^{112,153}.

Interfacial deposition is a process used for nanocapsule formation that involves a fifth oily compound that is miscible with the polymeric solvent but immiscible with the mixture¹¹². The polymer deposition occurs at the interface between oil and aqueous phase leading to the formation of nanocapsules¹⁵⁵. The major difference in this technique is that the used polymer is dissolved with the desired drug in a solvent mixture such as benzyl benzoate, acetone, and phospholipids. This mixture is subsequently injected into an aqueous medium, leading to the deposition of the polymer at the interface between water and solvent droplets¹⁵⁶.

d. Self-assembly

Self-assembly is a spontaneous process that allows some molecules to become designed in a specific desirable structure without any external interventions. Self-assembly leads to the generation of complex hierarchy of molecules without any defect¹⁵⁷. It is a widely occurring process in nature especially in molecular phenomenon such as crystal states where the building blocks tend to arrange in a 3-dimensional pattern, phospholipids aggregation into cell membranes, as well as DNA and RNA supramolecular systems. In self-assembly, molecules have chemical functionality of a certain reactivity or directionality that restricts the products with stable

thermodynamics¹⁵⁷. For example, non-covalent interactions such as hydrogen bonding, Van der Waals forces and metal-organic coordination bonds play major roles in stabilizing the self-assembled structures, and interestingly, this has led to the creation of a huge material chemistry field that deals with synthesizing porous frameworks¹⁵⁸.

Self-assembly is an interesting subject in modern chemistry mainly because of the ongoing work toward the production of novel molecular self-assembled species within the nanotechnology paradigm¹⁵⁹. For example, self-assembled nanoparticles are found in wires, rings and supper lattices. Self-assembled cadmium, selenide and ferritin nanoparticles of diblock copolymers are also found in thin films displaying spatially ordered and organic–bioparticle hybrid materials¹⁶⁰. In addition, a study by Boal *et al.*, showed the ability to design self-assembled gold nanoparticles with thermally controlled size and morphology¹⁶¹, while Wong *et al.*, formulated hollow silica and gold microspheres using lysine and cysteine polymer blocks¹⁶². Moreover, Rechard *et al.* generated self-assembled hexabenzocoronene nanotubes¹⁶³. Similarly, self-assembly methodologies were applied for constructing hydrogels at nano- and micro-scales¹⁶⁴.

- **Directed Self Assembly**

Directed self-assembly (DSA) also involves employing the fundamental principles of the conventional self-assembly of specific building blocks, yet it included several forces that facilitate the process¹⁶⁵. Various strategies and tools have been suggested to direct the process of self-assembly depending on tailored molecular interactions with external directing magnetic, electric or thermal fields to create self-assembled structures¹⁶¹. Besides using external directing fields, DSA commonly involves using directing agents, and templates such as 1D, 2D, or 3D surface-modified

object containing active sites suitable for selective nanoparticle deposition, to aid any intrinsically self-assembled molecules even those that are sensitive to temperature or pH. Molecular interactions created by different stimuli such as light, temperature, pH, presence of metal ions, and solvent nature provide control over DSA processes¹⁶⁶ (see **Figure 12**).

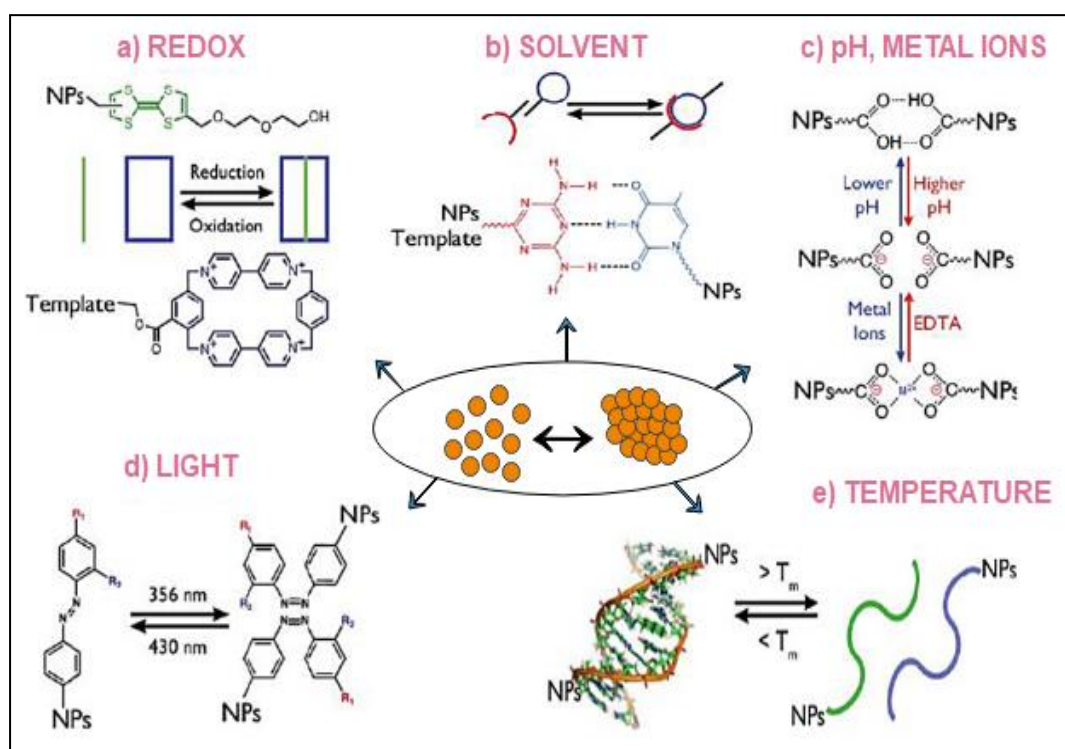


Figure 12. Molecular level of directed self-assembly. **(a)** Electrochemically active host-guest complexes can induce clustering or aggregation into polymeric sponges H-bonding. **(b)** Solvent mediated aggregation of particles by H-bonding. **(c)** Modulated concentration of H⁺ or metal ions induces reversible interparticle interactions by H-bonding or metal-ion coordination. **(d)** Photoisomerization of grafted molecules on the particles surface induces molecular dipole-dipole interactions. **(e)** Temperature induced denaturation of the DNA strand allows keeping particles dispersed, while a decrease in temperature causes aggregation.

4. Curcumin-based polymeric nanocapsules

Many polymeric nanocapsules of curcumin were formulated aiming to overcome its bioavailability limitations when applied clinically¹⁶⁷. Several studies have indicated that curcumin nanoencapsulation decelerates its hydrolytic and photochemical degradation^{2,167}. Strategies of curcumin nanoencapsulation into polymeric nanocapsules resulted in curcumin formulations that are of high drug loading capacity and enhanced stability, thus elucidating promising ways for curcumin delivery in biological systems¹⁶⁸.

For example, Beloqui *et al.* formulated pH-sensitive nanoparticles that combine curcumin with poly(lactide-co-glycolide) acid (PLGA) and a polymethacrylate polymer (Eudragit1 S100). Their results showed enhanced colonic delivery of curcumin in inflammatory bowel disease¹⁶⁹. Also, curcumin encapsulation in chitosan-based nanocapsules showed potent antibacterial effects against *E. coli*^{170,171}. In addition, the synthesis of curcumin conjugated silver¹⁷² and gold nanoparticles^{173,174} showed effective results when applied in nucleic acid sensing and anti-bacterial activities.

A recent study by Moussa *et al.* showed that the encapsulation of curcumin in cyclodextrin-metal organic frameworks enhanced the stability of curcumin¹⁷⁵. Another study by Mouslmani *et al.* indicated that the deposition of poly 9-(2-diallylaminoethyl)adenine HCl-co-sulfur dioxide on silica nanoparticles constructed hierarchically ordered nanocapsules that were potentially able to amplify guanine selectivity among nucleotide bases¹⁷⁶.

Numerous studies have been conducted to investigate the effects of different curcumin-loaded nanocapsules in the treatment of various cancer types. For instance, curcumin-loaded PLGA nanocapsules revealed high potential when applied as an

adjuvant therapy for prostate cancer¹⁷⁷. Likewise, poly(lactic-co-glycolic acid)- CUR nanoparticles (PLGA-CUR NPs) showed high antitumor effects against prostate cancer in a xenograft mice model¹⁷⁸. Moreover, the synthesis of a polymeric encapsulated formulation of curcumin with Nisopropylacrylamide (NIPAAM), N-vinyl-2-pyrrolidone (VP) and poly(ethyleneglycol)monoacrylate (PEG-A) revealed *in vitro* therapeutic efficacy against human pancreatic cancer cell lines¹⁷⁹. Furthermore, the conjugation of curcumin molecules with poly (lactic acid) (PLA) and their application into human hepatocellular carcinoma (HepG2) cells, showed cytotoxic effects and high intracellular targeting ability of micelles¹⁸⁰.

Additionally, curcumin-loaded monomethoxy poly(ethylene glycol)- poly(3-caprolactone) (MPEG-PCL) micelles inhibited the growth of colon carcinoma through blocking angiogenesis and inducing apoptosis both *in vitro* and *in vivo*¹⁸¹. Similarly, curcumin-loaded PEGylated PLGA nanocapsules were used in the delivery of curcumin to colon cancer cells in mice, and they showed potent antitumor effects¹⁸². Besides, several curcumin-loaded nanocapsules showed enhanced anti-colorectal cancer effects¹⁸³.

Curcumin self-assembly with β -cyclodextrin have been reported recently and results showed decrease in the degradation of curcumin, and enhanced stability, dispersibility and bioavailability⁸³. Moreover, Abbas *et al.* formulated curcumin-loaded nanoemulsion templates by self-assembly¹⁸⁴. Recently, self-assembled poly (L-lysine)-curcumin nanocapsules, referred to as "micro-curcumin", were synthesized¹⁸⁵. Moreover, the conjugation of curcumin with nano-aggregated chitosan oligosaccharide lactate was achieved through self-assembly process¹⁸⁶.

Curcumin-piperine nanocapsules coated with PEG overcame the bioavailability limitations associated with poor curcumin absorption, and exerted direct cancer cell targeting effects¹⁸⁷. Also, curcumin–piperine dual drug-loaded nanocapsules were able to target and treat multidrug-resistant cancers¹⁸⁸. On the other hand, a study by Shaikh *et al.*, showed that nanoparticle encapsulation of curcumin by emulsion technique improved the stability and oral bioavailability of curcumin by 9 folds compared to curcumin administration with piperine as absorption enhancer¹⁸⁹.

D. Polyallylamine Hydrochloride

The proposed requirements for polymeric nanocapsules caused a restriction in the use of a number of polymers. The commonly used polymers in drug delivery include glycolic, lactic acids, collagen, gelatin, bovine serum and human serum albumin, polylactic acid, poly-glycolic acid and their copolymers (polylactide-co-glycolides). Recently, nanocapsules for medical purposes were designed using polyvinylpyrrolidone, polylactic- and polyglycolic acids, polyalkyl cyanoacrylates, and polyallylamine hydrochloride (PAH). Among these promising biopolymers, polyallylamine hydrochloride (PAH) is of substantial significance (see **Figure 13**)¹⁹⁰.

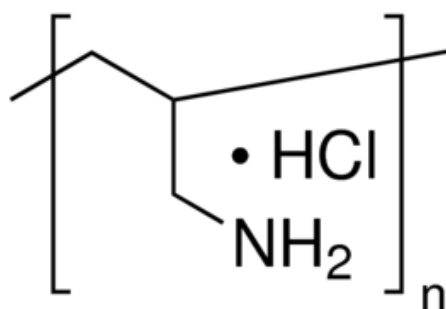


Figure 13. Chemical structure of polyallylamine hydrochloride (PAH).

1. Applications of PAHs

A study by Lu *et al.* showed successful LbL assembly of polyelectrolyte multilayer films involving poly(acrylic acid) and polyallylamine hydrochloride. These films were patterned by room-temperature imprinting with the aid of a polymer mold, and fabricated with different kinds of pattern structures¹⁹¹. In addition, another study by Li *et al.* revealed the ability to fabricate non-covalently assembled ionic responsive and fluorescent microcapsules made up of PAH and triethylamine. These capsules were characterized by high stability in acidic and basic media, as well as being easily tracked when applied in biological systems due to their autofluorescence¹⁹².

Another study by Janeesh *et al.* focused on synthesizing, characterizing and studying the biocompatibility and genotoxicity of PAH nanocapsules used for targeted drug delivery¹⁹³. In vitro and in vivo results of the use of such nanocapsules indicated the biocompatible nature of PAH nanocapsules at different concentrations. The activities of in vivo inflammatory markers such as cyclooxygenase (COX), nitric oxide synthase (NOS), interleukin-1 beta (IL-1b) and TNF- α did not witness significant changes. Likewise, no histopathological alterations were detected in many tissues which further confirm the biocompatibility and non-toxicity of PAH nanocapsules. Thus, it was suggested that PAH nanocapsules have great potential for in vivo drug-delivery applications¹⁹³.

Moreover, Zhang *et al.* were able to successfully design and assemble SiO₂ nanoparticles on the poly(allylamine hydrochloride)/multivalent anionic salt aggregates, and thus creating microcapsules with pH sensing properties. Due to their charge, these microcapsules have the ability to enter different cells and organelles especially those with acidic pH. Such localized pH sensing ability allowed the use of these capsules in

drug loading and real-time delivery of the carriers into target cells¹⁹⁴. Furthermore, PAH has been involved in the fabrication of DNA/PAH multilayered microcapsules. These capsules were prepared by LbL method where they were deposited in salt solutions to get optimum conditions for planar film growth. The templates were then dissolved to create porous DNA/PAH flexible capsules that could be later used in different future applications¹⁹⁵.

Regarding the ability of PAH nanoparticles to target cancer cells, some studies proved their efficiency in this field. For example, covalently assembled PAH/glutaraldehyde microcapsules were able to be uptaken by cells through endocytosis. These capsules showed dispersion in the cytoplasm without being colocalized into the nucleus. Such systems were used in gene transfer applications and the results showed significant alterations in the phenotype and function of the targeted cells including cell cycle, adhesion and migration processes¹⁹⁶. In addition, a study by Ruesing *et al.* revealed that PAH/DNA and PAH/siRNA nanocapsules prepared with calcium phosphate, were highly uptaken by HeLa cells and induced profound efficiency in gene transfer applications¹⁹⁷.

2. PAH driving forces

Aqueous PAH solutions were assessed by x-ray scattering at different salt concentrations. Results showed that at low salt concentration, a single broad peak was obtained observed indicating an ordered arrangement of PAH in solution. The scattering peak was found to be stable over 21 days, but it was lowered at high temperatures. The intermacroion spacing was shown to be smaller than that calculated from the polymer concentration, which suggests the existence of ordered structures. The spacing was

found to be decreasing with the increase of polymer's concentration, and it was increasing with the increase in salt concentration. These findings proved the intermolecular nature of PAH ordering¹⁹⁸.

Lu *et al.* designed well-defined Polyelectrolyte multilayer films made u of poly(acrylic acid) (PAA)/PAH and PAH/ poly(sodium 4-styrenesulfonate) (PSS). These films were fabricated based on electrostatic interactions as major driving forces for such room-temperature patterned structures¹⁹⁹. Other studies relied on entropically driven aggregations of bovine serum albumin (BSA) and PAH under different pH conditions and in the presence of salt to ensure a strong binding between these two partners. The concentration of BSA or PAH directly affected the molecular weight of the polyelectrolyte, and it was shown that the protein/polyelectrolyte interaction was endothermic²⁰⁰.

3. Curcumin and PAH

Recent methods of formulating poorly water-soluble materials such as curcumin, into nanoparticles involved dissolving the drug in an organic solvent miscible in water and adding into an aqueous polyelectrolyte solution. LbL assembled coating shells of cationic PAH and anionic PSS were designed with a high surface potentials and the efficiency in stabilizing curcumin nanocolloids²⁰¹. This method relied on dissolving curcumin in 60% ethanol/water solution followed by adding PAH. Then, sonication in the presence of water was performed to induce curcumin supersaturated conditions, subsequent crystal nucleation and LbL coating (see **Figure 14**).

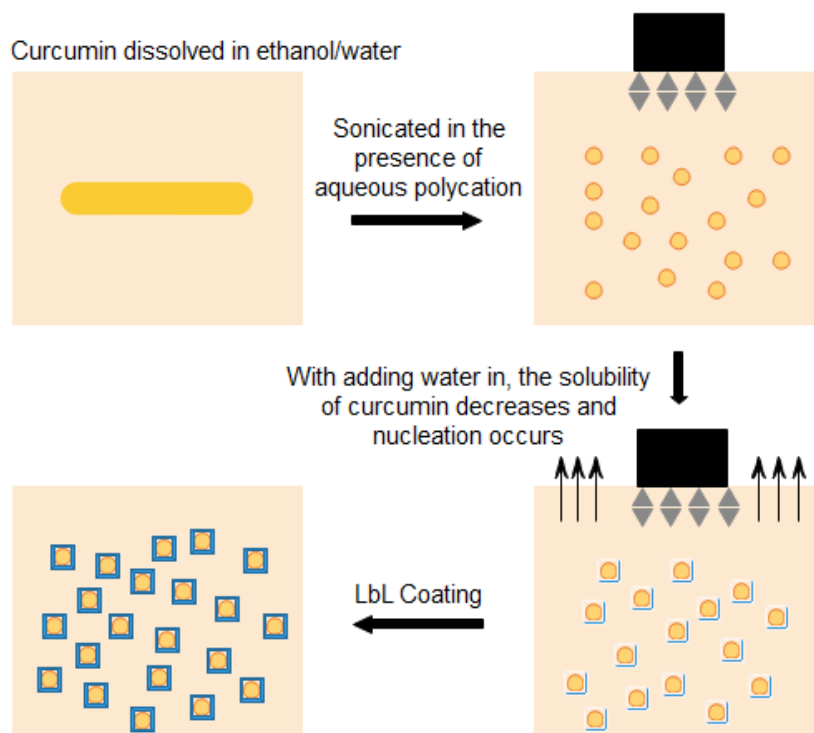


Figure 14. Conversion of curcumin powder into stable nanocolloids.

Recently, several ionically cross-linked capsules were generated from combining cationic polyamines with anionic salt. For instance, the crosslinkage of curcumin/PAH with dipotassium phosphate and their subsequent congregation with silica nanoparticles, generated self-assembled nanocapsule structures of 100-1000 nm size²⁰². These nanocapsules were prepared by mixing PAH with curcumin which had a strong interaction due to electrostatic and hydrophobic interactions between them. Such interactions have been shown to play a major role in the encapsulation chemistry²⁰³. Then, curcumin/PAH mixture solution was self-assembled by cross-linking the mixture chains with dipotassium phosphate in aqueous acidic medium that ensured that both polyamines by dipotassium phosphate have their respective charge in order to ionically crosslink. Later, a suspension of silica nanoparticles was added to this aggregated solution where the shell material diffused through the outer portion of the

polyamine/salt aggregate, through charge interaction with the positively charged polyamine. Finally, silica nanoparticles were deposited on the surface of PAH/dipotassium phosphate aggregates²⁰³. The overall net positive charge of curcumin–PAH–dipotassium phosphate aggregates assisted the assembly of negatively charged silica nanoparticles into ordered hierarchically nanocapsules.

SEM images showed that these nanocapsules were spherical in shape, and TEM images confirmed that the silica particles were at the surface with 100–250 nm thickness and the material at the center was thinner. In these negatively charged nanocapsules, fluorescence images showed that curcumin was distributed all over the capsule. Curcumin was highly bound to PAH as the latter had a strong binding affinity with curcumin that was confirmed by the high value of their association constant. In addition, the zeta potential of PAH and curcumin mixture proved that curcumin existed in its enolic form. Furthermore, it was shown that the release of curcumin from these nanocapsules was pH dependent, i.e. basic media induced the maximal release in comparison to acidic and neutral media. Also, the 2,2-Diphenyl-1-picrylhydrazyl (DPPH) scavenging activity of curcumin was decreasing with the decrease of capsule size as well as with the availability of β -diketone group in order to donate Hydrogen²⁰⁴.

CHAPTER III

MATERIALS AND METHODS

A. Chemicals and Reagents

Curcumin (CUR), Piperine (PIP) and PolyallylAmine Hydrochloride (PAH) were purchased from Sigma-Aldrich and used as received without further purification. Buffer stock solutions were purchased from Fisher and used after 10 times dilution to reach a final concentration of 100 μ M which is commonly used concentration for drug delivery studies. Acetone and methanol were supplied from Sigma-Aldrich and used as supplied.

For cellular assays, Dulbecco's Modified Eagle's medium (DMEM), penicillin/streptomycin (P/S), sodium/pyruvate were purchased from Lonza. Fetal Bovine Serum (FBS) was obtained from Sigma-Aldrich. Trypan Blue dye was supplied by Acros Organics. Caco-2 cells were graciously provided by Dr. Sawsan Kraidieh's Lab at the American University of Beirut. All other chemicals used were of analytical grade.

B. Methods

1. Preparation of CUR-PAH nanoparticles

CUR-PAH nanoparticles were prepared using the biodegradable polymer according to the nanoprecipitation method. 1:4 CUR:polymer ratio was prepared by mixing PAH (1 mg/mL in DDW for final volume 20 mL) and CUR (0.5 mg/mL in acetone for final volume 10 mL); the mixture was then stirred for 1 minute. Further, the

whole system was put on a hot plate at a constant heating rate and temperature= 60°C to totally evaporate the acetone and to reach a final aqueous volume of solution and NP = 20 mL. The NP suspension was then centrifuged at 15,000 rpm for 15 minutes. The supernatant was decanted to measure its absorbance by JASCO V-570 UV-VIS-NIR UV-vis spectrophotometer at $\lambda=428$ nm for encapsulation efficiency (EE), while the residue was re-suspended in 2 mL DDW then placed in liquid nitrogen for 2 minutes. After that, the frozen suspension was placed in the freeze-dryer for 6 hours in order to isolate the suspended solid NPs.

The same procedure was repeated for 1:2 and 1:1 CUR: PAH ratios whereby, 1 and 2 mg/mL CUR were used respectively for the fixed 1 mg/mL PAH.

2. Preparation of CUR-PIP-PAH nanoparticles

CUR-PIP-PAH nanoparticles (CUR-PIP-PAH NP) were prepared following the same above procedure with a fixed 1:2 CUR:PAH ratio but varying the concentration of the PIP used. Briefly, 1:4, 1:2 and 1:1 PIP:CUR ratios were prepared by weighing 2.5, 5 and 10 mg respectively of PIP and mixing them in 1 mg/mL CUR-acetone solution. Then, this prepared solution was mixed with PAH (1 mg/mL in DDW) and stirred for 1 minute. Later, the whole system was put on a hot plate at a constant heating rate and temperature= 60°C to totally evaporate the acetone and to reach a final aqueous volume of solution and NP = 20 mL. The NP suspension was then centrifuged at 15,000 rpm for 15 minutes. The supernatant was decanted to measure its absorbance by UV-vis spectrophotometer at 428 nm for encapsulation efficiency (EE), while the residue was re-suspended in 2 mL DDW then placed in liquid nitrogen for 2 minutes.

After that, the frozen suspension was placed in the freeze-dryer for 6 hours in order to isolate the suspended solid NPs.

3. Preparation of calibration curves

Different calibration curves were prepared to assess the drug loading, encapsulation efficiency and drug delivery of the two different NP types. For the drug loading analysis, initially, the 200 μM CUR stock solution was prepared by dissolving 1.1 mg of CUR in 15 mL methanol and vortexed for 2 minutes. A set of standard samples were made of different concentrations (5, 10, 15, 20, 25, 30, 35, 40, 45, 50, 55, 60, 65, 70, and 75 μM) by diluting different volumes (75, 150, 225, 300, 375, 450, 525, 600, 675, 750, 825, 900, 975, and 1050 μL) of the stock solution with methanol to reach a final volume of 3 mL diluted solutions. The absorbance of the diluted solutions was measured by UV-vis spectrophotometry. The calibration curve was plotted at maximum absorbance where $\lambda=428$ nm in order to determine CUR's concentration in the prepared samples.

As for the encapsulation efficiency, the same above procedure was followed however the stock solution was prepared by mixing 1.1 mg of CUR with 15 μL Triton-X (0.1%) and 5 mL of DDW. The solution was vortexed then sonicated for 2 minutes to totally dissolve CUR. After that, 10 mL of DDW were added to reach a final volume of 15 mL having a concentration = 200 μM . The standard samples of different concentrations were prepared following the same above-mentioned procedure but replacing (methanol) with (DDW). Subsequently, the absorbance of the diluted solutions was measured by UV-vis spectrophotometry. The calibration curve was

plotted at maximum absorbance where $\lambda=428$ nm in order to determine CUR's concentration in the prepared samples.

The calibration curves to assess the drug delivery at different pH (4, 6, 7, 8, and 10) were prepared using the above protocol whereby, the (DDW) used to prepare the stock solution was replaced with the (10x diluted buffer to have a final concentration of 100 μ M that is commonly used for drug delivery) of the corresponding pH. Similarly, the (DDW) used for dilutions was replaced with (10x diluted buffer + 0.1% Triton-X).

4. Drug Loading of curcumin nanocapsules

From each of the previously prepared CUR-PAH NP (1:1, 1:2 and 1:4 CUR: PAH ratios respectively) and CUR-PIP-PAH NP (1:4, 1:2 and 1:1 PIP:CUR ratios respectively), 0.031 mg of NP were dissolved in 3 mL of methanol then sonicated for 2 minutes. The absorbance of the obtained solutions was measured using UV-vis spectrophotometer at $\lambda=428$ nm.

The % Drug Loading (DL) in each type of capsule was calculated based on the below formula:

$$\% \text{ Drug Loading} = \frac{\text{mass of CUR obtained}}{\text{mass of weighed capsules}} \times 100 \quad \text{Equation (1)}$$

5. Encapsulation efficiency of curcumin nanocapsules

The absorbance of the supernatant collected from each of the previously prepared CUR-PAH NP (1:1, 1:2 and 1:4 CUR: PAH ratios respectively) and CUR-PIP-PAH NP (1:4, 1:2 and 1:1 PIP:CUR ratios respectively) was measured using UV-vis

spectrophotometer at $\lambda=428$ nm. The % Encapsulation Efficiency (EE) in each type of capsule was calculated based on the below formula:

$$\% EE = \frac{\text{mass of weighed CUR} - \text{mass of free CUR in supernatant}}{\text{mass of weighed CUR}} \quad \text{Equation (2)}$$

6. Characterization

a. Fourier Transform Infrared Spectroscopy (FTIR) Analysis

A ThermoNicolet 4700 Fourier Transform Infrared Spectrometer equipped with a Class 1 laser was used. The FTIR spectra of CUR, PIP, PAH, 1:2 CUR:PAH NP, and 1:2 PIP:CUR NP samples were performed on a scanning range between 400 and 4000 cm^{-1} .

b. Scanning Electron Microscopy (SEM) Analysis

The formation of NPs, their size and morphology were examined using a scanning electron microscope Tescan, Vega 3LMU with Oxford EDX detector (Inca XmaW20) at 15 KV whereby, 0.3 mg of CUR-PAH NP and CUR-PIP-PAH NP of different prepared ratios were dispersed in 10 ml DDW and then 25 μl of the prepared solution were deposited on an aluminum stub coated with carbon conductive adhesive tape. The samples were left to dry in open air overnight then SEM images were captured for further analysis.

c. X-Ray Diffraction Studies (XRD) Analysis

X-Ray Diffraction was done using Bruker d8 discover X-Ray diffractometer equipped with Cu-K α radiation ($\lambda=15405 \text{ \AA}$). The monochromator used was Johansson Type. The powder X-ray diffraction patterns of CUR, PIP, PAH, 1:2 CUR:PAH NP, and 1:2 PIP:CUR NP samples were recorded at 40 KV and 40 mA. The 2θ scanned angle was set between 2° to 70° at a scanning rate of $1^\circ/\text{min}$. These XRD patterns are used to investigate the crystal transformation of the above systems.

d. Dynamic Light Scattering (DLS) and Zeta Potential Analysis

The hydrodynamic diameter and zeta potential were done using Particle systems, Nano plus Zeta Potential/Nano Particle analyzer.

The hydrodynamic diameter and the surface charge of the two different NP delivery systems (CUR-PAH NP and CUR-PIP-PAH NP) was analyzed using particulate system Nonplus Zeta Potential/Nano Particle Analyzer. Samples were prepared by weighing 0.25 mg of NP and dispersing them in 10 mL DDW. The prepared solution was sonicated for 2 minutes and then the zeta potential of each sample was measured and set for 3 times repetition.

7. *In vitro* Analysis

For the drug release analysis, two types of NP were used (1:2 CUR:PAH ratio and 1:2 PIP:CUR ratio) at the five different pHs (4, 6, 7, 8, and 10).

Sample and separate method was conventionally used to study the *in vitro* drug release profile of CUR from the two different types of capsules. The general procedure followed was to weigh 0.5 mg of NPs and disperse them in 3 ml of the buffer of

selected pH having 0.1% Triton-X which is considered as a release medium. At time $t=0$ min, the solution was immediately centrifuged at 4000 rpm for 8 min, the supernatant was decanted and its absorbance was measured using UV-vis spectrophotometer at $\lambda=428$ nm. The solid particles were isolated and 3 ml of the release medium was added and the prepared solution was incubated at 37°C mimicking the physiological human body temperature. At predetermined time intervals (5 min, 10 min, 15 min, 30 min, 30 min, 1 hr., 1 hr., 2 hrs., 2 hrs., 2 hrs., 2 hrs., 3 hrs., 3 hrs., 3 hrs., and 3.5 hrs.; for a total of 24 hours-study), the solution was centrifuged at 4000 rpm for 8 min, the supernatant was decanted and its absorbance was measured using UV-vis spectrophotometer at $\lambda=428$ nm.

This study was done in triplicate so that their average additive absorbance and standard errors were plotted versus the average time. Using the calibration curve of each pH and the average additive absorbance, the percentage cumulative release versus the additive time was plotted in order to assess and analyze the drug release profile of each of the different NP type.

8. Culture of Caco-2 cells

Caco-2 cells were cultured in DMEM complete media that was prepared by adding 10% Fetal Bovine Serum (FBS), 1% sodium pyruvate and 1 % Penicillin/Streptomycin (P/S). Cells were grown in 10 cm Petri dish and incubated 37°C with a humid atmosphere containing 5% CO_2 till they reach 80 % confluence after 24 hrs.

9. Drug preparation for cell culture treatment

CUR: PAH (1:2 ratio) NP stock solution was freshly prepared at 100 μ M final concentration using DMEM complete media. After that, different concentrations were prepared from this stock solution (20, 25, 30 and 35 μ M) using above media and then sonicated for 2 minutes.

Different types of PIP: CUR NPs were used (1:4, 1:2 and 1:1 ratio) at 25 μ M concentration using the DMEM complete prepared media.

10. Cytotoxicity and cell viability studies

Caco-2 cells were plated in 6-well tissue culture plates at a density of 53000cells/m L. At 80 % confluence, cells were treated with the prepared NP media (different concentrations 1:2 CUR: PAH, and different ratios PIP: CUR).

At the 2 time points (24 and 48 hrs.), post treatment, pictures of the plates were taken using AXIOVERT 200 fluorescence inverted microscope with Zeiss AXIOCAM HRC, then the media was removed and cells were subsequently trypsinized and collected.

Cells were diluted with Trypan blue (1:1 volume/volume ratio) and counted using hemocytometer. Experiment was done in duplicates.

% viability was calculated using the following formula:

$$\% \text{ viability} = \frac{\text{number of living cells at specified concentration}}{\text{number of living cells at } 0 \mu \text{ M concentration of CUR (control)}} \times 100$$

CHAPTER IV

RESULTS AND DISCUSSION

A. FTIR Analysis

FTIR analysis was used to assess any significant change in the chemistry and fine structure by determining the intermolecular interactions between the different compounds of NPs. FTIR spectral data further supports our hypothesis (see **Figure 15**).

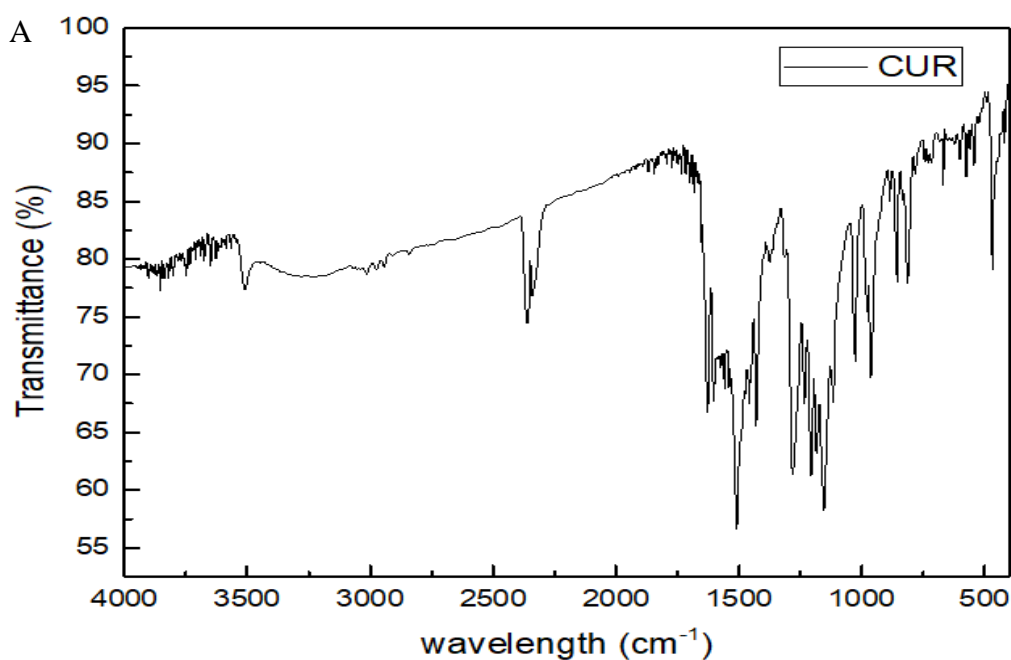
CUR showed significant peaks at 3510 cm^{-1} corresponding to the phenolic hydroxyl group (O-H) stretching (see **Figures 15A**) which was retained but shifted in the case of CUR-PAH NP (3416 cm^{-1}) and CUR-PIP-PAH NP (3567 cm^{-1}) (see **Figures 15C** and **15E**). Also, CUR showed a peak at 1627 cm^{-1} corresponding to aromatic C=C stretching which was retained but shifted in CUR-PAH NP (1626 cm^{-1}) and CUR-PIP-PAH NP (1668 cm^{-1}). Similarly, CUR peaks at 1602 cm^{-1} and 1508 cm^{-1} , corresponding to benzene ring and to carbonyl and ethylene groups stretching vibrations respectively, disappeared in both NPs. Further, CUR's peak at 1026 cm^{-1} corresponding to C-O-C stretching vibration was shifted to 1032 cm^{-1} in both NPs. Finally, CUR's peak at 963 cm^{-1} corresponding to the bending vibrations of C-H bond of alkene groups retained approximately the same in both NPs (962 cm^{-1}). It should be noted that CUR's major peaks are consistent with previous FTIR studies of curcumin²⁰⁵.

As for PAH, a significant peak at 2905 cm^{-1} associated with the symmetric and asymmetric stretching modes of methylene groups (see **Figure 15B**) was retained but shifted to a high wavelength in CUR-PAH NP (2927 cm^{-1}) and in CUR-PIP-PAH NP (2940 cm^{-1}) (see **Figures 15B** and **15C**). In addition, PAH peaks at 1647 cm^{-1} and 1516

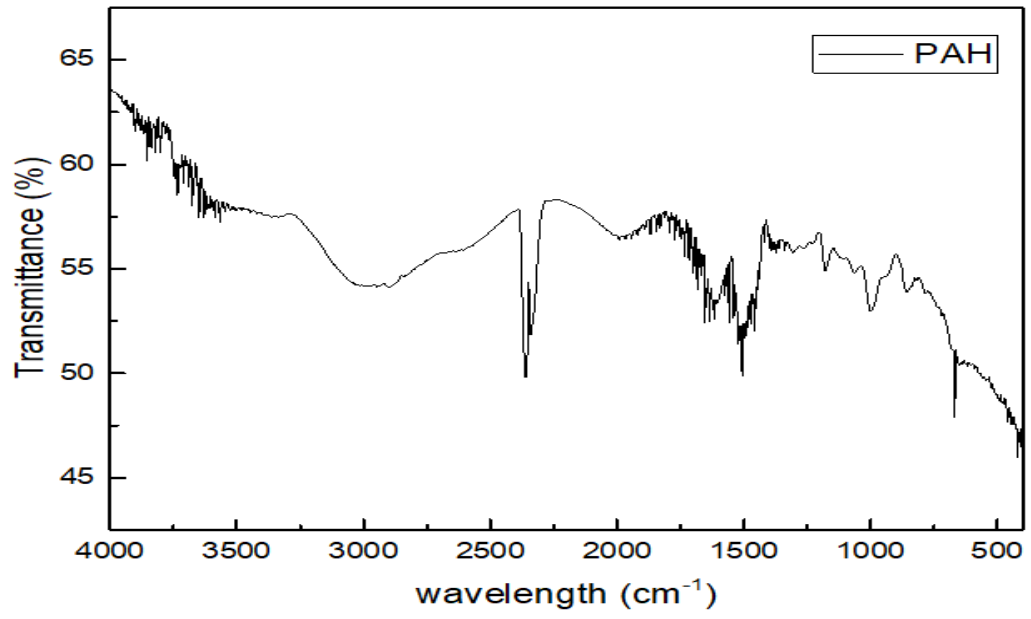
cm^{-1} associated with N-H asymmetric bending and C-H bending were retained in CUR-PAH NP (1513 cm^{-1}) and in CUR-PIP-PAH NP (1662 cm^{-1}). PAH peaks are also consistent with previous FTIR studies²⁰⁸.

The presence of these prominent peaks in control (CUR and PAH alone) as well as in CUR-PAH NP and CUR-PIP-PAH NP and their slight shifting suggests that (1) both CUR and PAH were present inside the NPs and (2) confirming a strong involvement of NH_2 of PAH and enol form of CUR inside the NPs.

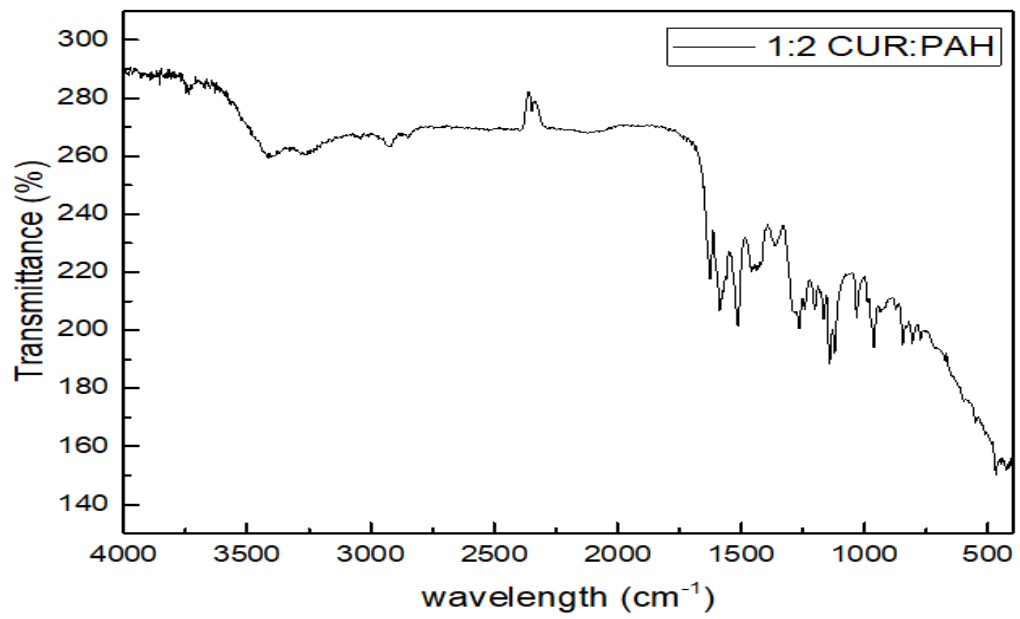
As for PIP, it showed significant peaks at 3009 cm^{-1} corresponding to aromatic C-H stretching, at 1634 cm^{-1} corresponding to symmetric and asymmetric stretching of C=C, at 1448 cm^{-1} corresponding to C-H stretching, at 1253 cm^{-1} corresponding to asymmetrical stretching of =C-O-C, and the most characteristic peak at 929 cm^{-1} corresponding to C-O stretching²⁰⁹ (see **Figure 15D**). Interestingly, all these peaks were retained the same in CUR-PIP-PAH NP indicating the incorporation of PIP into the NPs (see **Figure 15E**).



B



C



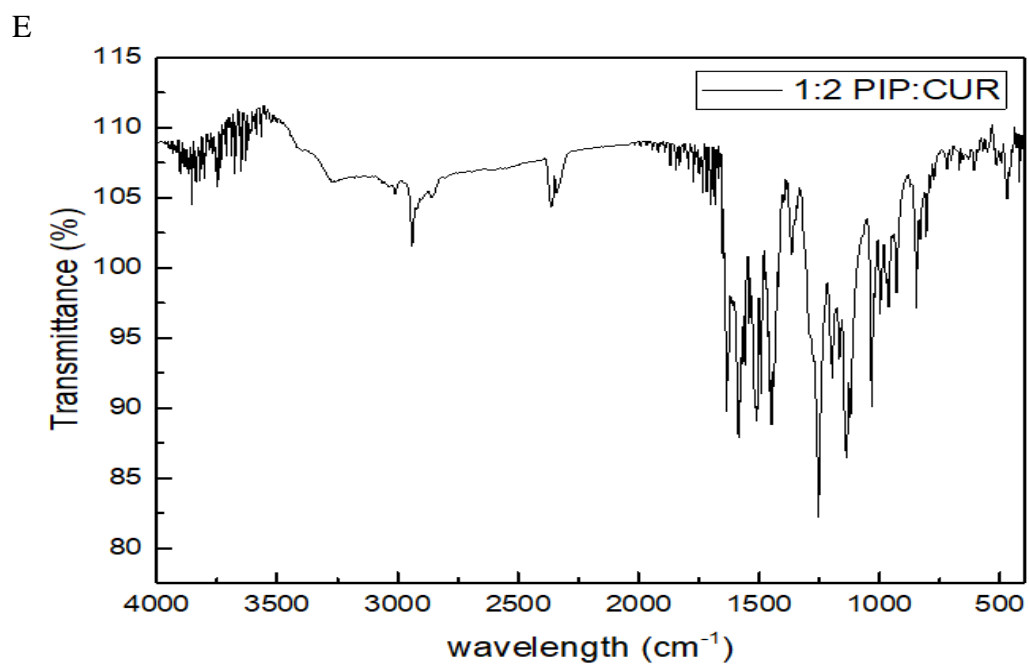
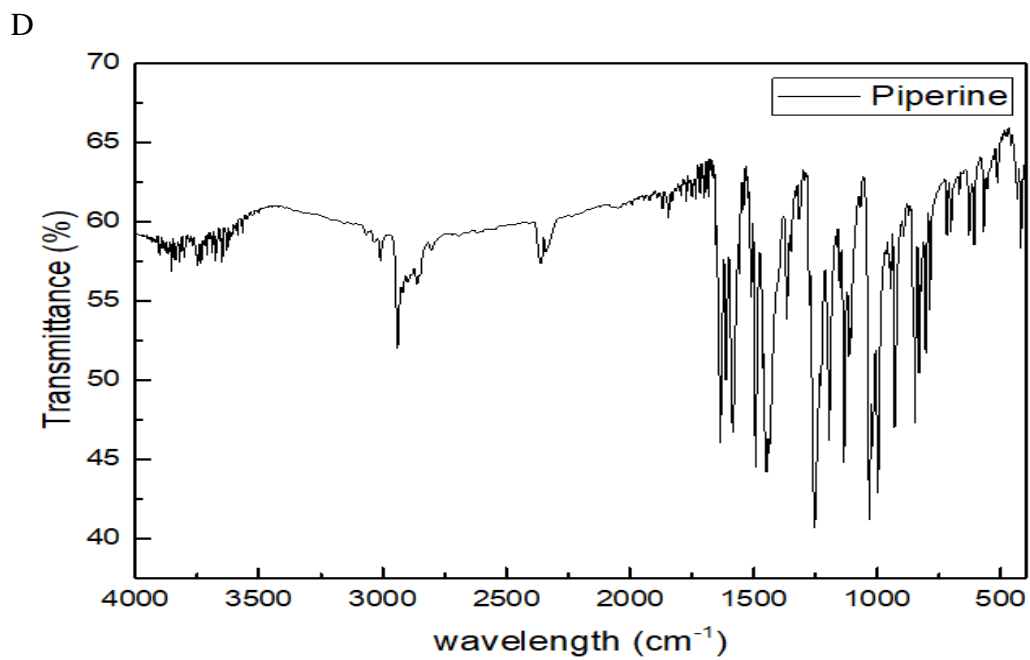


Figure 15. FT-IR spectra of CUR (A), PAH (B), CUR-PAH NP (C), PIP (D) and CUR-PIP-PAH NP (E).

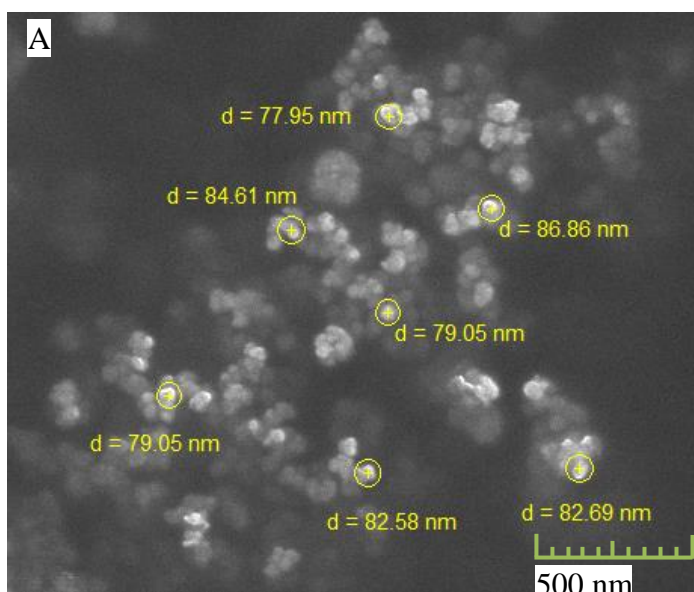
B. SEM Analysis

1. Formation and morphology

The SEM images of both types of nanocapsules having different CUR:PAH or PIP:CUR ratios showed the formation of nanospheres all along the deposited samples. CUR alone has a crystalline structure that appears under the SEM as rod-like shape. This change in morphology from rod-like to spherical proves the formation of desired nanocapsules that were prepared using the nanoprecipitation method.

2. Size

Briefly, 1:4 CUR:PAH ratio had an average diameter = 81.82 nm (see **Figure 16A**), 1:2 CUR:PAH ratio had an average diameter = 91.75 nm (see **Figure 16B**), and 1:1 CUR:PAH ratio had an average diameter = 100.66 nm (see **Figure 16C**). This shows that varying the initial concentration of CUR while keeping that of PAH constant did not have a significant impact on the size of the spherical formed NP whereby, the average diameter increased by 9.93 nm when going from 1:4 to 1:2 ratio and by 8.91 nm when going from 1:2 to 1:1 ratio.



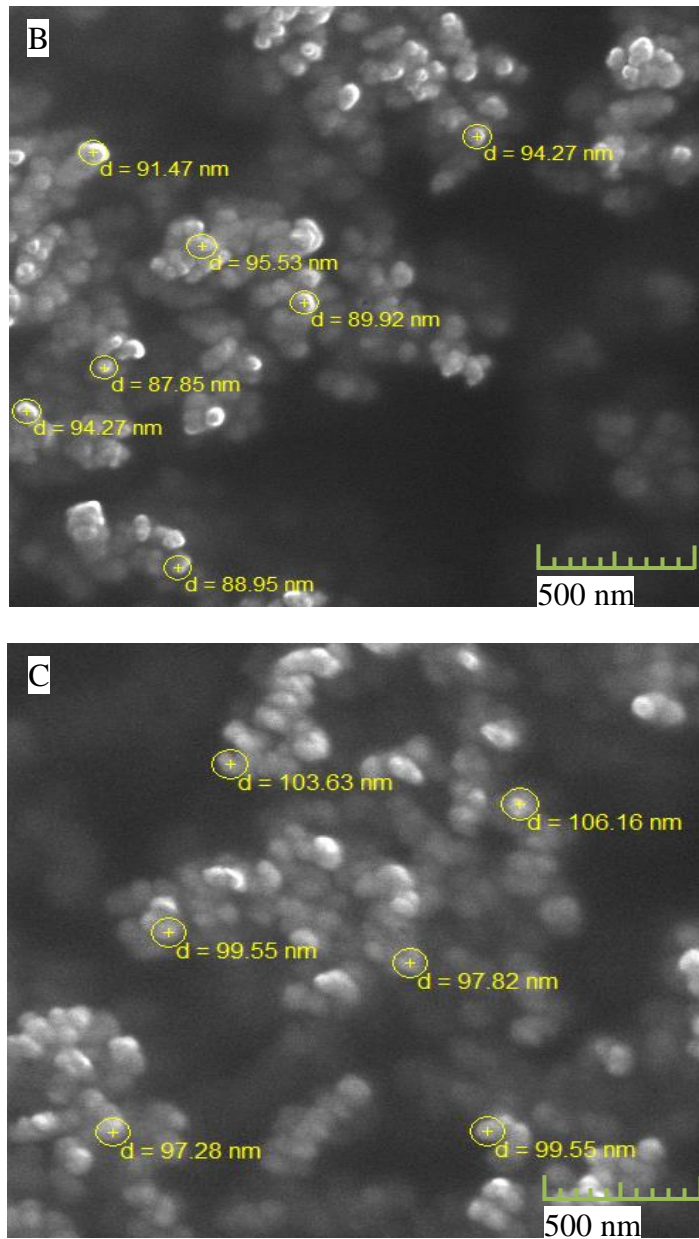
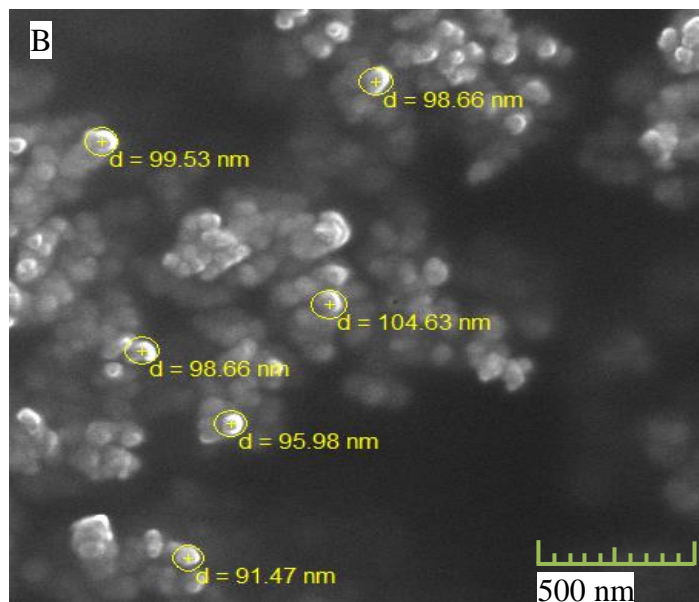
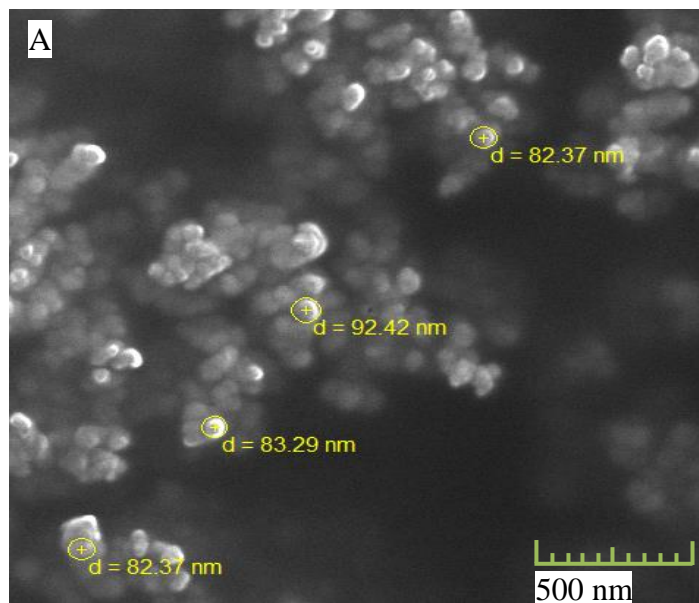


Figure 16. SEM images of 1:4 CUR:PAH (A), 1:2 CUR:PAH (B) and 1:1 CUR:PAH NPs (C).

Similarly, 1:4 PIP:CUR ratio had an average diameter of 85.11 nm (see **Figure 17A**), 1:2 PIP:CUR ratio had an average diameter of 98.15 nm (see **Figure 17B**), and 1:1 PIP:CUR ratio had an average diameter of 106.68 nm (see **Figure 17C**). From these

results, we can conclude that the increase in the concentration of PIP did not have a significant impact on increasing the average size of the produced NP.



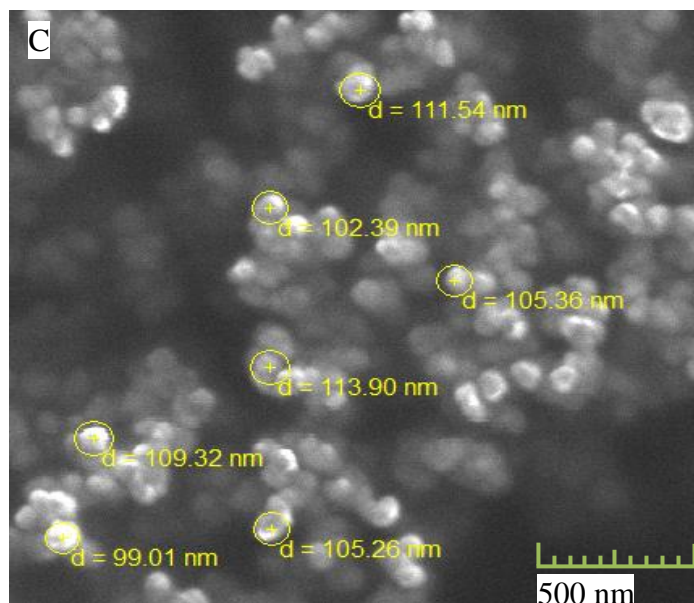


Figure 17. SEM images of 1:4 PIP:CUR (A), 1:2 PIP:CUR (B) and 1:1 PIP:CUR NPs (C).

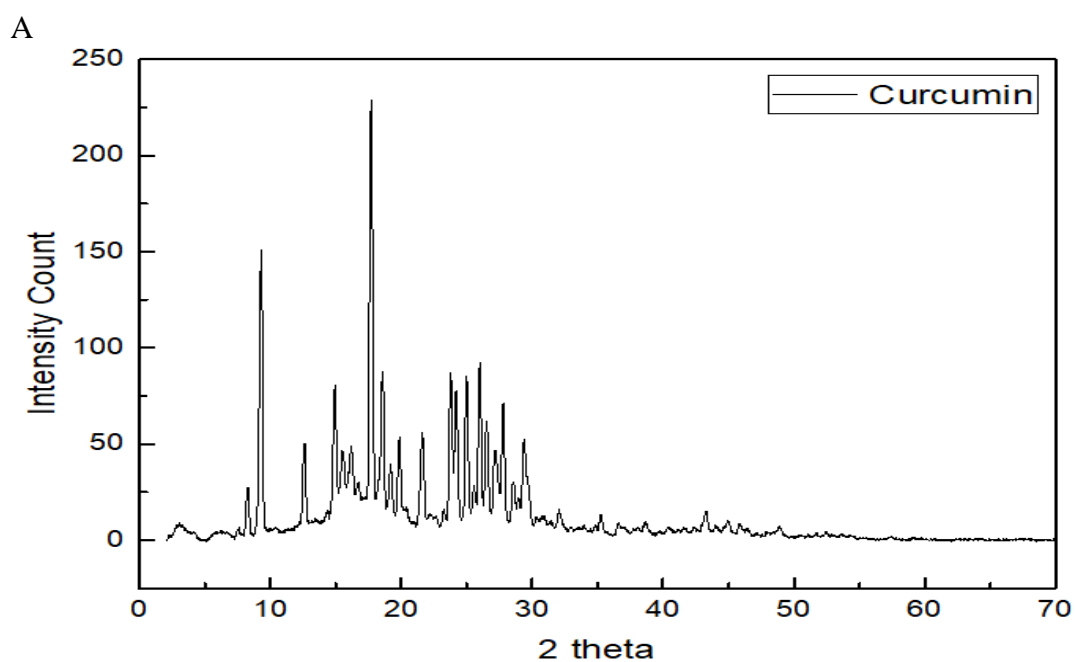
C. XRD Analysis

The XRD analysis was performed for CUR, PAH, PIP, 1:2 CUR:PAH and 1:2 PIP:CUR. The % crystallinity of CUR was 64.6 % while that of 1:2 CUR:PAH was 46.5%. Also, the % crystallinity of PIP was 62.0% and 1:2 PIP:CUR was 36.9 %.

These results prove that CUR, when encapsulated, underwent a modification in its crystallinity from crystalline to amorphous. These results were also proven by the size and patterns of the peaks. The major sharp peaks of CUR were observed at 2θ diffraction angles of 8.26° , 14.9° , 17.6° , 18.5° , 19.8° , 23.7° , 24.6° , and 26.5° suggesting that it possesses a highly crystalline structure²⁰⁶ (see **Figure 18A**).

The major unsmooth and very broad peaks of PAH were observed at 2θ diffraction angles of 3.006° and 15.71° indicating that PAH is an amorphous and very hygroscopic polymer (see **Figure 18B**).

The CUR:PAH NPs showed both CUR and PAH broad peaks at 2θ diffraction angles of 2.16° (attributed to the shifted PAH diffraction angle), 14.3° and 26.7° (attributed to the shifted CUR diffraction angles) (see **Figure 18C**). This indicates that (1) both CUR and PAH are present in the NPs and (2) proving the amorphous structure of the produced NPs.



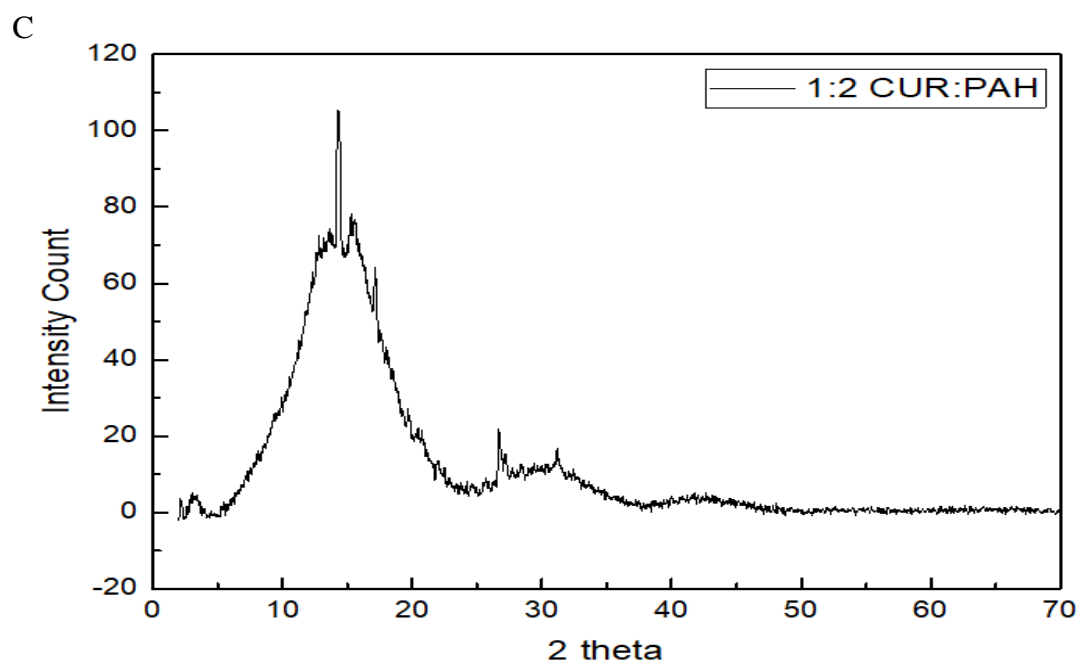
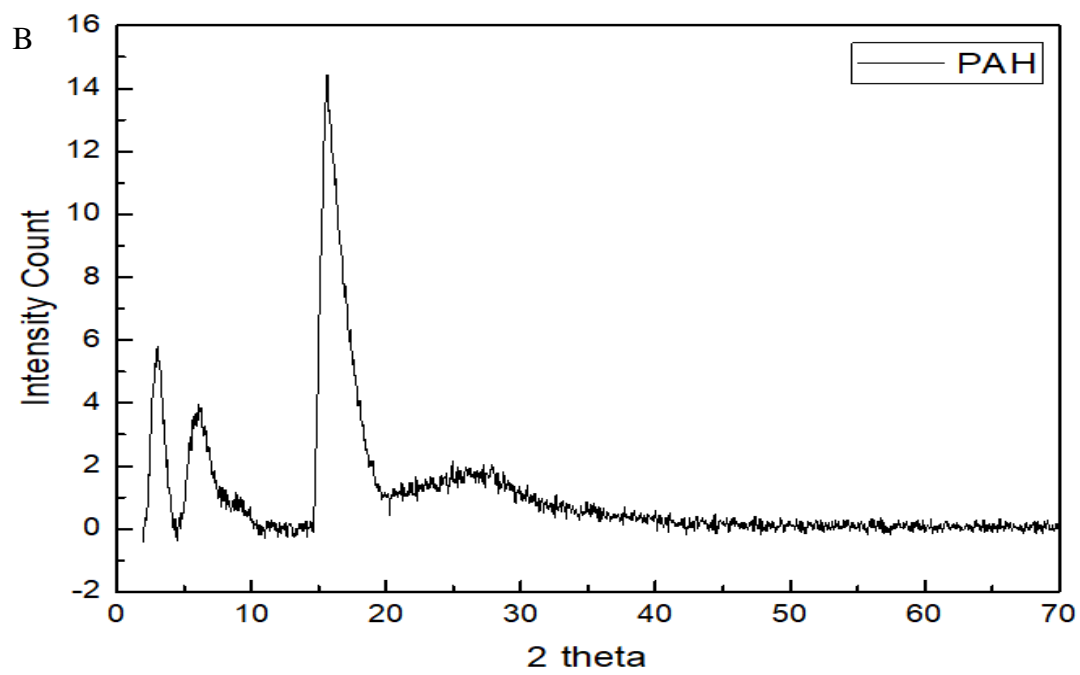
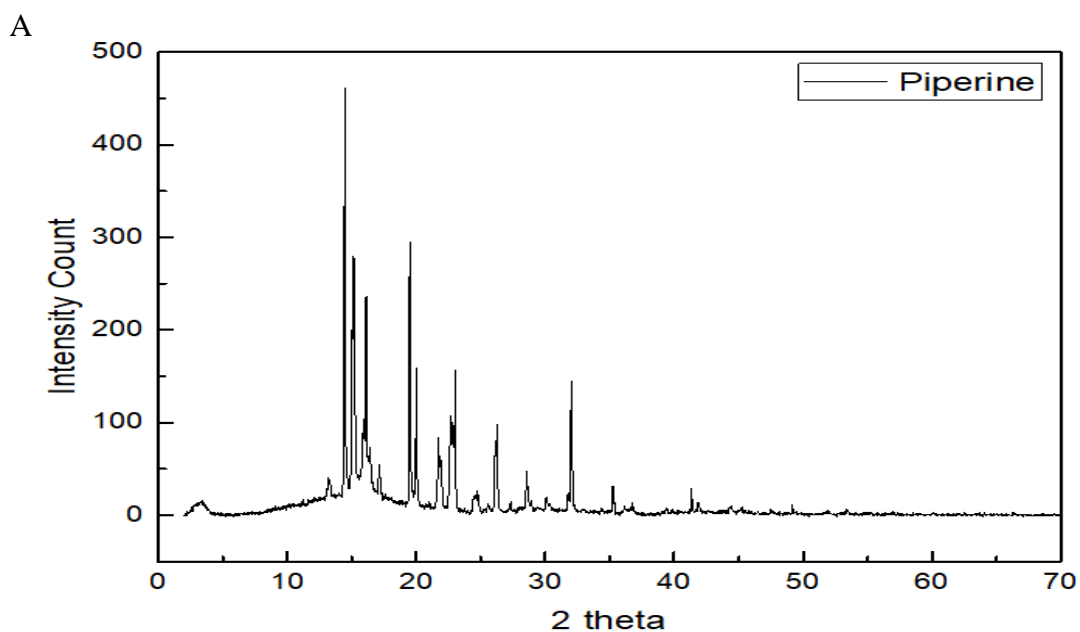


Figure 18. XRD images of curcumin (A), PAH (B), and 1:2 CUR:PAH (C).

Additionally, the major sharp peaks of PIP were observed at 2θ diffraction angles of 13.23° , 14.45° , 15.9° , 17.1° , 20.0° , 22.9° , 24.6° , 27.3° , and 31.8° (see **Figure 19A**). This indicates the highly ordered and crystalline structure of PIP.

Likewise, 1:2 PIP:CUR NPs showed broad peaks at different diffraction angles of 4° (attributed to shifted PAH diffraction angle), 25.0° and 26.6° (attributed exactly to CUR diffraction angles), and 17.1° , 20.4° , 27.1° and 31.2° (attributed to PIP diffraction angles) (see **Figure 19B**). This proves the successful incorporation of CUR, PAH and PIP in this NP, as well as the amorphous structure and disordered crystallinity of the prepared NPs.

This crystallinity modification shown in both types of NPs may be attributed to PAH that probably surrounded the crystal aggregates of CUR during NPs preparation, and thus formed the amorphous complex (proven by zeta potential).



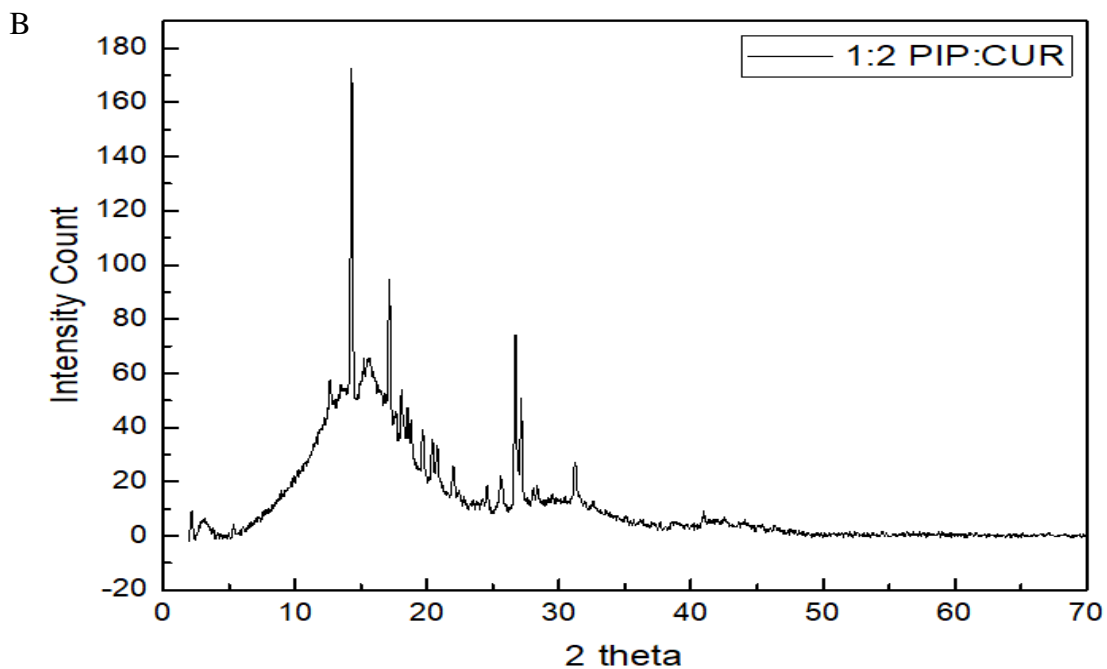


Figure 19. XRD images of PIP (A) and 1:2 PIP:CUR (B).

D. DLS and Zeta Potential Analysis

The hydrodynamic diameter of the two tested types of NPs served as a basic way to modulate the procedure of the capsules' preparation method. Whereby, when the freeze-dried isolated NPs capsules that were analyzed using DLS, a huge hydrodynamic diameter (2000-5000 nm) was observed proving that the NPs formed large aggregations on each other in the solution.

To avoid such considerable aggregation, the solid particles collected after centrifugation were dispersed in 2 mL DDW, placed in liquid nitrogen to freeze, then freeze-dried to isolate the suspended NPs. Upon DLS analysis of the re-suspended NPs in DDW, average hydrodynamic diameters of 207.3 nm, 243.6 nm, and 312.4 nm for 1:4, 1:2 and 1:1 CUR:PAH NPs respectively were obtained. However, the average hydrodynamic diameters of 1:4, 1:2, and 1:1 PIP:CUR NPs diameter were 236.2 nm, 298.4 nm, and 356.9 nm respectively.

A difference between the particle size analysis done by SEM, which measures the size of the particle in its solid state, and the DLS, that measures the hydrodynamic diameter of the aggregated particles in solution is noted. This difference is because the diameter obtained from DLS analysis includes the particle itself as well as the ionic interaction between the external PAH polymer and O atoms in the solvation layer surrounding the NPs. The solvation layer is the shell surrounding the particle consisting of water molecule and this gives a bigger diameter than the actual size²¹⁰.

Indeed, the observed DLS results prove that changing CUR ratio or PIP ratio did not have a significant impact on the size of the NP when keeping PAH's concentration fixed²⁰⁶.

As for the zeta potential analysis, CUR-PAH NP had an average positive zeta potential $\sim +30$ mV and CUR-PIP-PAH NP had an average positive zeta potential $\sim +27$ mV indicating that the cationic PAH polymer was externally surrounding CUR. The amount of amine group (NH_2^+) coated on the NPs surface has been shown to determine the surface charge of NPs.

Moreover, the +30 mV charge of the external NPs' surface resulted in a good stability profile, considerable repulsive forces between particles and less aggregation of NPs²⁰⁷. Results also indicated that CUR addition did not significantly affect the zeta potential which is matching with what is studied in the literature. More importantly, it is well documented a system having a positively charged surface is considered as a desirable system for the delivery of negatively charged drugs like CUR because the surrounding protein markers, DNA and cell membrane surface are slightly anionic, thus designing positively charged NPs facilitates the cellular uptake and accumulation of

NPs in the target cells. Literature has mentioned that cationic NPs can be considered as easy, safe and effective ways to carry therapeutic drugs²⁰⁷.

We can also deduce that the formation of NPs is stabilized by non-valent bonding such as Van der Waals forces and electrostatic interactions between the partially positive PAH polymer and the partially negative CUR. In addition, the internal H-bonding between the polymer and CUR are responsible for the structural behavior (amorphous structure indicated by XRD), morphological behavior (spherical NPs), drug loading of CUR (by diffusion), and the mechanism of drug release of CUR from NPs. Our findings are consistent with many articles in the literature which confirmed the above explanations by which H bonding can influence the conversion of dry crystals²⁰⁵.

% Encapsulation Efficiency (%EE)

After decanting the supernatant (obtained at the end of the preparation of different NPs types), its absorbance was measured spectrophotometrically. Then, using the %EE calibration curve prepared for this purpose, the mass of free CUR in supernatant was calculated. %EE was calculated using equation (2).

The %EE for CUR:PAH NPs of ratios 1:4, 1:2 and 1:1 was 83.1%, 92.7% and 88.5% respectively. The %EE for PIP:CUR NPs of ratios 1:4, 1:2 and 1:1 was 83.7%, 96.2% and 92.4% respectively. Adding PIP to the prepared NP while fixing the concentration of PAH and CUR led to improved %EE thus indicating that PIP facilitated the encapsulation of CUR within PAH.

% Drug Loading (%DL)

The % DL of CUR that is entrapped in the CUR-PAH NP is an important property in nanomedicine where it shall give an idea about the average dose required to be accumulated intracellularly in order to exert the desired therapeutic effects of the drug.

In our study, the absorbance of NP dissolved in methanol was measured spectrophotometrically. Then, using the drug loading calibration curve prepared for this purpose, the mass of CUR obtained was calculated. The % DL was calculated using equation (1).

The % DL for CUR:PAH NPs of ratios 1:4, 1:2 and 1:1 was 66.8%, 93.5% and 84% respectively. The % DL for PIP:CUR NPs of ratios 1:4, 1:2 and 1:1 was 67.9%, 94.6% and 85.2% respectively. This shows that increasing the amount of CUR added to a fixed quantity of PAH polymer led to an increase the drug loading which was best for 1:2 CUR:PAH ratio and 1:2 PIP:CUR ratio. It should be noted that similar findings of high % DL were also observed in many published articles that reported a greater loading of CUR into NPs than other matrices¹¹⁸. **Table 2** summarizes the % EE and % DL of the different CUR-PAH NP and CUR-PIP-PAH NP.

Table 2. % EE and % DL of different ratios of CUR-PAH NP and CUR-PIP-PAH NP.

Ratio	CUR-PAH NP			CUR-PIP-PAH NP		
	1:4	1:2	1:1	1:4	1:2	1:1
% EE	83.1%	92.7%	88.5%	83.7%	96.2%	92.4%
% DL	66.8%	93.5%	84%	67.9%,	94.6%	85.2%

E. *In Vitro* drug release analysis

To date, no standardized technique for the assessment of drug release from nanomedicines has been issued by regulatory authorities. *In vitro* release testing profiles are commonly used to predict the *in vivo* behavior of the encapsulated drug¹³⁷⁻¹³⁹. Properly designed *in vitro* release profiles can provide essential information regarding the drug dose, behavior, release mechanisms and kinetics. Such information enabled the development of different effective drug delivery systems.

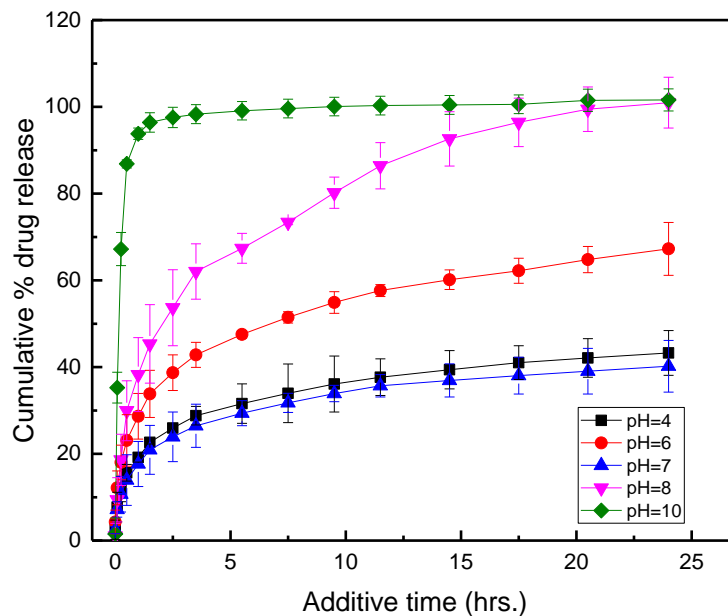
In our study, we relied on the Sample and Separate method which is used to analyze the real time drug release at the physiological human body temperature (37°C). This method is the most commonly used drug release method as it leads to the direct measurement of drug release as well as initial burst release using simple and practical requirements. Also, it is a reliable method for the characterization of the *in vitro* dosage form behavior of drugs which subsequently provides insights into the *in vivo* behavior¹³⁷.

Since the selection of the release media for NPs vary depending on the administration and target sites of the drug, we chose different pH media (4, 6, 7, 8, and 10) having 0.1% Triton-X surfactant to conduct the present study.

The enhanced physicochemical properties of different CUR NPs could be attributed to several factors: reduced size of particles, high-energy amorphous structure, crystalline transformations (as confirmed by XDR analysis), intermolecular H-bonding between the polar functional groups of drug molecules and amino groups of PAH polymer, and Van der Waals interactions between the hydrophobic moiety of drug molecules and PAH side chains (as depicted by FTIR analysis). Taken together, these factors improved the aqueous solubility and release of CUR²⁰⁵.

Figures 20A and 20B show the % cumulative release of 1:2 CUR-PAH NP and CUR-PIP-PAH NP respectively.

A



B

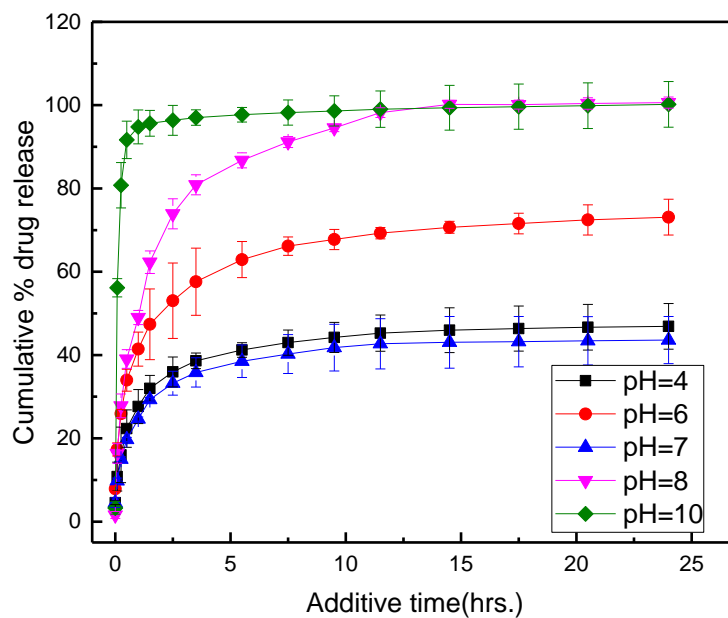


Figure 20. % Cumulative release of 1:2 CUR-PAH NP (A) and CUR-PIP-PAH NP (B).

At 2.5 hours, a release of about 25.9%, 38.7%, 23.9%, 53.6%, and 97.5% for 1:2 CUR:PAH nanoparticles at pHs 4, 6, 7, 8, and 10 respectively was observed. For the same time, a release of about 35.9%, 53.04%, 33.2%, 73.9%, and 96.3% for 1:2 PIP:CUR nanoparticles at pHs 4, 6, 7, 8, and 10 respectively.

At 9.5 hours, a release of about 36.1%, 54.8%, 33.8%, 80.2%, and 99.6% for 1:2 CUR:PAH nanoparticles at pHs 4, 6, 7, 8, and 10 respectively was observed. For the same time, a release of about 44.2%, 86.7%, 41.7%, 94.5%, and 99.04% for 1:2 PIP:CUR nanoparticles at pHs 4, 6, 7, 8, and 10 respectively.

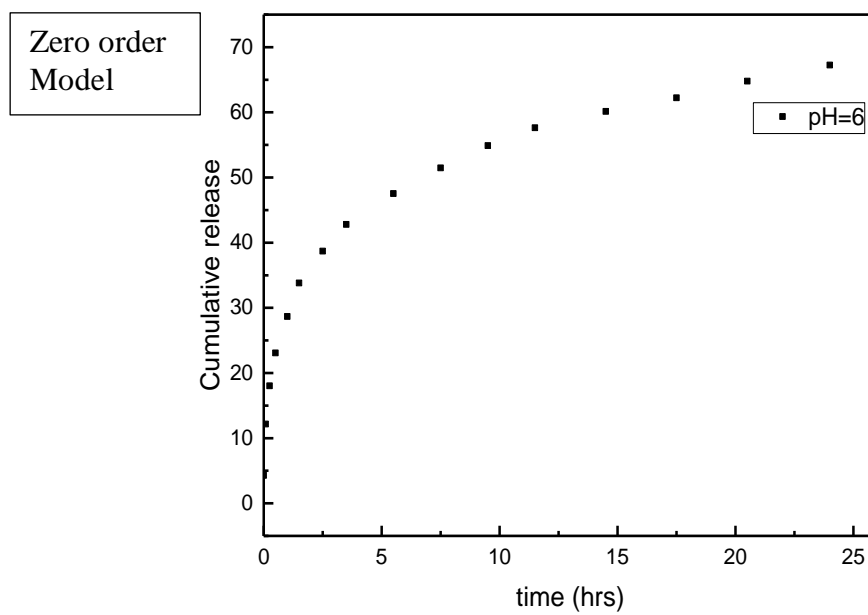
Finally, the total amount released after 24 hours was of about 43.26%, 67.25%, 40.1%, 99.46%, and 100% for 1:2 CUR:PAH nanoparticles at pHs 4, 6, 7, 8, and 10 respectively was observed. For the same time, a release of about 46.88%, 73.11%, 43.6%, 100%, and 100% for 1:2 PIP:CUR nanoparticles at pHs 4, 6, 7, 8, and 10 respectively.

Thus, it can be concluded from the above results that the addition of PIP to the prepared CUR NPs enhanced the % drug release at different pH and time intervals. The graphs showed more release in basic media compared to acidic and neutral media (as mentioned earlier in literature). We speculate that when the pH

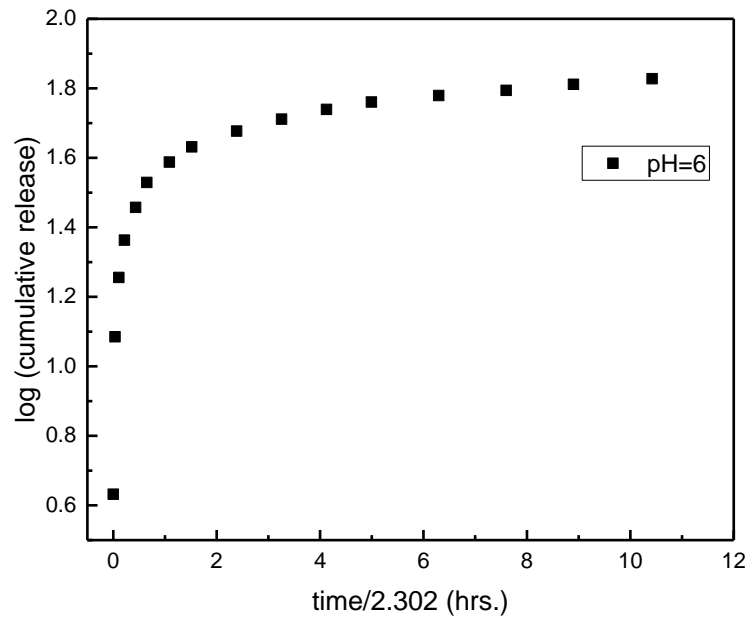
Increases to pH =10 in basic medium the amino group (NH_2) in the polymer becomes (NH_3^+). The positive/positive interactions formed destabilize the capsule leading to its breaking down and eventually allowing curcumin to diffuse out of nanocapsules easier.

Drug release kinetic models

After assessing the drug release profiles of curcumin, we went further to determine the best fit release kinetic model. To achieve this, we plotted graphs of zero-order, first-order and Higuchi kinetic models (see **Figure 21**) and then determined the R^2 of each curve (see **Tables 3 and 4**).



First order Model



Higuchi Model

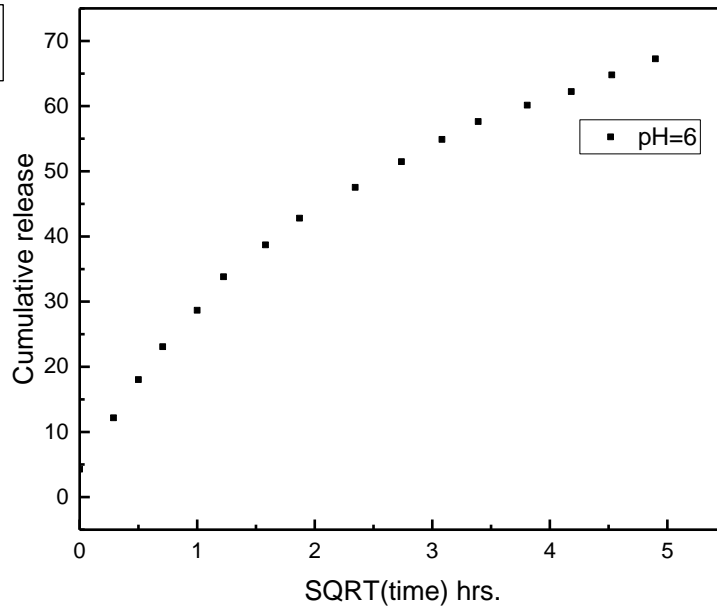


Figure 21. Plots showing the drug release of CUR:PAH NPs plotted using three different mathematical models: (a) zero order kinetic model, (b) first order kinetic model, and (c) Higuchi kinetic model.

Table 3. R² values of zero-order, first-order and Higuchi kinetic models for 1:2 CUR:PAH NPs release at different pH.

R² \ pH	4	6	7	8	10
Zero-order Model	0.7469	0.7705	0.7469	0.7889	0.2463
First-order Model	0.4583	0.488	0.4693	0.3801	0.1249
Higuchi Model	0.9273	0.9412	0.9284	0.9508	0.4386

Table 4. R² values of zero-order, first-order and Higuchi kinetic models for 1:2 PIP:CUR NPs release at different pH.

R² \ pH	4	6	7	8	10
Zero-order Model	0.5799	0.6183	0.587	0.6045	0.1962
First-order Model	0.3869	0.4183	0.4047	0.3007	0.1058
Higuchi Model	0.8081	0.8393	0.8159	0.8302	0.3608

Based on the R² values, the best kinetic model that fits the drug release can be determined by the linear plot having the highest R² values. From our results, it is apparent that CUR follows the Higuchi kinetic release model in its 2 types of NPs whereby, the highest R² values of 1:2 CUR:PAH NPs were 0.9273, 0.9412, 0.9284, 0.9508, and 0.4386 at pHs 4, 6, 7, 8, and 10 respectively. Similarly, the highest R² values of 1:2 PIP:CUR NPs were 0.8081, 0.8393, 0.8159, 0.8302, and 0.3608 at pHs 4, 6, 7, 8, and 10 respectively.

Since the R² values at pH 10 of both CUR-PAH NP and CUR-PIP-PAH NP were low (0.4386 and 0.3608 respectively), we checked if the release occurred in two phases: 1st phase during the 1st hour, and 2nd phase during the remaining time to reach

24 hours. R^2 values of zero-order, first-order and Higuchi kinetic models for CUR-PAH NP and CUR-PIP-PAH NP release at the 2 phases are shown in **Table 5**. Results showed that the R^2 values of both nanocapsule types during the two phases were highest when fitted into the Higuchi model (0.9948 and 0.6458 for CUR-PAH NP, and 0.9858 and 0.8483 for CUR-PIP-PAH NP for the 1st and 2nd phase respectively). This indicates that CUR was released from both types of capsules by diffusion but with a difference in the diffusion rate. This can be explained by the fast deprotonation of the cationic PAH polymer in extreme basic medium (pH 10) causing a disruption in the electrostatic forces and H-bonding between the polymer and CUR. This leads to an increase in the diffusion rate of CUR out of the nanocapsules during the 1st phase while a decrease in its diffusion rate during the second phase occurs due to the minimal release of CUR (10-15% only).

Table 5. R^2 values of zero-order, first-order and Higuchi kinetic models for CUR-PAH NP and CUR-PIP-PAH NP release at 2 phases of pH=10.

	CUR-PAH NP		CUR-PIP-PAH NP	
	1 st Phase	2 nd Phase	1 ST Phase	2 nd Phase
Zero-order Model	0.8942	0.6826	0.8491	0.7066
First-order Model	0.722	0.4727	0.6707	0.6946
Higuchi Model	0.9948	0.6458	0.9858	0.8483

Thus, the drug release profile of curcumin follows Higuchi model. Higuchi model is the best model that explains the process of drug release from a matrix system and is commonly applied to diffusion-controlled systems^{133,140}. The above results indicate that CUR is released from its nanosystem by the process of diffusion.

F. Cytotoxic effect of CUR-PAH NP and CUR-PIP-PAH NP

As indicated in **Figure 22**, the prepared 1:2 CUR:PAH NP treatment showed a time and dose dependent cytotoxic effect on Caco-2 cells. As shown, the IC_{50} (half maximal Inhibitory Concentration) of 1:2 CUR:PAH NP was around 25 μ M at 24 hrs, and above which higher concentrations didn't show an increase in the cytotoxicity. Interestingly, the IC_{50} of CUR alone was 74.9 μ M for Caco-2 cells at 24 hrs as reported in a study by Abdeldayem *et al.*²¹¹.

Thus having a lower IC_{50} value (25 μ M for NPs) compared to CUR alone (74.9 μ M) for the same cell line at the same time point indicates that our prepared 1:2 CUR:PAH NP enhances the cytotoxic effect of CUR alone by around 3 times.

Since 25 μ M of the prepared 1:2 CUR: PAH NP was most effective in decreasing % viability of Caco-2 cells after both 24 and 48 hrs, thus it was used for further investigation.

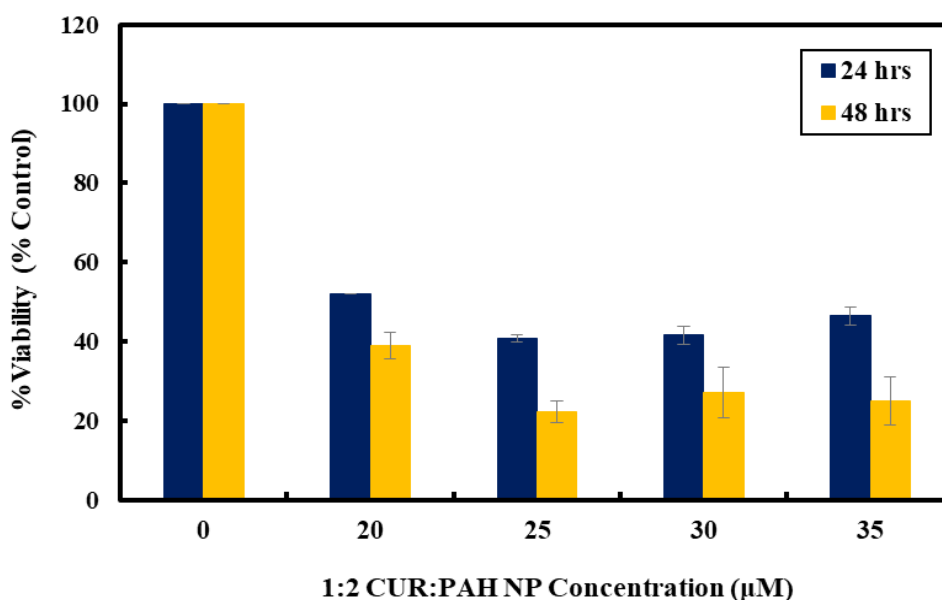
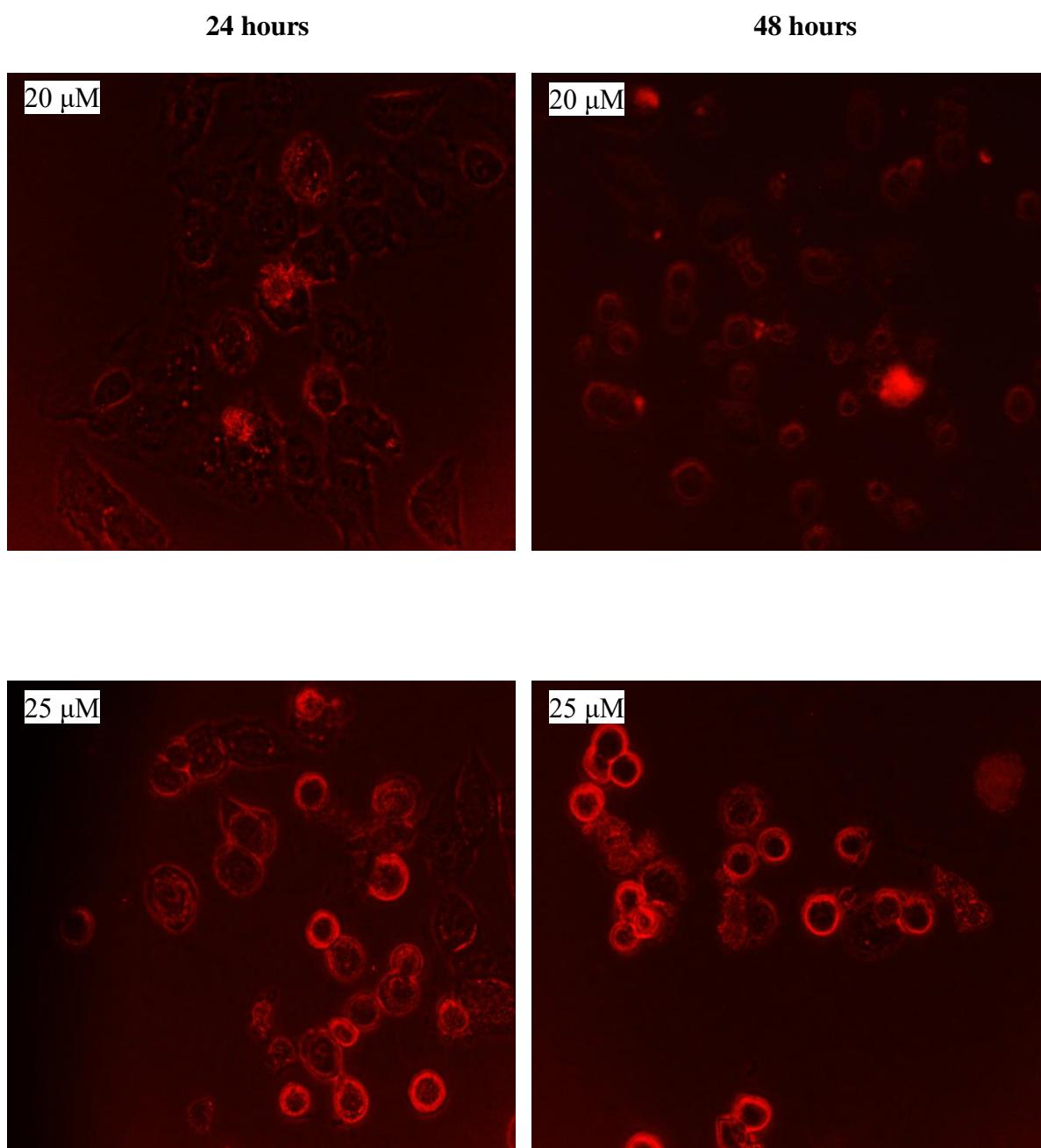


Figure 22. % Viability of Caco-2 cells treated with different concentrations of 1:2 CUR:PAH NPs.

Figure 23 shows the fluorescence images of Caco-2 cell uptake of different concentrations of CUR-PAH NP at 24 and 48 hours. It can be seen that 25 μM CUR-PAH NP shows the prominent localization of CUR into Caco-2 cells as well as a significant morphological change in the surface of cells characterized by blebbing and shrinkage which indicate apoptosis²¹².



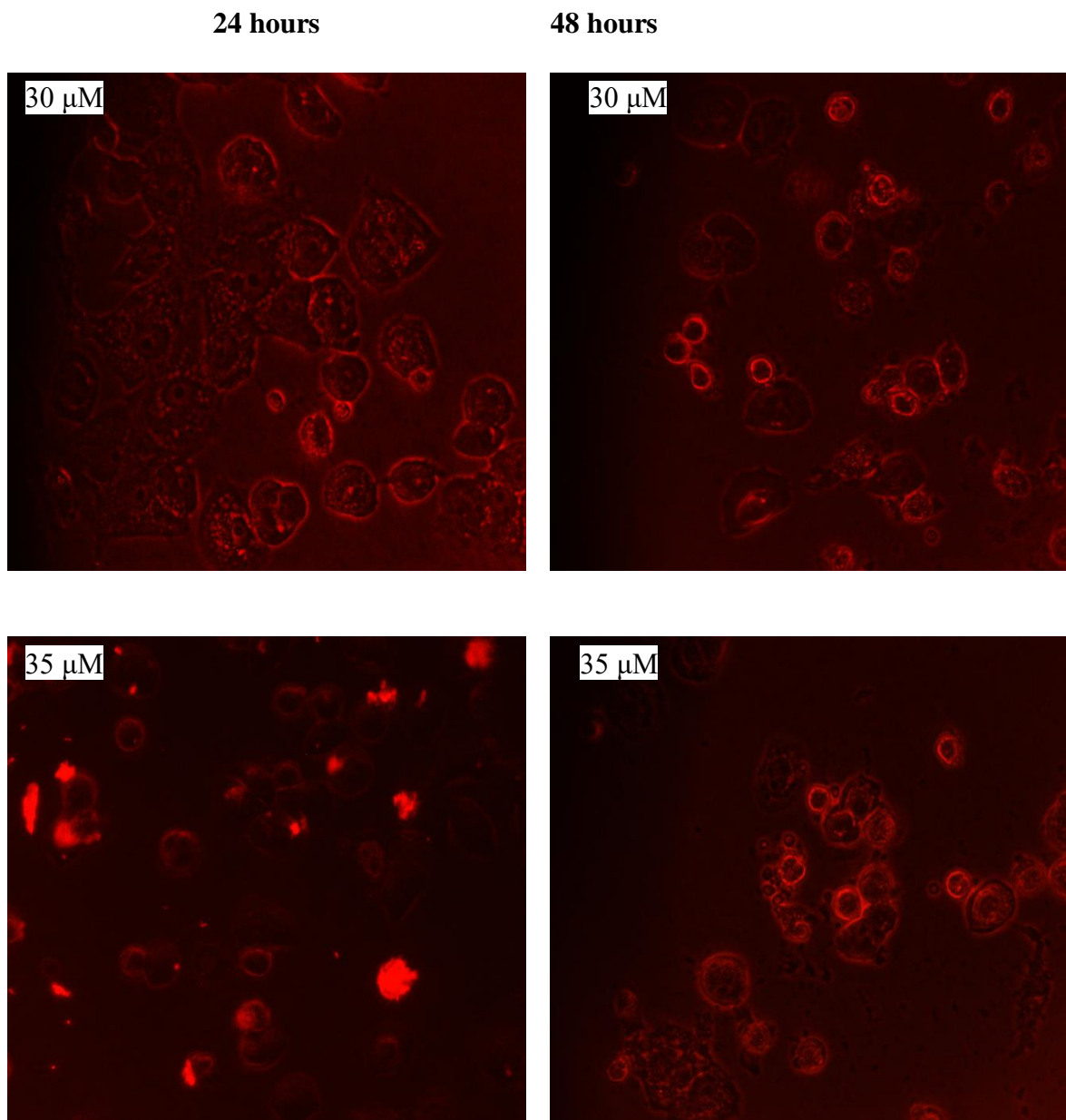


Figure 23. Fluorescence inverted microscope images of Caco-2 cell uptake of different concentrations of CUR-PAH NP at 24 and 48 hours.

As shown in **Figure 24**, the % viability of Caco2 cells decreased when treated with different types of CUR drugs compared to the control. This decrease proves that CUR, whether administered free or as nanoparticles, exerts a cytotoxic effect against Caco2 cells after 24 and 48 hours at a concentration of 25 μ M concentration (as mentioned earlier). Moreover, it can be seen that the % viability of the different types of

the administered NPs (CUR-PAH NP and CUR-PIP-PAH NP) showed lower % viability compared to CUR alone. Thus, as proven in many well-documented papers, the nanoprecipitation method enhances the bioavailability of CUR into Caco2 cells and correspondingly enhances the cytotoxic effect of CUR¹⁸¹⁻¹⁸³.

Furthermore, when PIP was incorporated into CUR-PAH NP at different ratios (1:4, 1:2 and 1:1), the % viability of cells decreased by 10%, 12% and 8% respectively compared to the 1:2 CUR:PAH NP. Hence, PIP improves the bioavailability of CUR inside the cancer cells where more CUR particles become accumulated inside the tumor cells which further enhances the cytotoxic effects of CUR NPs¹⁸⁷⁻¹⁸⁹.

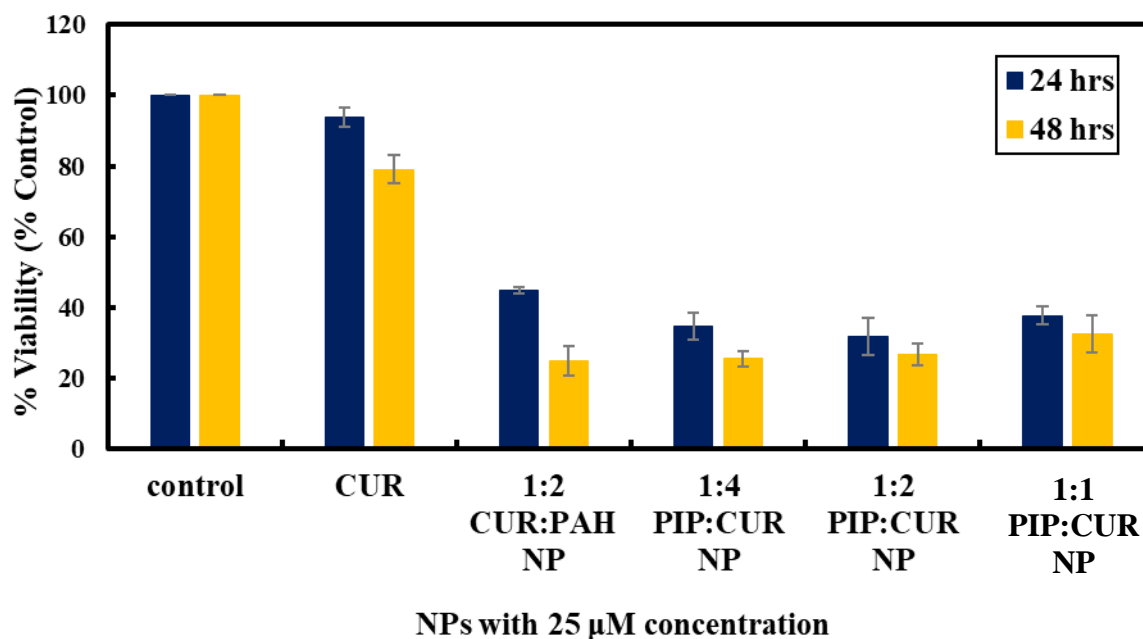
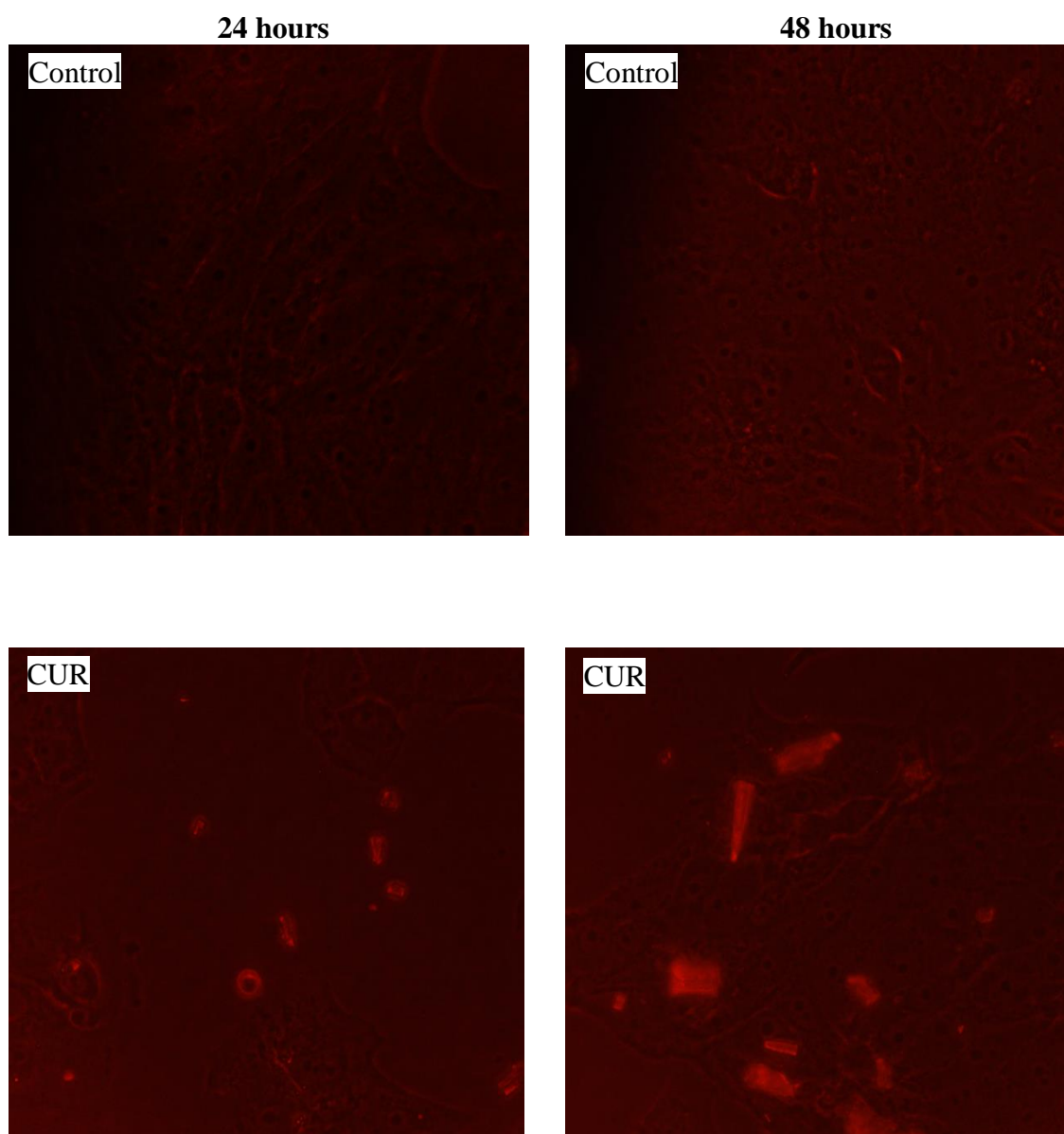


Figure 24. % Viability of Caco-2 cells treated with CUR, 1:2 CUR:PAH, and different ratios of PIP:CUR NPs.

Figure 25 shows the fluorescence images of untreated control, CUR treated, and 1:2 PIP:CUR treated Caco-2 cells at 24 and 48 hours. It can be seen that 1:2

PIP:CUR NPs showed significant localization of CUR into Caco-2 cells and thus enhance CUR bioavailability and delivery into cancer cells. Moreover, significant morphological changes in the surface of cells are observed which further confirm the enhanced apoptotic effects of CUR²¹².



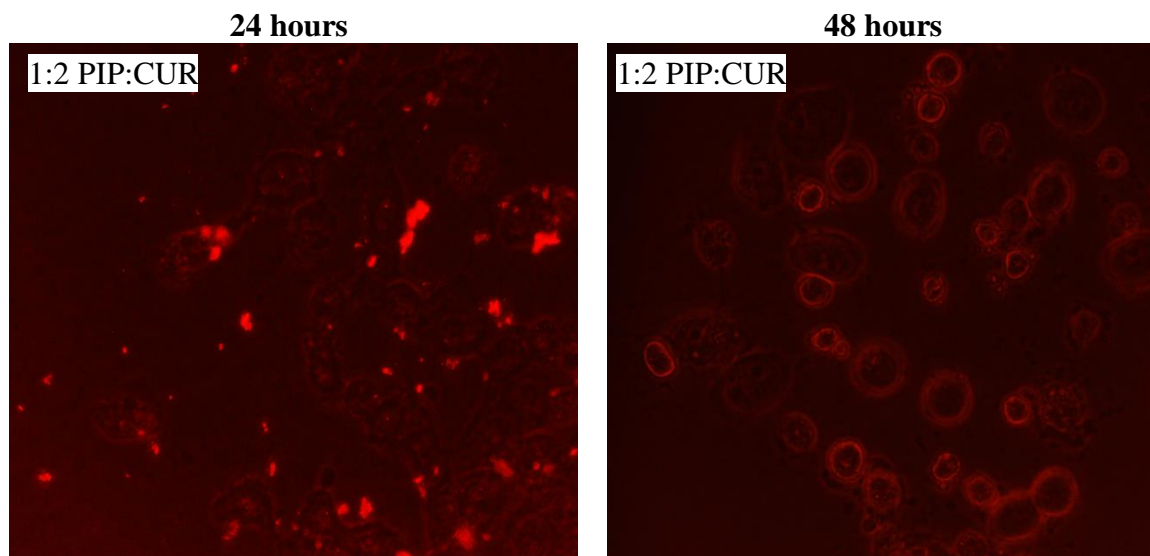


Figure 25. Fluorescence inverted microscope images of untreated Caco-2 cells (control), CUR and 1:2 PIP:CUR NPs treated cells at 24 and 48 hours.

CHAPTER V

IN VIVO STUDY

To decipher the *in vivo* effects of CUR-PAH NP against colorectal cancer (CRC), an intermediate-term commonly used mouse model of CRC was induced by the carcinogen 1,2-dimethylhydrazine (DMH)²¹³. Twenty-four female Balb/c mice were divided into four experimental groups as shown in **Table 6**.

Table 6. Experimental protocol.

Group A (control)	Mice were intraperitoneally (i.p.) injected with saline at 20 mg/Kg of body weight. Saline is the vehicle used to suspend DMH. Mice were injected once a week over a period of 12 weeks.
Group B (DMH 12-weeks)	Mice received DMH dissolved in saline (20 mg/Kg, i.p.) once per week over 12 weeks to induce CRC, and no further treatment for the next 6 weeks where they received only water.
Group C (DMH + Free polymer)	Mice received Free polymer starting 1 week after the twelfth DMH injection and continued over additional 6 weeks (5days/week).
Group D (post-treatment)	Mice received CUR-PAH NP (1:2 CUR:PAH ratio) starting 1 week after the twelfth DMH injection and continued over additional 6 weeks (5days/week).

In this study, we assessed the effect of CUR-PAH NP on the Wnt/ β -catenin signaling pathway which is aberrantly activated in CRC; targeting this pathway has revealed important insights towards novel therapies^{214,215}. The results of real time polymerase chain reaction (qRT-PCR) showed that CUR-PAH NP post-treatment

corrected the major aberrant alterations in the Wnt pathway observed compared to untreated DMH-induced CRC mice. Significant downregulation in the gene expression levels of Wnt, β -catenin and cyclin D1 by 20, 18, and 16 folds respectively, and upregulation in the gene expression level of adenomatous polyposis coli (APC) by 0.9 folds were observed in mice post-treated with CUR-PAH NP (see **Figure 26**).

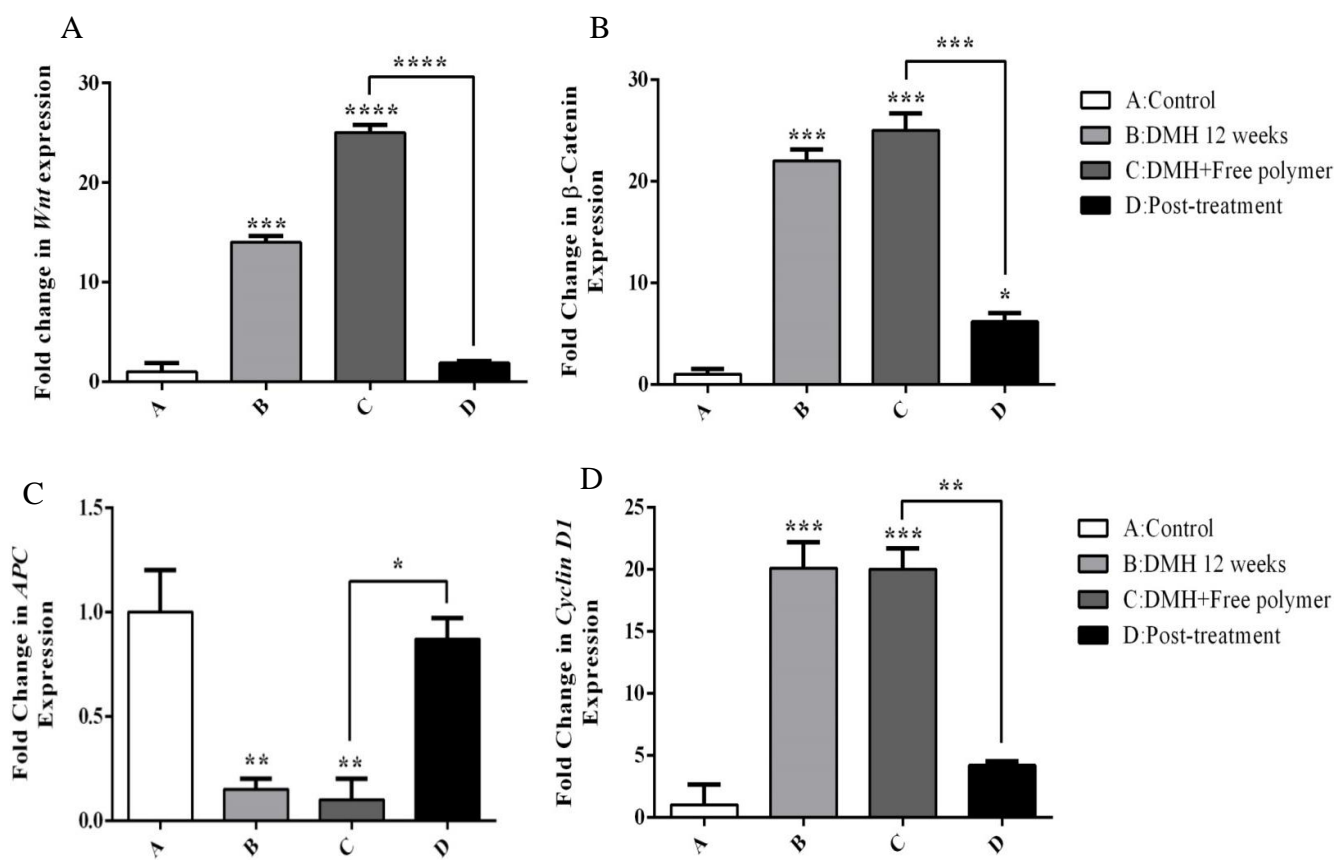


Figure 26. Effect of CUR-PAH NP on the expression of Wnt (A), β -Catenin (B), APC (C), and Cyclin D1 (D) genes. Expression levels of control and treated samples were normalized to their respective GAPDH, and the fold change was determined relative to the control. All bars represent mean of three determinations \pm SEM. (*), (**), (***), and (****) on bars correspond to p-value < 0.05 , < 0.01 , < 0.001 , and < 0.0001 respectively.

These results are consistent with previous studies where there is considerable evidence that the curcumin possesses anti-proliferative and apoptotic effects against various human cancer cell lines including colorectal cancer⁴³⁻⁴⁷.

Besides the Wnt signaling pathway, CRC is known to involve life-threatening complications of inflammation, where the pro-inflammatory enzymes cyclooxygenase-2 (COX-2) and inducible nitric oxide synthase (iNOS) were shown to favor carcinogenesis²¹⁶. Our results showed a significant increase in the level of COX-2 and activity of iNOS in DMH mice compared; however, post treatments with CUR-PAH NP resulted in significant downregulation in COX-2 levels by 83% and iNOS activities by 47% (see **Figure 27**). Likewise, our results demonstrate that CUR-PAH NP acted as COX-2 and iNOS inhibitors which is consistent with previous studies^{22,46,47}.

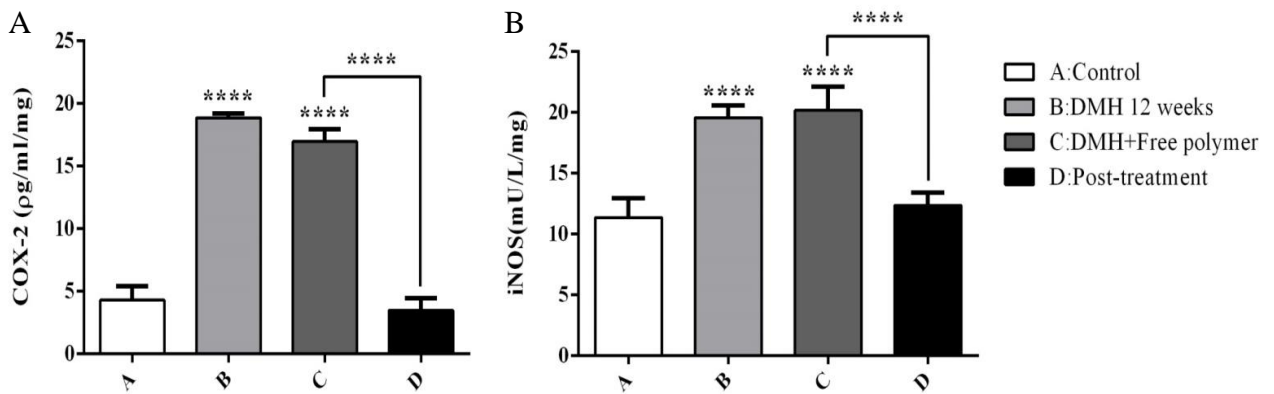


Figure 27. Effect of CUR-PAH NP on the COX-2 level and iNOS activity. Data are represented as mean \pm SD. (****) corresponds to p-value < 0.0001.

CHAPTER VI

CONCLUSION

This study aimed at developing two novel types of curcumin loaded biodegradable polymeric nanocapsules CUR-PAH NP and CUR-PIP-PAH NP. These Ns were successfully designed by self-assembled nanoprecipitation method. Their characteristics were identified by FTIR, XRD, SEM, DLS, and Zeta potential, their drug loading was assessed under different pH, and their effects against colon cancer were investigated both *in vitro* and *in vivo*. FTIR analysis proved CUR incorporation into both NPs, XRD proved the amorphous character of NPs, SEM showed the spherical shape of NPs. The drug loading and encapsulation efficiency of the two NP types were high. PIP, when added at a ratio of 1:2 PIP:CUR was shown to enhance encapsulation and the release of CUR which was optimum under basic medium compared to acidic and neutral conditions. Regarding their biological activity, both NPs interestingly exerted cytotoxic effects against colon cancer cells which were confirmed by % viability and fluorescent images that showed the cellular localization of NPs inside the Caco-2 cells as well as the distorted morphology of these cells indicating apoptosis. Similarly, the *in vivo* administration of CUR-PAH NP to mice with DMH induced CRC showed the ability to suppress cancer cell proliferation and inflammation through downregulating the Wnt signaling pathway as well as inhibiting COX-2 and iNOS enzymes. All in all, our findings indicate that CUR-PAH NP and CUR-PIP-PAH NP could be safely used as a promising approach for pharmaceutical applications including cancer drug delivery.

REFERENCES

1. Akram, M.; Shahab-Uddin, A. A.; Usmanghani, K.; Hannan, A.; Mohiuddin, E.; Asif, M., Curcuma longa and curcumin: a review article. *Rom J Biol Plant Biol* **2010**, *55* (2), 65-70.
2. Mohanty, C.; Das, M.; Sahoo, S. K., Emerging role of nanocarriers to increase the solubility and bioavailability of curcumin. *Expert opinion on drug delivery* **2012**, *9* (11), 1347-1364.
3. Goel, A.; Kunnumakkara, A. B.; Aggarwal, B. B., Curcumin as “Curecumin”: from kitchen to clinic. *Biochemical pharmacology* **2008**, *75* (4), 787-809.
4. Hewlings, S. J.; Kalman, D. S., Curcumin: A Review of Its' Effects on Human Health. *Foods* **2017**, *6* (10).
5. Gupta, S. C.; Kismali, G.; Aggarwal, B. B., Curcumin, a component of turmeric: from farm to pharmacy. *Biofactors* **2013**, *39* (1), 2-13.
6. Hatcher, H.; Planalp, R.; Cho, J.; Torti, F.; Torti, S., Curcumin: from ancient medicine to current clinical trials. *Cellular and Molecular Life Sciences* **2008**, *65* (11), 1631-1652.
7. Araujo, C. C.; Leon, L. L., Biological activities of Curcuma longa L. *Memorias do Instituto Oswaldo Cruz* **2001**, *96* (5), 723-8.
8. Aggarwal, B. B.; Takada, Y.; Oommen, O. V., From chemoprevention to chemotherapy: common targets and common goals. *Expert opinion on investigational drugs* **2004**, *13* (10), 1327-38.
9. Noorafshan, A.; Ashkani-Esfahani, S., A review of therapeutic effects of curcumin. *Current pharmaceutical design* **2013**, *19* (11), 2032-46.
10. Sundar Dhilip Kumar, S.; Houreld, N. N.; Abrahamse, H., Therapeutic Potential and Recent Advances of Curcumin in the Treatment of Aging-Associated Diseases. *Molecules* **2018**, *23* (4).
11. Liu, X. F.; Hao, J. L.; Xie, T.; Mukhtar, N. J.; Zhang, W.; Malik, T. H.; Lu, C. W.; Zhou, D. D., Curcumin, A Potential Therapeutic Candidate for Anterior Segment Eye Diseases: A Review. *Frontiers in pharmacology* **2017**, *8*, 66.
12. Mantzorou, M.; Pavlidou, E.; Vasios, G.; Tsagalioti, E.; Giaginis, C., Effects of curcumin consumption on human chronic diseases: A narrative review of the most recent clinical data. *Phytotherapy research : PTR* **2018**, *32* (6), 957-975.
13. Zheng, J.; Cheng, J.; Zheng, S.; Feng, Q.; Xiao, X., Curcumin, A Polyphenolic Curcuminoid With Its Protective Effects and Molecular Mechanisms in Diabetes and Diabetic Cardiomyopathy. *Frontiers in pharmacology* **2018**, *9*, 472.
14. Yang, Y. S.; Su, Y. F.; Yang, H. W.; Lee, Y. H.; Chou, J. I.; Ueng, K. C., Lipid-lowering effects of curcumin in patients with metabolic syndrome: a randomized,

- double-blind, placebo-controlled trial. *Phytotherapy research : PTR* **2014**, 28 (12), 1770-7.
15. Qin, S.; Huang, L.; Gong, J.; Shen, S.; Huang, J.; Ren, H.; Hu, H., Efficacy and safety of turmeric and curcumin in lowering blood lipid levels in patients with cardiovascular risk factors: a meta-analysis of randomized controlled trials. *Nutrition journal* **2017**, 16 (1), 68.
16. Lin, J. K.; Shih, C. A., Inhibitory effect of curcumin on xanthine dehydrogenase/oxidase induced by phorbol-12-myristate-13-acetate in NIH3T3 cells. *Carcinogenesis* **1994**, 15 (8), 1717-21.
17. Sreejayan; Rao, M. N., Nitric oxide scavenging by curcuminoids. *The Journal of pharmacy and pharmacology* **1997**, 49 (1), 105-7.
18. Abe, Y.; Hashimoto, S.; Horie, T., Curcumin inhibition of inflammatory cytokine production by human peripheral blood monocytes and alveolar macrophages. *Pharmacological research* **1999**, 39 (1), 41-7.
19. Reddy, A. C.; Lokesh, B. R., Studies on anti-inflammatory activity of spice principles and dietary n-3 polyunsaturated fatty acids on carrageenan-induced inflammation in rats. *Annals of nutrition & metabolism* **1994**, 38 (6), 349-58.
20. Venkatesan, N.; Chandrakasan, G., Modulation of cyclophosphamide-induced early lung injury by curcumin, an anti-inflammatory antioxidant. *Molecular and cellular biochemistry* **1995**, 142 (1), 79-87.
21. Zheng, Z.; Sun, Y.; Liu, Z.; Zhang, M.; Li, C.; Cai, H., The effect of curcumin and its nanoformulation on adjuvant-induced arthritis in rats. *Drug design, development and therapy* **2015**, 9, 4931-42.
22. Chainani-Wu, N., Safety and anti-inflammatory activity of curcumin: a component of tumeric (*Curcuma longa*). *The Journal of Alternative & Complementary Medicine* **2003**, 9 (1), 161-168.
23. Daily, J. W.; Yang, M.; Park, S., Efficacy of Turmeric Extracts and Curcumin for Alleviating the Symptoms of Joint Arthritis: A Systematic Review and Meta-Analysis of Randomized Clinical Trials. *Journal of medicinal food* **2016**, 19 (8), 717-29.
24. Cavaleri, F., Presenting a New Standard Drug Model for Turmeric and Its Prized Extract, Curcumin. *International journal of inflammation* **2018**, 2018, 5023429.
25. Toda, S.; Miyase, T.; Arichi, H.; Tanizawa, H.; Takino, Y., Natural antioxidants. III. Antioxidative components isolated from rhizome of *Curcuma longa* L. *Chemical & pharmaceutical bulletin* **1985**, 33 (4), 1725-8.
26. Cohly, H. H.; Taylor, A.; Angel, M. F.; Salahudeen, A. K., Effect of turmeric, turmerin and curcumin on H₂O₂-induced renal epithelial (LLC-PK1) cell injury. *Free radical biology & medicine* **1998**, 24 (1), 49-54.
27. Manikandan, P.; Sumitra, M.; Aishwarya, S.; Manohar, B. M.; Lokanadam, B.; Puvanakrishnan, R., Curcumin modulates free radical quenching in myocardial ischaemia in rats. *The international journal of biochemistry & cell biology* **2004**, 36 (10), 1967-80.

28. Calabrese, V.; Butterfield, D. A.; Stella, A. M., Nutritional antioxidants and the heme oxygenase pathway of stress tolerance: novel targets for neuroprotection in Alzheimer's disease. *The Italian journal of biochemistry* **2003**, *52* (4), 177-81.
29. Yang, F.; Lim, G. P.; Begum, A. N.; Ubeda, O. J.; Simmons, M. R.; Ambegaokar, S. S.; Chen, P. P.; Kayed, R.; Glabe, C. G.; Frautschy, S. A.; Cole, G. M., Curcumin inhibits formation of amyloid beta oligomers and fibrils, binds plaques, and reduces amyloid in vivo. *The Journal of biological chemistry* **2005**, *280* (7), 5892-901.
30. Maheshwari, R. K.; Singh, A. K.; Gaddipati, J.; Srimal, R. C., Multiple biological activities of curcumin: a short review. *Life sciences* **2006**, *78* (18), 2081-2087.
31. Farzaei, M. H.; Zobeiri, M.; Parvizi, F.; El-Senduny, F. F.; Marmouzi, I.; Coy-Barrera, E.; Naseri, R.; Nabavi, S. M.; Rahimi, R.; Abdollahi, M., Curcumin in Liver Diseases: A Systematic Review of the Cellular Mechanisms of Oxidative Stress and Clinical Perspective. *Nutrients* **2018**, *10* (7).
32. Perrone, D.; Ardito, F.; Giannatempo, G.; Dioguardi, M.; Troiano, G.; Lo Russo, L.; De Lillo, A.; Laino, L.; Lo Muzio, L., Biological and therapeutic activities, and anticancer properties of curcumin. *Experimental and therapeutic medicine* **2015**, *10* (5), 1615-1623.
33. Doello, K.; Ortiz, R.; Alvarez, P. J.; Melguizo, C.; Cabeza, L.; Prados, J., Latest in Vitro and in Vivo Assay, Clinical Trials and Patents in Cancer Treatment using Curcumin: A Literature Review. *Nutrition and cancer* **2018**, *70* (4), 569-578.
34. Wilken, R.; Veena, M. S.; Wang, M. B.; Srivatsan, E. S., Curcumin: A review of anti-cancer properties and therapeutic activity in head and neck squamous cell carcinoma. *Molecular cancer* **2011**, *10* (1), 12.
35. Limtrakul, P.; Lipigorngoson, S.; Namwong, O.; Apisariyakul, A.; Dunn, F. W., Inhibitory effect of dietary curcumin on skin carcinogenesis in mice. *Cancer letters* **1997**, *116* (2), 197-203.
36. Deshpande, S. S.; Ingle, A. D.; Maru, G. B., Chemopreventive efficacy of curcumin-free aqueous turmeric extract in 7,12-dimethylbenz[a]anthracene-induced rat mammary tumorigenesis. *Cancer letters* **1998**, *123* (1), 35-40.
37. Ushida, J.; Sugie, S.; Kawabata, K.; Pham, Q. V.; Tanaka, T.; Fujii, K.; Takeuchi, H.; Ito, Y.; Mori, H., Chemopreventive effect of curcumin on N-nitrosomethylbenzylamine-induced esophageal carcinogenesis in rats. *Japanese journal of cancer research : Gann* **2000**, *91* (9), 893-8.
38. Sreepriya, M.; Bali, G., Effects of administration of Embelin and Curcumin on lipid peroxidation, hepatic glutathione antioxidant defense and hematopoietic system during N-nitrosodiethylamine/Phenobarbital-induced hepatocarcinogenesis in Wistar rats. *Molecular and cellular biochemistry* **2006**, *284* (1-2), 49-55.
39. Mahady, G. B.; Pendland, S. L.; Yun, G.; Lu, Z. Z., Turmeric (*Curcuma longa*) and curcumin inhibit the growth of *Helicobacter pylori*, a group 1 carcinogen. *Anticancer research* **2002**, *22* (6C), 4179-81.

40. Allegra, A.; Innao, V.; Russo, S.; Gerace, D.; Alonci, A.; Musolino, C., Anticancer activity of curcumin and its analogues: Preclinical and clinical studies. *Cancer investigation* **2017**, *35* (1), 1-22.
41. Shishodia, S.; Chaturvedi, M. M.; Aggarwal, B. B., Role of curcumin in cancer therapy. *Current problems in cancer* **2007**, *31* (4), 243-305.
42. Tuorkey, M., Curcumin a potent cancer preventive agent: Mechanisms of cancer cell killing. *Interventional Medicine and Applied Science* **2014**, *6* (4), 139-146.
43. Siegel, R. L.; Miller, K. D.; Jemal, A., Cancer statistics, 2018. *CA: a cancer journal for clinicians* **2018**, *68* (1), 7-30.
44. Dulbecco, P.; Savarino, V., Therapeutic potential of curcumin in digestive diseases. *World journal of gastroenterology* **2013**, *19* (48), 9256-70.
45. Karunagaran, D.; Rashmi, R.; Kumar, T., Induction of apoptosis by curcumin and its implications for cancer therapy. *Current cancer drug targets* **2005**, *5* (2), 117-129.
46. Plummer, S. M.; Holloway, K. A.; Manson, M. M.; Munks, R. J.; Kaptein, A.; Farrow, S.; Howells, L., Inhibition of cyclo-oxygenase 2 expression in colon cells by the chemopreventive agent curcumin involves inhibition of NF- κ B activation via the NIK/IKK signalling complex. *Oncogene* **1999**, *18* (44), 6013.
47. Anand, P.; Sundaram, C.; Jhurani, S.; Kunnumakkara, A. B.; Aggarwal, B. B., Curcumin and cancer: an “old-age” disease with an “age-old” solution. *Cancer letters* **2008**, *267* (1), 133-164.
48. Wargovich, M. J.; Chen, C. D.; Jimenez, A.; Steele, V. E.; Velasco, M.; Stephens, L. C.; Price, R.; Gray, K.; Kelloff, G. J., Aberrant crypts as a biomarker for colon cancer: evaluation of potential chemopreventive agents in the rat. *Cancer epidemiology, biomarkers & prevention : a publication of the American Association for Cancer Research, cosponsored by the American Society of Preventive Oncology* **1996**, *5* (5), 355-60.
49. Kawamori, T.; Lubet, R.; Steele, V. E.; Kelloff, G. J.; Kaskey, R. B.; Rao, C. V.; Reddy, B. S., Chemopreventive effect of curcumin, a naturally occurring anti-inflammatory agent, during the promotion/progression stages of colon cancer. *Cancer research* **1999**, *59* (3), 597-601.
50. Bar-Sela, G.; Epelbaum, R.; Schaffer, M., Curcumin as an anti-cancer agent: review of the gap between basic and clinical applications. *Current medicinal chemistry* **2010**, *17* (3), 190-197.
51. Roy, M.; Chakraborty, S.; Siddiqi, M.; Bhattacharya, R. K., Induction of Apoptosis in Tumor Cells by Natural Phenolic Compounds. *Asian Pacific journal of cancer prevention : APJCP* **2002**, *3* (1), 61-67.
52. Chearwae, W.; Anuchapreeda, S.; Nandigama, K.; Ambudkar, S. V.; Limtrakul, P., Biochemical mechanism of modulation of human P-glycoprotein (ABCB1) by curcumin I, II, and III purified from Turmeric powder. *Biochemical pharmacology* **2004**, *68* (10), 2043-52.

53. Sharma, R. A.; McLelland, H. R.; Hill, K. A.; Ireson, C. R.; Euden, S. A.; Manson, M. M.; Pirmohamed, M.; Marnett, L. J.; Gescher, A. J.; Steward, W. P., Pharmacodynamic and pharmacokinetic study of oral Curcuma extract in patients with colorectal cancer. *Clinical cancer research : an official journal of the American Association for Cancer Research* **2001**, *7* (7), 1894-900.
54. Garcea, G.; Berry, D. P.; Jones, D. J.; Singh, R.; Dennison, A. R.; Farmer, P. B.; Sharma, R. A.; Steward, W. P.; Gescher, A. J., Consumption of the putative chemopreventive agent curcumin by cancer patients: assessment of curcumin levels in the colorectum and their pharmacodynamic consequences. *Cancer epidemiology, biomarkers & prevention : a publication of the American Association for Cancer Research, cosponsored by the American Society of Preventive Oncology* **2005**, *14* (1), 120-5.
55. Braumann, C.; Guenther, N.; Loeffler, L. M.; Dubiel, W., Liver metastases after colonic carcinoma--palliative chemotherapy plus curcumin. *International journal of colorectal disease* **2009**, *24* (7), 859-60.
56. He, Z. Y.; Shi, C. B.; Wen, H.; Li, F. L.; Wang, B. L.; Wang, J., Upregulation of p53 expression in patients with colorectal cancer by administration of curcumin. *Cancer investigation* **2011**, *29* (3), 208-13.
57. Lestari, M. L.; Indrayanto, G., Curcumin. In *Profiles of drug substances, excipients and related methodology*, Elsevier: 2014; Vol. 39, pp 113-204.
58. Indira Priyadarsini, K., Chemical and structural features influencing the biological activity of curcumin. *Current pharmaceutical design* **2013**, *19* (11), 2093-2100.
59. Metzler, M.; Pfeiffer, E.; Schulz, S. I.; Dempe, J. S., Curcumin uptake and metabolism. *Biofactors* **2013**, *39* (1), 14-20.
60. Manolova, Y.; Deneva, V.; Antonov, L.; Drakalska, E.; Momekova, D.; Lambov, N., The effect of the water on the curcumin tautomerism: a quantitative approach. *Spectrochimica acta. Part A, Molecular and biomolecular spectroscopy* **2014**, *132*, 815-20.
61. Sharma, R.; Gescher, A.; Steward, W., Curcumin: the story so far. *European journal of cancer* **2005**, *41* (13), 1955-1968.
62. Kolev, T. M.; Velcheva, E. A.; Stamboliyska, B. A.; Spiteller, M., DFT and experimental studies of the structure and vibrational spectra of curcumin. *International Journal of Quantum Chemistry* **2005**, *102* (6), 1069-1079.
63. Balasubramanian, K., Molecular orbital basis for yellow curry spice curcumin's prevention of Alzheimer's disease. *Journal of agricultural and food chemistry* **2006**, *54* (10), 3512-20.
64. Khopde, S. M.; Indira Priyadarsini, K.; Palit*, D. K.; Mukherjee, T., Effect of Solvent on the Excited-state Photophysical Properties of Curcumin[¶]. *Photochemistry and photobiology* **2000**, *72* (5), 625-631.

65. Shen, L.; Ji, H. F., Theoretical study on physicochemical properties of curcumin. *Spectrochimica acta. Part A, Molecular and biomolecular spectroscopy* **2007**, *67* (3-4), 619-23.
66. Kong, L.; Indira Priyadarsini, K.; Zhang, H.-Y., A theoretical investigation on intramolecular hydrogen-atom transfer in curcumin. *Journal of Molecular Structure: THEOCHEM* **2004**, *684* (1), 111-116.
67. Baiz, C. R.; Dunietz, B. D., Theoretical studies of conjugation effects on excited state intramolecular hydrogen-atom transfer reactions in model systems. *The journal of physical chemistry. A* **2007**, *111* (40), 10139-43.
68. Patra, D.; Barakat, C., Synchronous fluorescence spectroscopic study of solvatochromic curcumin dye. 2011; Vol. 79, p 1034-41.
69. Patra, D.; Barakat, C.; Tafech, R. M., Study on effect of lipophilic curcumin on sub-domain IIA site of human serum albumin during unfolded and refolded states: a synchronous fluorescence spectroscopic study. *Colloids and surfaces. B, Biointerfaces* **2012**, *94*, 354-61.
70. Moussa, Z.; Chebl, M.; Patra, D., Fluorescence of tautomeric forms of curcumin in different pH and biosurfactant rhamnolipids systems: Application towards on-off ratiometric fluorescence temperature sensing. 2017; Vol. 173.
71. Patra, D.; Moussawi, R., Photoluminescence studies of curcumin doped ZnO nanoparticles. 2015; p 374-377.
72. Ghosh, R.; Mondal, J. A.; Palit, D. K., Ultrafast dynamics of the excited states of curcumin in solution. *The Journal of Physical Chemistry B* **2010**, *114* (37), 12129-12143.
73. Joe, B.; Vijaykumar, M.; Lokesh, B., Biological properties of curcumin-cellular and molecular mechanisms of action. *Critical reviews in food science and nutrition* **2004**, *44* (2), 97-111.
74. Bong, P. H., Spectral and photophysical behaviors of curcumin and curcuminoids. *Bulletin of the Korean Chemical Society* **2000**, *21* (1), 81-86.
75. Shen, L.; Zhang, H. Y.; Ji, H. F., Successful application of TD-DFT in transient absorption spectra assignment. *Organic letters* **2005**, *7* (2), 243-6.
76. Galasso, V.; Kovac, B.; Modelli, A.; Ottaviani, M. F.; Pichierri, F., Spectroscopic and theoretical study of the electronic structure of curcumin and related fragment molecules. *The journal of physical chemistry. A* **2008**, *112* (11), 2331-8.
77. Chignell, C. F.; Bilskj, P.; Reszka, K. J.; Motten, A. G.; Sik, R. H.; Dahl, T. A., Spectral and photochemical properties of curcumin. *Photochemistry and photobiology* **1994**, *59* (3), 295-302.
78. Erez, Y.; Simkovitch, R.; Shomer, S.; Gepshtein, R.; Huppert, D., Effect of acid on the ultraviolet-visible absorption and emission properties of curcumin. *The Journal of Physical Chemistry A* **2014**, *118* (5), 872-884.

79. Schneider, C.; Gordon, O. N.; Edwards, R. L.; Luis, P. B., Degradation of Curcumin: From Mechanism to Biological Implications. *Journal of agricultural and food chemistry* **2015**, *63* (35), 7606-14.
80. Anand, P.; Kunnumakkara, A. B.; Newman, R. A.; Aggarwal, B. B., Bioavailability of curcumin: problems and promises. *Molecular pharmaceutics* **2007**, *4* (6), 807-818.
81. Burgos-Morón, E.; Calderón-Montaña, J. M.; Salvador, J.; Robles, A.; López-Lázaro, M., The dark side of curcumin. *International journal of cancer* **2010**, *126* (7), 1771-1775.
82. Bansal, S. S.; Goel, M.; Aqil, F.; Vadhanam, M. V.; Gupta, R. C., Advanced drug-delivery systems of curcumin for cancer chemoprevention. *Cancer prevention research* **2011**, canprevres. 0006.2010.
83. Yallapu, M. M.; Jaggi, M.; Chauhan, S. C., Curcumin nanoformulations: a future nanomedicine for cancer. *Drug discovery today* **2012**, *17* (1-2), 71-80.
84. Sun, M.; Su, X.; Ding, B.; He, X.; Liu, X.; Yu, A.; Lou, H.; Zhai, G., Advances in nanotechnology-based delivery systems for curcumin. *Nanomedicine* **2012**, *7* (7), 1085-1100.
85. Naksuriya, O.; Okonogi, S.; Schiffelers, R. M.; Hennink, W. E., Curcumin nanoformulations: a review of pharmaceutical properties and preclinical studies and clinical data related to cancer treatment. *Biomaterials* **2014**, *35* (10), 3365-3383.
86. Prasad, S.; Tyagi, A. K.; Aggarwal, B. B., Recent developments in delivery, bioavailability, absorption and metabolism of curcumin: the golden pigment from golden spice. *Cancer research and treatment: official journal of Korean Cancer Association* **2014**, *46* (1), 2.
87. Ghalandarlaki, N.; Alizadeh, A. M.; Ashkani-Esfahani, S., Nanotechnology-applied curcumin for different diseases therapy. *BioMed research international* **2014**, *2014*.
88. Banerjee, S.; Chakravarty, A. R., Metal complexes of curcumin for cellular imaging, targeting, and photoinduced anticancer activity. *Accounts of chemical research* **2015**, *48* (7), 2075-2083.
89. Jäger, R.; Lowery, R. P.; Calvanese, A. V.; Joy, J. M.; Purpura, M.; Wilson, J. M., Comparative absorption of curcumin formulations. *Nutrition journal* **2014**, *13* (1), 11.
90. Singh, R.; Lillard Jr, J. W., Nanoparticle-based targeted drug delivery. *Experimental and molecular pathology* **2009**, *86* (3), 215-223.
91. Hoffman, A. S., The origins and evolution of "controlled" drug delivery systems. *Journal of controlled release : official journal of the Controlled Release Society* **2008**, *132* (3), 153-63.
92. Hans, M.; Lowman, A., Biodegradable nanoparticles for drug delivery and targeting. *Current Opinion in Solid State and Materials Science* **2002**, *6* (4), 319-327.
93. Faraji, A. H.; Wipf, P., Nanoparticles in cellular drug delivery. *Bioorganic & medicinal chemistry* **2009**, *17* (8), 2950-2962.

94. Liu, Y.; Miyoshi, H.; Nakamura, M., Nanomedicine for drug delivery and imaging: a promising avenue for cancer therapy and diagnosis using targeted functional nanoparticles. *International journal of cancer* **2007**, *120* (12), 2527-2537.
95. Khanbabaie, R.; Jahanshahi, M., Revolutionary impact of nanodrug delivery on neuroscience. *Current neuropharmacology* **2012**, *10* (4), 370-92.
96. Shi, J.; Kantoff, P. W.; Wooster, R.; Farokhzad, O. C., Cancer nanomedicine: progress, challenges and opportunities. *Nat Rev Cancer* **2017**, *17* (1), 20-37.
97. Farokhzad, O. C.; Langer, R., Impact of nanotechnology on drug delivery. *ACS nano* **2009**, *3* (1), 16-20.
98. Couvreur, P., Nanoparticles in drug delivery: past, present and future. *Advanced drug delivery reviews* **2013**, *65* (1), 21-3.
99. Dahoumane, S. A.; Jeffryes, C.; Mechouet, M.; Agathos, S. N., Biosynthesis of Inorganic Nanoparticles: A Fresh Look at the Control of Shape, Size and Composition. *Bioengineering* **2017**, *4* (1).
100. Pugazhendhi, A.; Edison, T.; Karuppusamy, I.; Kathirvel, B., Inorganic nanoparticles: A potential cancer therapy for human welfare. *International journal of pharmaceutics* **2018**, *539* (1-2), 104-111.
101. Bonifácio, B. V.; da Silva, P. B.; dos Santos Ramos, M. A.; Negri, K. M. S.; Bauab, T. M.; Chorilli, M., Nanotechnology-based drug delivery systems and herbal medicines: a review. *International journal of nanomedicine* **2014**, *9*, 1.
102. Ranade, V. V.; Cannon, J. B., *Drug Delivery Systems, Third Edition*. Taylor & Francis: 2011.
103. Lu, Y.; Li, Y.; Wu, W., Injected nanocrystals for targeted drug delivery. *Acta pharmaceutica Sinica. B* **2016**, *6* (2), 106-13.
104. Mishra, N.; Pant, P.; Porwal, A.; Jaiswal, J.; Aquib Samad, M.; Tiwari, S., *Targeted Drug Delivery: A Review*. 2016; Vol. 6.
105. Wassei, J. K.; Tung, V. C.; Jonas, S. J.; Cha, K.; Dunn, B. S.; Yang, Y.; Kaner, R. B., Stenciling graphene, carbon nanotubes, and fullerenes using elastomeric lift-off membranes. *Advanced materials* **2010**, *22* (8), 897-901.
106. Abbasi, E.; Aval, S. F.; Akbarzadeh, A.; Milani, M.; Nasrabadi, H. T.; Joo, S. W.; Hanifehpour, Y.; Nejati-Koshki, K.; Pashaei-Asl, R., Dendrimers: synthesis, applications, and properties. *Nanoscale research letters* **2014**, *9* (1), 247.
107. Mendes, L. P.; Pan, J.; Torchilin, V. P., Dendrimers as Nanocarriers for Nucleic Acid and Drug Delivery in Cancer Therapy. *Molecules (Basel, Switzerland)* **2017**, *22* (9), E1401.
108. Soppimath, K. S.; Aminabhavi, T. M.; Kulkarni, A. R.; Rudzinski, W. E., Biodegradable polymeric nanoparticles as drug delivery devices. *Journal of controlled release : official journal of the Controlled Release Society* **2001**, *70* (1-2), 1-20.

109. Kataoka, K.; Harada, A.; Nagasaki, Y., Block copolymer micelles for drug delivery: design, characterization and biological significance. *Advanced drug delivery reviews* **2001**, *47* (1), 113-31.
110. Kopecek, J., Polymer-drug conjugates: origins, progress to date and future directions. *Advanced drug delivery reviews* **2013**, *65* (1), 49-59.
111. Kumari, A.; Yadav, S. K.; Yadav, S. C., Biodegradable polymeric nanoparticles based drug delivery systems. *Colloids and surfaces. B, Biointerfaces* **2010**, *75* (1), 1-18.
112. Reis, C. P.; Neufeld, R. J.; Veiga, F., Preparation of Drug-Loaded Polymeric Nanoparticles. In *Nanomedicine in Cancer*, Pan Stanford: 2017; pp 197-240.
113. Mora-Huertas, C.; Fessi, H.; Elaissari, A., Polymer-based nanocapsules for drug delivery. *International journal of pharmaceutics* **2010**, *385* (1-2), 113-142.
114. Prabhu, R. H.; Patravale, V. B.; Joshi, M. D., Polymeric nanoparticles for targeted treatment in oncology: current insights. *International journal of nanomedicine* **2015**, *10*, 1001-18.
115. Wilken, R.; Veena, M. S.; Wang, M. B.; Srivatsan, E. S., Curcumin: A review of anti-cancer properties and therapeutic activity in head and neck squamous cell carcinoma. *Molecular cancer* **2011**, *10*, 12.
116. Mahmood, K.; Zia, K. M.; Zuber, M.; Salman, M.; Anjum, M. N., Recent developments in curcumin and curcumin based polymeric materials for biomedical applications: a review. *International journal of biological macromolecules* **2015**, *81*, 877-890.
117. Mars, A.; Hamami, M.; Bechnak, L.; Patra, D.; Raouafi, N., Curcumin-graphene quantum dots for dual mode sensing platform: Electrochemical and fluorescence detection of APOe4, responsible of Alzheimer's disease. 2018; Vol. 1036.
118. Rejinold, N. S.; Muthunarayanan, M.; Divyarani, V. V.; Sreerekha, P. R.; Chennazhi, K. P.; Nair, S. V.; Tamura, H.; Jayakumar, R., Curcumin-loaded biocompatible thermoresponsive polymeric nanoparticles for cancer drug delivery. *Journal of colloid and interface science* **2011**, *360* (1), 39-51.
119. Anitha, A.; Deepagan, V.; Rani, V. D.; Menon, D.; Nair, S.; Jayakumar, R., Preparation, characterization, in vitro drug release and biological studies of curcumin loaded dextran sulphate–chitosan nanoparticles. *Carbohydrate Polymers* **2011**, *84* (3), 1158-1164.
120. Gangwar, R. K.; Tomar, G. B.; Dhumale, V. A.; Zinjarde, S.; Sharma, R. B.; Datar, S., Curcumin conjugated silica nanoparticles for improving bioavailability and its anticancer applications. *Journal of agricultural and food chemistry* **2013**, *61* (40), 9632-9637.
121. Manju, S.; Sreenivasan, K., Gold nanoparticles generated and stabilized by water soluble curcumin–polymer conjugate: blood compatibility evaluation and targeted drug delivery onto cancer cells. *Journal of colloid and interface science* **2012**, *368* (1), 144-151.

122. Zamarioli, C. M.; Martins, R. M.; Carvalho, E. C.; Freitas, L. A. P., Nanoparticles containing curcuminoids (*Curcuma longa*): development of topical delivery formulation. *Revista Brasileira de Farmacognosia* **2015**, *25* (1), 53-60.
123. Mimeault, M.; Batra, S. K., Potential applications of curcumin and its novel synthetic analogs and nanotechnology-based formulations in cancer prevention and therapy. *Chinese medicine* **2011**, *6* (1), 31.
124. Subramani, P. A.; Panati, K.; Narala, V. R., Curcumin nanotechnologies and its anticancer activity. *Nutrition and cancer* **2017**, *69* (3), 381-393.
125. Yen, F.-L.; Wu, T.-H.; Tzeng, C.-W.; Lin, L.-T.; Lin, C.-C., Curcumin nanoparticles improve the physicochemical properties of curcumin and effectively enhance its antioxidant and antihepatoma activities. *Journal of agricultural and food chemistry* **2010**, *58* (12), 7376-7382.
126. Sahu, A.; Kasoju, N.; Bora, U., Fluorescence study of the curcumin– casein micelle complexation and its application as a drug nanocarrier to cancer cells. *Biomacromolecules* **2008**, *9* (10), 2905-2912.
127. Langer, R. S.; Peppas, N. A., Present and future applications of biomaterials in controlled drug delivery systems. *Biomaterials* **1981**, *2* (4), 201-14.
128. Allen, T. M.; Cullis, P. R., Drug delivery systems: entering the mainstream. *Science* **2004**, *303* (5665), 1818-22.
129. Hofmeister, I.; Landfester, K.; Taden, A., Controlled formation of polymer nanocapsules with high diffusion-barrier properties and prediction of encapsulation efficiency. *Angewandte Chemie* **2015**, *54* (1), 327-30.
130. Leo, E.; Scatturin, A.; Vighi, E.; Dalpiaz, A., Polymeric nanoparticles as drug controlled release systems: a new formulation strategy for drugs with small or large molecular weight. *Journal of nanoscience and nanotechnology* **2006**, *6* (9-10), 3070-9.
131. Tiede, K.; Boxall, A. B.; Tear, S. P.; Lewis, J.; David, H.; Hasselov, M., Detection and characterization of engineered nanoparticles in food and the environment. *Food additives & contaminants. Part A, Chemistry, analysis, control, exposure & risk assessment* **2008**, *25* (7), 795-821.
132. Mouzouvi, C. R. A.; Umerska, A.; Bigot, A. K.; Saulnier, P., Surface active properties of lipid nanocapsules. *PloS one* **2017**, *12* (8), e0179211.
133. Dash, S.; Murthy, P. N.; Nath, L.; Chowdhury, P., Kinetic modeling on drug release from controlled drug delivery systems. *Acta Pol Pharm* **2010**, *67* (3), 217-23.
134. Uhrich, K. E.; Cannizzaro, S. M.; Langer, R. S.; Shakesheff, K. M., Polymeric systems for controlled drug release. *Chemical reviews* **1999**, *99* (11), 3181-98.
135. Ahuja, N.; Katare, O. P.; Singh, B., Studies on dissolution enhancement and mathematical modeling of drug release of a poorly water-soluble drug using water-soluble carriers. *European Journal of Pharmaceutics and Biopharmaceutics* **2007**, *65* (1), 26-38.

136. Fu, Y.; Kao, W. J., Drug release kinetics and transport mechanisms of non-degradable and degradable polymeric delivery systems. *Expert opinion on drug delivery* **2010**, 7 (4), 429-444.
137. D'Souza, S., A Review of In Vitro Drug Release Test Methods for Nano-Sized Dosage Forms. *Advances in Pharmaceutics* **2014**, 2014, 12.
138. Amatya, S.; Park, E. J.; Park, J. H.; Kim, J. S.; Seol, E.; Lee, H.; Choi, H.; Shin, Y.-H.; Na, D. H., Drug release testing methods of polymeric particulate drug formulations. *Journal of Pharmaceutical Investigation* **2013**, 43 (4), 259-266.
139. Wallace, S. J.; Li, J.; Nation, R. L.; Boyd, B. J., Drug release from nanomedicines: Selection of appropriate encapsulation and release methodology. *Drug delivery and translational research* **2012**, 2 (4), 284-92.
140. Higuchi, T., Mechanism of sustained-action medication. Theoretical analysis of rate of release of solid drugs dispersed in solid matrices. *Journal of pharmaceutical sciences* **1963**, 52 (12), 1145-1149.
141. Ho, B. N.; Pfeffer, C. M.; Singh, A. T. K., Update on Nanotechnology-based Drug Delivery Systems in Cancer Treatment. *Anticancer research* **2017**, 37 (11), 5975-5981.
142. Din, F. U.; Aman, W.; Ullah, I.; Qureshi, O. S.; Mustapha, O.; Shafique, S.; Zeb, A., Effective use of nanocarriers as drug delivery systems for the treatment of selected tumors. *International journal of nanomedicine* **2017**, 12, 7291-7309.
143. Schmaljohann, D., Thermo- and pH-responsive polymers in drug delivery. *Advanced drug delivery reviews* **2006**, 58 (15), 1655-70.
144. Decher, G., Fuzzy nanoassemblies: toward layered polymeric multicomposites. *science* **1997**, 277 (5330), 1232-1237.
145. Lvov, Y.; Decher, G.; Moehwald, H., Assembly, structural characterization, and thermal behavior of layer-by-layer deposited ultrathin films of poly (vinyl sulfate) and poly (allylamine). *Langmuir* **1993**, 9 (2), 481-486.
146. Kittitheeranun, P.; Sajomsang, W.; Phanpee, S.; Treetong, A.; Wutikhun, T.; Suktham, K.; Puttipipatkachorn, S.; Ruktanonchai, U. R., Layer-by-layer engineered nanocapsules of curcumin with improved cell activity. *International journal of pharmaceutics* **2015**, 492 (1-2), 92-102.
147. Ariga, K.; Hill, J. P.; Ji, Q., Layer-by-layer assembly as a versatile bottom-up nanofabrication technique for exploratory research and realistic application. *Physical chemistry chemical physics : PCCP* **2007**, 9 (19), 2319-40.
148. Wang, Y.; Angelatos, A. S.; Caruso, F., Template Synthesis of Nanostructured Materials via Layer-by-Layer Assembly. *Chemistry of Materials* **2008**, 20 (3), 848-858.
149. Liu, Y.; Yang, J.; Zhao, Z.; Li, J.; Zhang, R.; Yao, F., Formation and characterization of natural polysaccharide hollow nanocapsules via template layer-by-layer self-assembly. *Journal of colloid and interface science* **2012**, 379 (1), 130-40.

150. Leroux, J. C.; Allémann, E.; Doelker, E.; Gurny, R., New approach for the preparation of nanoparticles by an emulsification-diffusion method. 1995; Vol. 41, p 14-18.
151. Kumar, S.; Dilbaghi, N.; Rani, R.; Bhanjana, G., Nanotechnology as Emerging Tool for Enhancing Solubility of Poorly Water-Soluble Drugs. 2012; Vol. 2.
152. Fessi, H.; Puisieux, F.; Devissaguet, J. P.; Ammoury, N.; Benita, S., Nanocapsule formation by interfacial polymer deposition following solvent displacement. *International journal of pharmaceutics* **1989**, 55 (1), R1-R4.
153. Beck-Broichsitter, M.; Rytting, E.; Lehardt, T.; Wang, X.; Kissel, T., Preparation of nanoparticles by solvent displacement for drug delivery: a shift in the "ouzo region" upon drug loading. *European journal of pharmaceutical sciences : official journal of the European Federation for Pharmaceutical Sciences* **2010**, 41 (2), 244-53.
154. Piñón-Segundo, E.; Ganem-Quintanar, A.; Rafael Garibay-Bermúdez, J.; Juan Escobar-Chávez, J.; López-Cervantes, M.; Quintanar-Guerrero, D., Preparation of Nanoparticles by Solvent Displacement Using a Novel Recirculation System. *Pharmaceutical Development and Technology* **2006**, 11 (4), 493-501.
155. Prathap Chandran, S.; Ghatak, J.; Satyam, P. V.; Sastry, M., Interfacial deposition of Ag on Au seeds leading to Au@Ag shell in organic media. *Journal of colloid and interface science* **2007**, 312 (2), 498-505.
156. Brinker, C. J.; Lu, Y.; Sellinger, A.; Fan, H., Evaporation-induced self-assembly: nanostructures made easy. *Advanced materials* **1999**, 11 (7), 579-585.
157. Rosler, A.; Vandermeulen, G. W.; Klok, H. A., Advanced drug delivery devices via self-assembly of amphiphilic block copolymers. *Advanced drug delivery reviews* **2012**, 53 (1), 95-108.
158. Hill, J. P.; Shrestha, L. K.; Ishihara, S.; Ji, Q.; Ariga, K., Self-assembly: from amphiphiles to chromophores and beyond. *Molecules* **2014**, 19 (6), 8589-609.
159. Kim, D.; Kim, E.; Lee, J.; Hong, S.; Sung, W.; Lim, N.; Park, C. G.; Kim, K., Direct synthesis of polymer nanocapsules: self-assembly of polymer hollow spheres through irreversible covalent bond formation. *Journal of the American Chemical Society* **2010**, 132 (28), 9908-19.
160. Lin, Y.; Böker, A.; He, J.; Sill, K.; Xiang, H.; Abetz, C.; Li, X.; Wang, J.; Emrick, T.; Long, S., Self-directed self-assembly of nanoparticle/copolymer mixtures. *Nature* **2005**, 434 (7029), 55.
161. Boal, A. K.; Ilhan, F.; DeRouchey, J. E.; Thurn-Albrecht, T.; Russell, T. P.; Rotello, V. M., Self-assembly of nanoparticles into structured spherical and network aggregates. *Nature* **2000**, 404 (6779), 746.
162. Wong, M. S.; Cha, J. N.; Choi, K.-S.; Deming, T. J.; Stucky, G. D., Assembly of Nanoparticles into Hollow Spheres Using Block Copolypeptides. *Nano letters* **2002**, 2 (6), 583-587.

163. Richards, G. J.; Hill, J. P.; Labuta, J.; Wakayama, Y.; Akada, M.; Ariga, K., Self-assembled pyrazinacene nanotubes. *Physical chemistry chemical physics : PCCP* **2011**, *13* (11), 4868-76.
164. Ozbas, B.; Kretsinger, J.; Rajagopal, K.; Schneider, J. P.; Pochan, D. J., Salt-Triggered Peptide Folding and Consequent Self-Assembly into Hydrogels with Tunable Modulus. *Macromolecules* **2004**, *37* (19), 7331-7337.
165. Olson, M. A.; Coskun, A.; Klajn, R.; Fang, L.; Dey, S. K.; Browne, K. P.; Grzybowski, B. A.; Stoddart, J. F., Assembly of polygonal nanoparticle clusters directed by reversible noncovalent bonding interactions. *Nano letters* **2009**, *9* (9), 3185-90.
166. Grzelczak, M.; Vermant, J.; Furst, E. M.; Liz-Marzán, L. M., Directed self-assembly of nanoparticles. *ACS nano* **2010**, *4* (7), 3591-3605.
167. Mazzarino, L.; Dora, C. L.; Bellettini, I. C.; Minatti, E.; Cardoso, S. G.; Lemos-Senna, E., Curcumin-loaded polymeric and lipid nanocapsules: preparation, characterization and chemical stability evaluation. *Lat Am J Pharm* **2010**, *29* (6), 933-40.
168. Rahimi, H. R.; Nedaeinia, R.; Shamloo, A. S.; Nikdoust, S.; Oskuee, R. K., Novel delivery system for natural products: Nano-curcumin formulations. *Avicenna journal of phytomedicine* **2016**, *6* (4), 383.
169. Beloqui, A.; Coco, R.; Memvanga, P. B.; Ucakar, B.; des Rieux, A.; Pr at, V., pH-sensitive nanoparticles for colonic delivery of curcumin in inflammatory bowel disease. *International journal of pharmaceutics* **2014**, *473* (1-2), 203-212.
170. Shlar, I.; Poverenov, E.; Vinokur, Y.; Horev, B.; Droby, S.; Rodov, V., High-throughput screening of nanoparticle-stabilizing ligands: Application to preparing antimicrobial curcumin nanoparticles by antisolvent precipitation. *Nano-Micro Letters* **2015**, *7* (1), 68-79.
171. Goycoolea, F.; Valle-Gallego, A.; Stefani, R.; Menchicchi, B.; David, L.; Rochas, C.; Santander-Ortega, M.; Alonso, M., *Chitosan-based nanocapsules: Physical characterization, stability in biological media and capsaicin encapsulation*. 2012; Vol. 290.
172. El Khoury, E.; Abiad, M.; Kassaify, Z.; Patra, D., Green Synthesis of Curcumin Conjugated Nano Silver for the Applications in Nucleic Acid Sensing and Anti-bacterial Activity. 2015; Vol. 127C.
173. Patra, D.; Moussawi, R., Curcumin conjugated gold nanoparticles for nucleic acid sensing. 2015; p 401-404.
174. Moussawi, R.; Patra, D., Synthesis of Au Nanorods through Pre-Reduction with Curcumin: Preferential Enhancement of Au Nanorods Formation Prepared from CTAB Capped over Citrate Capped Au Seeds. 2015; Vol. 119, p 150803161314005.
175. Moussa, Z.; Hmadeh, M.; Abiad, M.; Dib, O.; Patra, D., Encapsulation of curcumin in cyclodextrin-metal organic frameworks: Dissociation of loaded CD-MOFs enhances stability of curcumin. 2016; Vol. 212.

176. Mouslmani, M.; Bouhadir, K.; Patra, D., Poly (9-(2-diallylaminoethyl)adenine HCl-co-sulfur dioxide) deposited on silica nanoparticles constructs hierarchically ordered nanocapsules: Curcumin conjugated nanocapsules as a novel strategy to amplify guanine selectivity among nucleobases. 2015; Vol. 68.
177. Mukerjee, A.; Vishwanatha, J. K., Formulation, characterization and evaluation of curcumin-loaded PLGA nanospheres for cancer therapy. *Anticancer research* **2009**, *29* (10), 3867-3875.
178. Yallapu, M. M.; Khan, S.; Maher, D. M.; Ebeling, M. C.; Sundram, V.; Chauhan, N.; Ganju, A.; Balakrishna, S.; Gupta, B. K.; Zafar, N., Anti-cancer activity of curcumin loaded nanoparticles in prostate cancer. *Biomaterials* **2014**, *35* (30), 8635-8648.
179. Bisht, S.; Feldmann, G.; Soni, S.; Ravi, R.; Karikar, C.; Maitra, A.; Maitra, A., Polymeric nanoparticle-encapsulated curcumin ("nanocurcumin"): a novel strategy for human cancer therapy. *Journal of nanobiotechnology* **2007**, *5* (1), 3.
180. Yang, R.; Zhang, S.; Kong, D.; Gao, X.; Zhao, Y.; Wang, Z., Biodegradable polymer-curcumin conjugate micelles enhance the loading and delivery of low-potency curcumin. *Pharmaceutical research* **2012**, *29* (12), 3512-3525.
181. Gou, M.; Men, K.; Shi, H.; Xiang, M.; Zhang, J.; Song, J.; Long, J.; Wan, Y.; Luo, F.; Zhao, X., Curcumin-loaded biodegradable polymeric micelles for colon cancer therapy in vitro and in vivo. *Nanoscale* **2011**, *3* (4), 1558-1567.
182. Klippstein, R.; Wang, J. T. W.; El-Gogary, R. I.; Bai, J.; Mustafa, F.; Rubio, N.; Bansal, S.; Al-Jamal, W. T.; Al-Jamal, K. T., Passively Targeted Curcumin-Loaded PEGylated PLGA Nanocapsules for Colon Cancer Therapy In Vivo. *small* **2015**, *11* (36), 4704-4722.
183. Udompornmongkol, P.; Chiang, B. H., Curcumin-loaded polymeric nanoparticles for enhanced anti-colorectal cancer applications. *Journal of biomaterials applications* **2015**, *30* (5), 537-46.
184. Abbas, S.; Karangwa, E.; Bashari, M.; Hayat, K.; Hong, X.; Sharif, H. R.; Zhang, X., Fabrication of polymeric nanocapsules from curcumin-loaded nanoemulsion templates by self-assembly. *Ultrasonics sonochemistry* **2015**, *23*, 81-92.
185. Patra, D.; Sleem, F., A new method for pH triggered curcumin release by applying poly(L-lysine) mediated nanoparticle-congregation. *Analytica chimica acta* **2013**, *795*, 60-8.
186. Chebl, M.; Abiad, M.; Moussa, Z.; Patra, D., Two Modes of Associations of Curcumin with Pre- and Nano-Aggregated Chitosan Oligosaccharide Lactate: Ionic Strength and Hydrophobic Bile Salt Modulate Partition of Drug and Self-Assembly Process. 2016; Vol. 120.
187. Moorthi, C.; Krishnan, K.; Manavalan, R.; Kathiresan, K., Preparation and characterization of curcumin-piperine dual drug loaded nanoparticles. *Asian Pacific journal of tropical biomedicine* **2012**, *2* (11), 841-848.
188. Moorthi, C.; Kathiresan, K., Curcumin-Piperine/Curcumin-Quercetin/Curcumin-Silibinin dual drug-loaded nanoparticulate combination therapy: A novel approach to

target and treat multidrug-resistant cancers. *Journal of Medical Hypotheses and Ideas* **2013**, 7 (1), 15-20.

189. Shaikh, J.; Ankola, D.; Beniwal, V.; Singh, D.; Kumar, M. R., Nanoparticle encapsulation improves oral bioavailability of curcumin by at least 9-fold when compared to curcumin administered with piperine as absorption enhancer. *European Journal of Pharmaceutical Sciences* **2009**, 37 (3-4), 223-230.

190. Wang, Y.; Bansal, V.; Zelikin, A. N.; Caruso, F., Templated Synthesis of Single-Component Polymer Capsules and Their Application in Drug Delivery. *Nano letters* **2008**, 8 (6), 1741-1745.

191. Lu, Y.; Chen, X.; Hu, W.; Lu, N.; Sun, J.; Shen, J., Room-Temperature Imprinting Poly(acrylic acid)/Poly(allylamine hydrochloride) Multilayer Films by Using Polymer Molds. *Langmuir* **2007**, 23 (6), 3254-3259.

192. Li, H.; Zheng, H.; Tong, W.; Gao, C., Non-covalent assembly of poly(allylamine hydrochloride)/triethylamine microcapsules with ionic strength-responsiveness and auto-fluorescence. *Journal of colloid and interface science* **2017**, 496, 228-234.

193. Janeesh, P. A.; Sami, H.; Dhanya, C. R.; Sivakumar, S.; Abraham, A., Biocompatibility and genotoxicity studies of polyallylamine hydrochloride nanocapsules in rats. *RSC Advances* **2014**, 4 (47), 24484-24497.

194. Zhang, P.; Song, X.; Tong, W.; Gao, C., Nanoparticle/Polymer assembled microcapsules with pH sensing property. *Macromolecular bioscience* **2014**, 14 (10), 1495-504.

195. Vinogradova, O. I.; Lebedeva, O. V.; Vasilev, K.; Gong, H.; Garcia-Turiel, J.; Kim, B. S., Multilayer DNA/poly(allylamine hydrochloride) microcapsules: assembly and mechanical properties. *Biomacromolecules* **2005**, 6 (3), 1495-502.

196. Wang, B.; Zhang, Y.; Mao, Z.; Gao, C., Cellular uptake of covalent poly(allylamine hydrochloride) microcapsules and its influences on cell functions. *Macromolecular bioscience* **2012**, 12 (11), 1534-45.

197. Ruesing, J.; Rotan, O.; Gross-Heitfeld, C.; Mayer, C.; Epple, M., Nanocapsules of a cationic polyelectrolyte and nucleic acid for efficient cellular uptake and gene transfer. *Journal of Materials Chemistry B* **2014**, 2 (29), 4625-4630.

198. Yoshikawa, Y.; Matsuoka, H.; Ise, N., 'Ordered' Structure of Polyallylamine Hydrochloride in Dilute Solutions as Studied by Small Angle X-ray Scattering. *British polymer journal* **1986**, 18 (4), 242-246.

199. Lu, Y.; Hu, W.; Ma, Y.; Zhang, L.; Sun, J.; Lu, N.; Shen, J., Patterning Layered Polymeric Multilayer Films by Room-Temperature Nanoimprint Lithography. *Macromolecular Rapid Communications* **2006**, 27 (7), 505-510.

200. Ball, V.; Winterhalter, M.; Schwinte, P.; Lavalle, P.; Voegel, J. C.; Schaaf, P., Complexation Mechanism of Bovine Serum Albumin and Poly(allylamine hydrochloride). *The Journal of Physical Chemistry B* **2002**, 106 (9), 2357-2364.

201. Zheng, Z.; Zhang, X.; Carbo, D.; Clark, C.; Nathan, C.; Lvov, Y., Sonication-assisted synthesis of polyelectrolyte-coated curcumin nanoparticles. *Langmuir* **2010**, *26* (11), 7679-81.
202. Mouslmani, M. A. Poly-amine based tailored made ordered nanocapsule: preparation fluorescence study and application. 2014.
203. Rana, R.; Murthy, V. S.; Yu, J.; Wong, M. S., *Nanoparticle Self-Assembly of Hierarchically Ordered Microcapsule Structures*. 2005; Vol. 17, p 1145-1150.
204. Mouslmani, M.; Rosenholm, J. M.; Prabhakar, N.; Peurla, M.; Baydoun, E.; Patra, D., Curcumin associated poly (allylamine hydrochloride)-phosphate self-assembled hierarchically ordered nanocapsules: size dependent investigation on release and DPPH scavenging activity of curcumin. *RSC Advances* **2015**, *5* (24), 18740-18750.
205. Yen, F. L.; Wu, T. H.; Tzeng, C. W.; Lin, L. T.; Lin, C. C., Curcumin nanoparticles improve the physicochemical properties of curcumin and effectively enhance its antioxidant and antihepatoma activities. *Journal of agricultural and food chemistry* **2010**, *58* (12), 7376-82.
206. Jithan, A.; Madhavi, K.; Madhavi, M.; Prabhakar, K., Preparation and characterization of albumin nanoparticles encapsulating curcumin intended for the treatment of breast cancer. *International journal of pharmaceutical investigation* **2011**, *1* (2), 119-25.
207. Honary, S.; Zahir, F., Effect of Zeta Potential on the Properties of Nano-Drug Delivery Systems - A Review (Part 2). *Tropical Journal of Pharmaceutical Research*. **2013**, *12* (2), 265-273.
208. Zhao, H. C.; Wu, X. T.; Tian, W. W.; Ren, S. T., Synthesis and Thermal Property of Poly(Allylamine Hydrochloride). *Advanced Materials Research* **2011**, *150-151*, 1480-1483.
209. Gorgani, L.; Mohammadi, M.; Najafpour, G. D.; Nikzad, M., Piperine—The Bioactive Compound of Black Pepper: From Isolation to Medicinal Formulations. *Comprehensive Reviews in Food Science and Food Safety* **2017**, *16* (1), 124-140.
210. Eaton, P. ; Quaresma, P.; Soares, C.; Neves, C.; de Almeida, M. P.; Pereira, E.; West, P., A direct comparison of experimental methods to measure dimensions of synthetic nanoparticles. *Ultramicroscopy* **2017**, *182*, 179-190.
211. Abdeldayem, S. ; Hamdallah, Z. ; Abdelfattah, B. ; Ali, F. ; Mohamed, A., INVITRO Evaluation of Anti-Cancer Activity of 5-Flourouracil and Curcumin in Single and Combined Forms Against Breast and Colon Cancer Cell Lines. *Int J of Adv Res* **2016**, *4*(6), 1649-1657.
212. Syed Abdul Rahman, S. N.; Abdul Wahab, N.; Abd Malek, S. N., In Vitro Morphological Assessment of Apoptosis Induced by Antiproliferative Constituents from the Rhizomes of *Curcuma zedoaria*. *Evidence-based complementary and alternative medicine : eCAM* **2013**, *2013*, 257108.

213. Washington, M. K.; Powell, A. E.; Sullivan, R.; Sundberg, J. P.; Wright, N.; Coffey, R. J.; Dove, W. F., Pathology of rodent models of intestinal cancer: progress report and recommendations. *Gastroenterology* **2013**, *144* (4), 705-17.
214. Li, Z.-Y.; Liu, W.-P.; Zhao, M.-R., Crosstalk between Wnt/ β -catenin and Hedgehog/Gli signaling pathways in colon cancer and implications for therapy AU - Song, Li. *Cancer Biology & Therapy* **2015**, *16* (1), 1-7.
215. Fonseca, B. F.; Predes, D.; Cerqueira, D. M.; Reis, A. H.; Amado, N. G.; Cayres, M. C.; Kuster, R. M.; Oliveira, F. L.; Mendes, F. A.; Abreu, J. G., Derricin and derricin inhibit Wnt/beta-catenin signaling and suppress colon cancer cell growth in vitro. *PloS one* **2015**, *10* (3), e0120919.
216. DiDonato, J. A.; Mercurio, F.; Karin, M., NF- κ B and the link between inflammation and cancer. *Immunological Reviews* **2012**, *246* (1), 379-400.